Final Scientific/Technical Report

Reporting Period: June 01, 2008 through May 31, 2011

Submission Date: August 05, 2013

Agreement Number: DE-FG02-08ER64566

Project Title: Electrode Induced Removal and Recovery of Uranium (VI) from Acidic Subsurfaces

Investigators: Kelvin B. Gregory (PI)

Carnegie Mellon University, Pittsburgh, PA
Department of Civil and Environmental Engineering

Researchers: Dr. Juan Peng and Fei Lian

Contact: Kelvin B. Gregory, 412-268-9811, kelvin@cmu.edu

Executive Summary

Uranium (U) and technetium (Tc) are principal environmental contaminants in groundwater at several U.S. Department of Energy facilities. Area 3 of the U.S. DOE Y-12 site in Oak Ridge, TN is a challenging environment for subsurface remediation. It exhibits buffered low pH (<4) and high concentration of nitrate in addition to high U and Tc level. As a result, conventional in situ bioremediation and permeable reactive barrier (PRB) technologies for reductive immobilization and precipitation of these radionuclides are challenging. Recently, electrode-based remediation has emerged as an alternative approach for managing radionuclide contamination of groundwater. By capturing ions in the electric double layer of polarized electrodes, this approach can localize metal sequestration on a material that may be removed from the subsurface for recovery of the metals at the surface and enable permanent site restoration. However, little is known about the performance of electrodes under environmental conditions or how aqueous geochemical factors will impact remediation and recovery of radionuclides from the subsurface. The overarching objective of this research is to provide an improved understanding of how aqueous geochemical conditions impact the removal of U and Tc from groundwater and how engineering design may be utilized to optimize removal of these radionuclides. Experiments were designed to address the unique conditions in Area 3 of ORNL while also providing broader insight into the geochemical effectors of the removal rates and extent for U and Tc. The specific tasks of this work were to: 1) quantify the impact of common aqueous geochemical and operational conditions on the rate and extent of U removal and recovery from water, 2) investigate the removal of Tc with polarized graphite electrode, and determine the influence of geochemical and operational conditions on Tc removal and recovery, 3) determine whether U and Tc may be treated simultaneous from Area 3 groundwater, and examine the bench-scale performance of electrode-based treatment, and 4) determine the capacity of graphite electrodes for U(VI) removal and develop a mathematical, kinetic model for the removal of U(VI) from aqueous solution. Findings from Tasks 1 are in review for publication. Manuscripts that present findings from Tasks 2 and 4 are in draft format.

Initial removal rates of U(VI) were approximately first-order and increased from 0.01 hr-1 at pH 2 to 0.06 hr-1 at pH 6. U(VI) recovery rate was also closely related to pH. The slower removal rates exhibited at lower pH were overcome by increasing the applied potential, but with diminishing returns at above 2.5 V. U(VI) was removed faster at lower concentrations. The presence of Al^{3+}, Mg^{2+}, and Na^{+} did not influence U(VI) removal at lower applied potential (2.5 V) but showed different impacts on U(VI) removal at higher potential (5.0 V). Ionic strength and humic acid as a surrogate for natural organic matter did not influence U(VI) removal.

Pertechnetate may be removed with an externally-applied potential as low as 1.5 V. The observed removal rate for technetium increased with higher externally applied potential, but with diminishing returns above 2.5 V. Technetium was readily recovered in solution after removing the external potential. As with U(VI), the extent of technetium removal and recovery was strongly related to pH. Technetium was removed and recovered faster and to a greater extent at higher pH. The finding that Tc was mainly recovered from the cathode suggests that the primary removal mechanism was electroreduction at the electrode surface at 2.5 V. Ionic strength and humic acid did not exhibit an impact on technetium removal rates over the range of conditions studied.

Experiments with actual site water from Area 3 showed that simultaneous U and Tc removal can be achieved with both potentiostat-powered batch reactors and power supply-poised flow-through reactors. Despite low pH (~3) and high concentration of nitrate (~300 mM), both U (cation) and Tc (anion) were rapidly removed at the cathode within 3-7 days.

Graphite electrodes have a finite capacity for uranium electrosorption that was modeled using a Langmuir isotherm. A kinetic, mathematic model was developed based on empirical first order kinetics, to predict k_{obs} for U(VI) removal under the influence of some major environmental and operational effectors. The S/m ratio term that was developed is a surface area (S) to molar mass of adsorbate (m) ratio term was created to stress the combined effect of electrode surface area, solution volume, and adsorbate concentration. Double layer capacity, C_d was selected as a term to define the influence of applied potential. Ionic strength considerations were based on Gouy-Chapman-Stern (GCS) theory. The mathematical model to predict removal rates, $k_{obs} = 0.022(pH - 1.6)\ln(0.85C_d \frac{S}{m})$, accurately predicted k_{obs} for U(VI) removal over a broad range of solution ionic strengths that are relevant to groundwater (10^{-3} – 0.24 M).

Overall the body of work suggests that an electrode-based approach for the remediation of acidic subsurface environments, such as those observed in Area 3 of ORNL may be successful for the removal for both U(VI) and Tc. Carbonaceous (graphite) electrode materials are likely to be the least costly means to maximize removal rates and efficiency by maximizing the electrode surface area. Future work should aim at developing a small-scale field test around high surface area carbon aerogel electrodes to evaluate the feasibility of an electrode-based remedial approach under field conditions.

Introduction

Uranium (U) and technetium (Tc) are principle contaminants of concern at several U.S. Department of Energy (DOE) facilities, including Oak Ridge National Lab, the Hanford Site, and the Paducah Gas Diffusion Plant due to high concentrations, high mobility in groundwater, and their potential for adverse effects on human and environmental health. Groundwater in Area 3 at Oak Ridge National Laboratory (ORNL), where radionuclide contamination is the highest, exhibits low pH (~3.0) and concentrations of uranium as high as 210 μM, technetium as high as 40 nCi/L. The groundwater also contains high concentrations of other metals (Ca, Mg, Al, etc) and nitrate (up to 160 mM). Due to the special site geology and hydrogeology, the complexity of contaminants, and the extent and magnitude of contaminated area, yet no practical U and Tc remedial strategy was found to be effective in long term operation.

Recently, a graphite electrode-based approach for removal of radionuclides from groundwater was demonstrated. With a graphite electrode carrying a potentiostat-poised cathodic potential, U(VI) was rapidly removed from contaminated artificial groundwater at circumneutral pH {Gregory, 2005}. When potential was removed, U(VI) rapidly returned to solution under abiotic conditions, whereas with the presence of cells, recovery was observed until air was bubbled through the system. This study shows significant promise for applying electrode-based technique to in situ U and Tc remediation. By localizing metals/radionuclides on an electrode surface and enabling their recovery outside the subsurface, it offers the opportunity for permanent restoration, which is one very significant advantage over all other in situ methods proposed for remediation of U and Tc. Additionally, electrode-based remedial approaches offer the opportunity to adjust the electric field in which the target contaminant is migrating as well as the delivery of electron donor in real time and in accordance to changing site conditions. While these advantages and opportunities are substantial, electrode-based remediation is a nascent technology. Little is known about how aqueous geochemical factors and design considerations will impact the initial abiotic removal of radionuclide. Indeed, the selection, design, and implementation of electrode based-remedial approaches will rely on a thorough understanding of how aqueous geochemical and operational conditions affect removal rates, extents of removal, and subsequent recovery of radionuclides from electrode surfaces. The aim of this research was to fill those knowledge gaps to better enable a future field-scale pilot test of electrode-based remediation at ORNL Area 3 or other DOE legacy sites with metal contamination.

Project Accomplishments

The following describes the results obtained relating to each project task and the implications of those results on the applicability of the electrode-based remedial approach for removal and recovery of radionuclide contamination from subsurface environments.

Task 1: Impact of Aqueous Geochemical and Operational Conditions on U Removal

The objective of this task was to investigate the impacts of common geochemical factors in groundwater (pH, initial U(VI) concentration, other cations, ionic strength and humic acid) and applied potential on uranium removal during the initial, rapid abiotic removal process at the electrode surface as well as recovery. Findings from this task have been submitted for publication. The manuscript is appended to the report as Manuscript 1.

Removal and Recovery of U(VI) from FRC Area 3 Site Water

The extraction of U(VI) from FRC Area 3 site water using electrodes was examined using a 3-electrode, potentiostat-poised reactor. This reactor was identical to previous studies by the PI {Gregory, 2005}. The application of electric potential at the working electrode (-0.5 V vs Ag/AgCl) initiated the rapid removal of U(VI) from a slurry of low pH sediment and groundwater from the FRC Area 3 site (**Figure 1**). 86% of the initial U(VI) was removed after 29 days. No U(VI) removal occurred in the control reactors that lacked external potential. On day 29, U(VI) was respiked into the reactors from an aqueous stock solution of U(VI)-acetate to achieve a concentration of 310 μM. On day 88, 86% of the respiked U(VI) had been removed and over the next 71 days, very little additional U(VI) was removed. Although the initial U(VI) removal rates (over the first 48 hours) were similar for both amendments, removal rate for the respike was slower over the duration of the experiment.

Recovery of U(VI) from the electrodes began immediately following the removal of potential from the working electrode on day 159. 52% of removed U(VI) returned to solution within 24 hours. The remaining U(VI) returned solution over the next 85 days. The average recovery of U(VI) was 68.0% on day 244 and no further U(VI) returned to solution.

The rapid removal and recovery of uranium from the low pH groundwater on polarized electrodes was consistent with entrapment of uranium ions in the electrical double layer at the electrode reported previously using circumneutral pH solutions {Xu, 2000; Gregory, 2005}. Previous studies suggested that reduction of U(VI) to U(IV) in groundwater solutions by a graphite electrode poised at -0.5 V vs Ag/AgCl was not a significant source of abiotic removal {Gregory, 2005} and was also insignificant for potentials ranging from -0.45 V to -0.9 V versus Ag/AgCl electrode {Xu, 2000}. Theoretically, reduction of U(VI) to U(IV) requires a working electrode potential of ~-0.6 V versus Ag/AgCl. The potential further decreases to -0.70 V for reduction of 280 μM U(VI) to U(IV) ($UO_{2(s)}$) at pH3. Therefore the removal and recovery of U(VI) may be attributed to charging/discharging of the electric double layer (EDL) around cathode {Farmer, 1997; Ying, 2002} or cationic adsorption/desorption {Alfarra, 2002}.

The total fraction of U(VI) removed from the FRC Areas 3 site samples was similar to previous studies examining removal of U(VI) from a biological growth media using electrodes {Gregory, 2005}. However, the rates of removal were much lower from the FRC Area 3 samples despite nearly identical reactors and electrode materials. For example, only 39% of the initial U(VI) was removed within 1 day from the FRC Area 3 samples whereas 99.0% of removal was observed from the media samples {Gregory, 2005}. The difference in U(VI) removal rates between the two samples was likely the result of aqueous constituents of the water between the two studies. For example, initial U(VI) concentration, pH, metal concentrations and ionic strength at FRC Area 3 are all higher than in Gregory et al (2005). The more concentrated conditions may have the effect of dissipating the electrical double later that develops around the electrode, slowing the removal rates of U(VI) at the electrode surface.

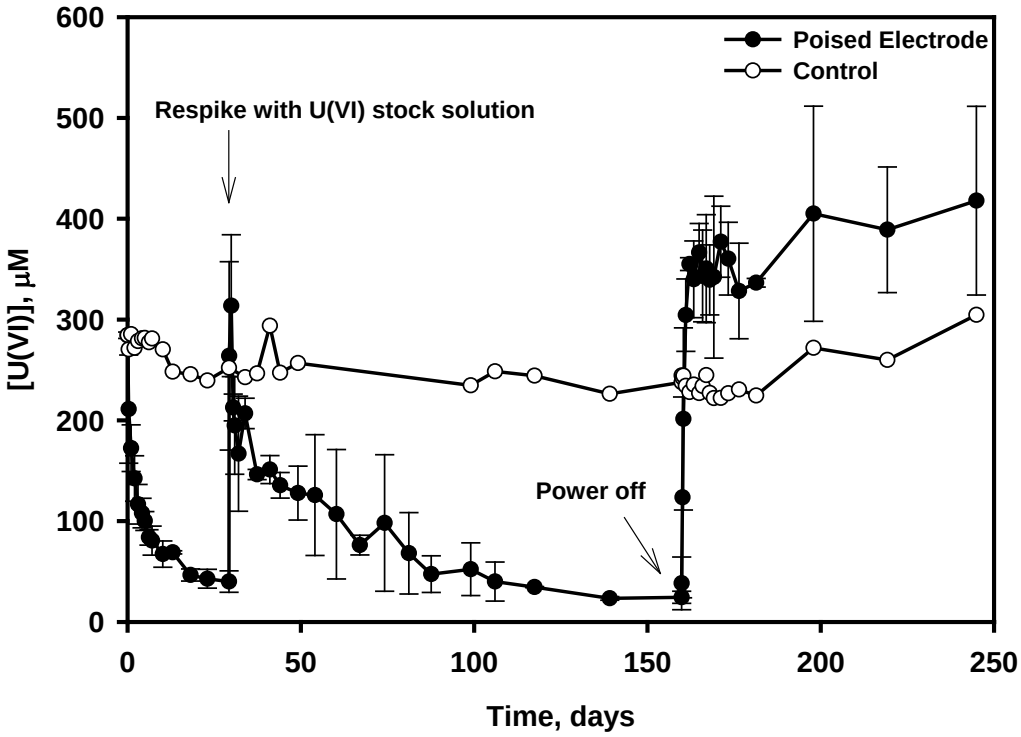

Figure 1. Removal and recovery of U(VI) in batch incubations of uranium-contaminated soil and groundwater from Oak ridge, TN. Working electrode was poised at -0.5 V (vs a Ag/AgCl reference) via a potentiostat. After 29 days, more U(VI) was added. Power was turned off on day 159. Error bars represent the average and standard deviation of duplicate reactors.

Influence of pH on U(VI) Removal

The impact of pH on the initial removal rate of U(VI) (k_{obs}) was examined in a 2-electrode system using pH adjusted water between pH 2 and 6 (**Figure 2**). Initial removal rates were approximated using pseudo first order kinetics. The rates were dependent on pH, increasing from 0.01 hr^{-1} to 0.06 hr^{-1} as pH increased from 2 to 6. The pH dependence of U(VI) removal on carbon-based electrodes may be attributed to the rapid charging of the EDL by protons at low pH.

However, the pH dependence may also arise from differences in the mobility of the predominant uranium species at each pH as well. For example, at pH 2, over 90% of U(VI) is expected to exist as free UO_2^{2+}. As the pH increases, the fraction of UO_2^{2+} decreases and the predominant species changes to $(UO_2)_2(OH)_2^{2+}$ and at pH 5-6 $(UO_2)_3(OH)_5^{+}$ becomes the dominant species. The mobility of an ion in an electric field is a factor that indicates how fast a given species can move through solution in an electric field and may be estimated according to Equation 1 {Bard, 2001}:

$$u_i = \frac{|z_i|e}{6\pi\eta r_i} \qquad \text{Equation 1}$$

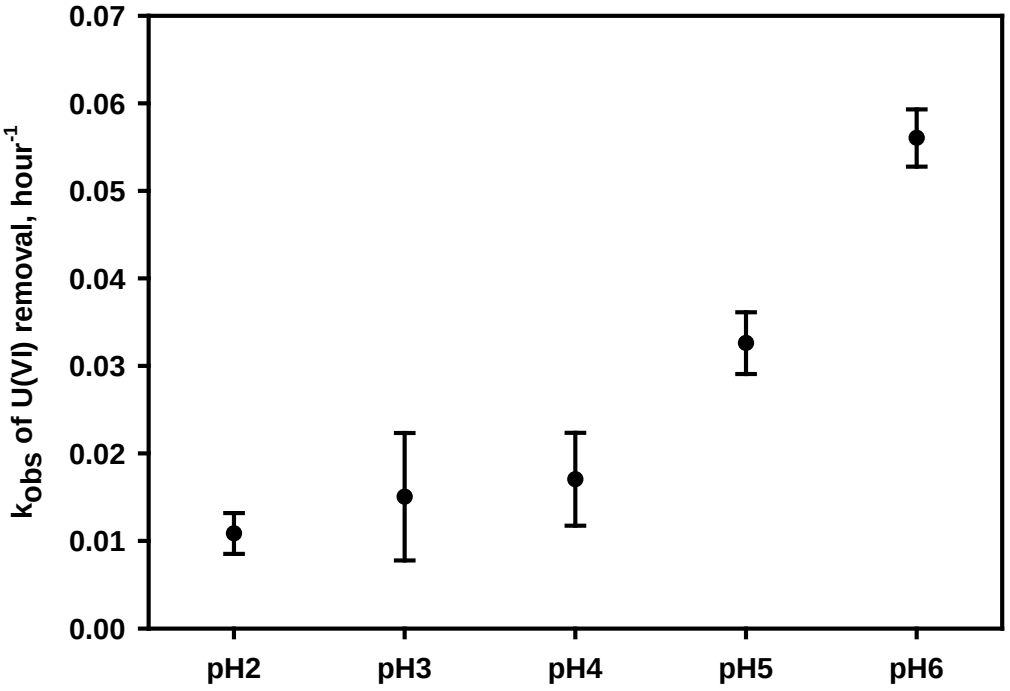

Figure 2. Impact of solution pH on initial removal rates (k_{obs}) of U(VI). Initial removal rates were approximately first order. The external potential was 2.0 V and starting concentration of U(VI), 150 µM. Error bars represent the average and standard deviation of duplicate reactors.

Where u_i is the mobility (m^2/ s•V) of species *i* in an electric field, z_i is the charge of species *i*, *e* is electronic charge (1.602×10^{-19} coulombs), η is the viscosity of the solution (g/m•s), and r_i is the radius of species *i* (m). Equation 1 predicts that UO_2^{2+} has higher mobility than either $(UO_2)_2(OH)_2^{2+}$ or $(UO_2)_3(OH)_5^{+}$ in electric field, due to the charge it carries and its relatively smaller ionic radius. Mobility of H^+ (3.63×10^{-3} cm^2/s•V) is about eleven times higher than that of UO_2^{2+}(3.32×10^{-4} cm^2/s•V) in diluted solution (**Table 1**). With the estimated mobility, the net flux of a particular species in the EDL may be estimated by Equation 2 {Newman, 2004}:

$$J_i = -u_i c_i \nabla\Phi - D_i \nabla c_i \qquad \text{Equation 2}$$

where J_i is the net flux of a charged ion in an electric field (mol/m^2s) (convection is not considered near the electrode surface). The first group of terms on the right hand side of Equatoin 2 accounts for ionic migration, where, c_i is the concentration of species *i* (mol/L), $\nabla\Phi$ is the potential gradient (V/m). The second group of terms accounts for diffusion, where D_i is the diffusion coefficient of species *i* (m^2/s) ($D_i = \frac{u_i RT}{|z_i| F}$, where z_i is the charge of species *i*, u_i is the mobility of species *i*, F is Faraday's constant, R is universal gas constant, and T is absolute

temperature) and ∇c_i is the concentration gradient of species *i* (mol/m^4). For example, although carrying the same charge, flux of $(UO_2)_2(OH)_2^{2+}$ should be smaller than that of UO_2^{2+} (Equation 1) since mobility (u_i) of $(UO_2)_2(OH)_2^{2+}$ is lower in the same electric field. At higher pH, $(UO_2)_2(OH)_2^{2+}$ or $(UO_2)_3(OH)_5^{+}$ are the dominant U(V)) species, since they both have lower mobility than UO_2^{2+}, U(VI) species do not move faster at higher pH than at lower pH according to Equation 2. Assuming ions reaching the electrode surface first will have the priority to be electrosorbed, the analyses above clearly suggests that U(VI) speciation is not the reason for increase of U(VI) removal at high pH, since U(VI) species move faster at lower pH at an electric field.

Table 1 Values of radii, mobility and diffusion coefficients of major cations at infinite dilution in water at 25 °C.

Components	z_i	r_i Å	u_i cm^2/s•V	D_i 10^{-5} cm^{2}s^{-1}
H^+	1	0.28 [a]	3.63×10^{-3} [b]	9.311 [c]
UO_2^{2+}	2	5.76 [b]	3.32×10^{-4} [b]	0.426 [c]
Na^+	1	1.84 [a]	5.20×10^{-4} [b]	1.334 [c]
Mg^{2+}	2	3.47 [a]	5.50×10^{-4} [b]	0.706 [c]
Al^{3+}	3	4.39 [a]	6.32×10^{-4} [b]	0.541 [c]

[a]{Nightingale, 1959 #53}
[b]calculated from diffusion coefficient with F=96485.3 coulombs, η=8.9×10^{-3} Pa·s, R=8.314 J/mol•K, T=298 K
[c]{Vanýsek, 2008-2009 #51}

At low pH, both uranium cations and protons move towards the electric double layer at the cathode. Protons have a much greater mobility and the flux of protons is 73 times of that of UO_2^{2+} ions at pH 3 with 150 μM U(VI). Therefore protons move faster than U(VI) cations and enter the electric double layer earlier than uranium. The accumulation of protons will dissipate charge at the electrode surface, limiting its ability to hold uranium. As pH increases, protons gradually lose their advantage. Increasing pH from 3 to 6 will decrease migration flux of protons by 3 orders of magnitude. Since ionic radius of $(UO_2)_2(OH)_2^{2+}$ or $(UO_2)_3(OH)_5^{+}$ are unknown, it is hard to compare flux of protons with that of U(VI) species at pH beyond 4. However, when pH exceeds 3.8, concentration of protons is no longer larger than U(VI), suggesting that the impact of proton competition for the electrical double layer lessens at pH beyond 4, and gives rise to faster removal rates for uranium.

In addition to reducing the effect of competition for the EDL between protons and uranium, increasing pH may deprotonate acidic surface functional groups on graphite such as carboxyl groups (pK_a=3~8), and provide a negative charge to the electrode surface {Seron, 1996}. Cationic U(VI) species may form complexes with negatively charged functional groups {Alfarra, 2002}, and contribute to faster U(VI) removal. Although surface complexation and electrostatic interactions in the EDL may be contribute to U(VI) removal, U(VI) could not outcompete H^+ under either circumstances at lower pH due to disadvantages in concentration and flux. Lower pH increases the impact of proton competition as well as decreases available surface functional groups where U(VI) may adsorb. Regardless of the mechanism, the aggregate impact of lower pH is greatly decreased U(VI) removal rates.

Influence of pH on U(VI) Recovery

The impact of pH on the recovery of U(VI) from electrodes was examined in a two electrode systems which had previously removed 150 μM U(VI). Solution pH between 2 and 6 were explored in synthetic groundwater that simulated geochemical conditions in Area 3. Recovery was initiated by merely removing potential from the electrodes. Over 50% of the total U(VI) returned to the solution within 10 hours at all pH evaluated in the study (**Figure 4**). Additional U(VI) was recovered slowly afterwards. It was found that recovery of U(VI) over the first 9 hours at different pH fitted well into zero order kinetics. Results showed that pH was as important in U(VI) recovery process as it was for U(VI) removal. The pH-depended recovery of uranium from electrode surfaces is different than previous observations for recovery of electrosorbed Li^+ {Alfarra, 2002}, NaF and $Cu(NO_3)_2$ {Ying, 2002} at reversed potentials, in which pH was not reported to impact rates of recovery, regardless of impact of pH on cation removal.

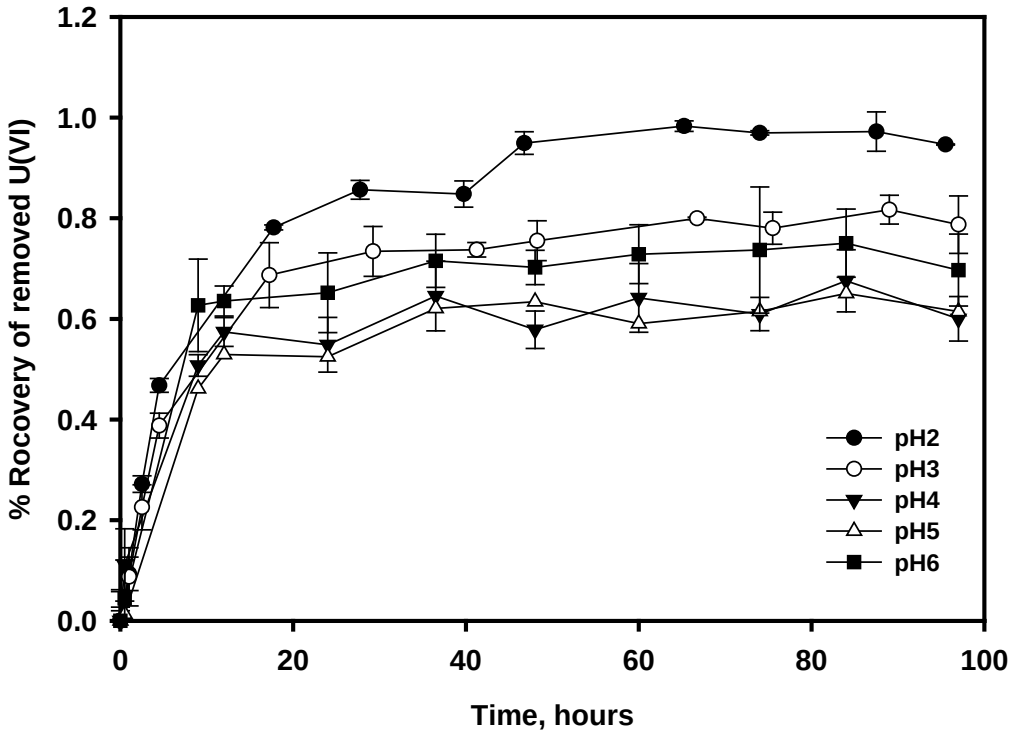

Figure 3. Recovery of removed U(VI) after the poise of electrodes were removed at pH 2-6 and 2.0 V. Error bars represent the average and standard deviation of duplicates.

The pH-dependence for uranium is likely related to U(VI) speciation with pH and complexation phenomena. As discussed previously, at higher pH, the dominant U(VI) species, $(UO_2)_2(OH)_2^{2+}$ or $(UO_2)_3(OH)_5^+$, have lower diffusion coefficient than UO_2^{2+} and may diffuse back to bulk solution at slower rate. But at pH 6, initial k_{obs} starts to increase. With all other conditions unchanged, carbonate speciation may contribute to this phenomenon. As pH approaches 6, more carbonate species exist as HCO_3^- instead of $H_2CO_{3(aq)}$ than at pH 5. Naturally dissolved HCO_3^- and CO_3^{2-} in pH 6 solution are about 501.2 μM and 0.025 μM, respectively. Dominant U(VI)

species at pH 6, $(UO_2)_3(OH)_5^+$, may react with HCO_3^- or CO_3^{2-} and speed up U(VI) recovery by forming uncharged species such as $UO_2(CO_3)_{(aq)}$, $UO_2(OH)_{2(aq)}$, and other more mobile species {Burns, 1999}.

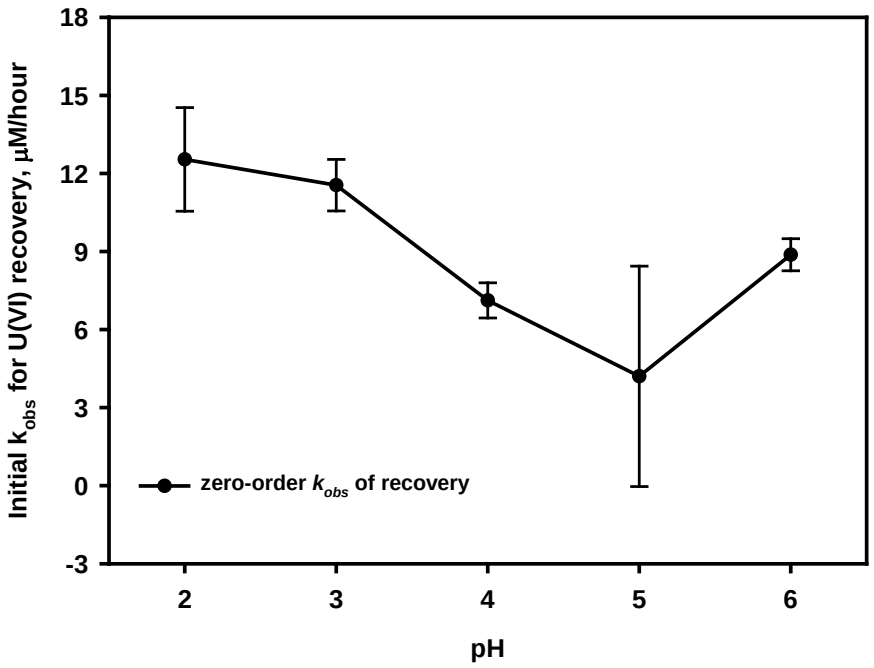

Figure 4. Initial recovery rate of removed U(VI) varies with different pHs. Recovery of U(VI) is a zero-order reaction during the beginning of the recovery, and k_{obs} was calculated from zero-order linear fitting. Error bars represent the average and standard deviation of duplicate reactors.

Influence of Applied Potential on U(VI) Removal

The previous calculations show that removal rates of uranium are adversely impacted by competition with faster moving and higher concentration protons in the EDL. However, the flux of ions through the EDL is also partially determined by the applied potential gradient at the electrode (Equation 2). Moreover, increasing the applied potential will also change the potential distribution in the EDL by enhancing cathodic potential and increase the capacity of EDL {Bard, 2001}. The impact of applied potential between the electrodes on the removal rates of uranium and its ability to overcome the detrimental impacts of low pH were examined through step-wise adjustments and estimation of initial removal rates. The investigation was run for over 240 hours. As for the initial k_{obs} plotted in **Figure 5**, no appreciable increase in k_{obs} was occurred as the potential was adjusted from 0.5 V to 1.5 V. However, between 1.5 and 2.5 V, k_{obs} increased from 0.15 hr^{-1} to 0.67 hr^{-1}. The rate observed at pH 3 with an external potential of 2.5 V was similar to the rate at 0.5 V and pH 6, confirming that the adverse impact of low pH may be overcome by increasing the externally applied potential at the electrodes. However, the benefit on uranium removal rate diminished with further increases in potential between the electrodes. This diminishing return was examined further and described below.

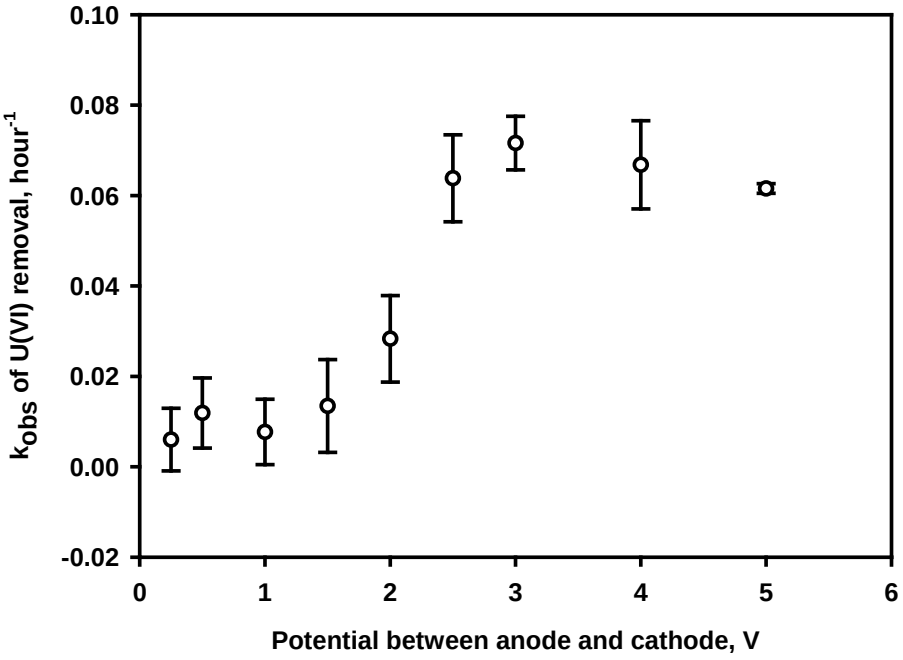

Figure 5. k_{obs} at different external potentials at pH 3 with 150 μM U(VI) solution within 24 hours. Error bars represent the average and standard deviation of duplicate reactors.

The diminishing return on the applied potential was examined by measuring the potential of the anode and cathode independently during stepwise adjustments. **Figure 6** shows that the absolute value of cathode potential against Ag/AgCl increased by over 80% with external potential increased from 2.0 V and 2.5 V, but by smaller percentages as the external potential was increased beyond 2.5 V. This is consistent with the doubling of k_{obs} from 2.0 V to 2.5 V, and the plateau beyond 2.5 V as shown in **Figure 5**. Due to low conductivity of the solution, large ohmic loss greatly reduced potential difference between cathode and anode. As mentioned previously, although thermodynamically feasible, significant reduction of U(VI) to U(IV) was not observed when working electrode was poised at -0.9 V versus Ag/AgCl electrode {Xu, 2000}, which suggests that diminishing return should not be attributed to U(VI) reduction to U(IV). Some other factors hindered U(VI) removal. Since our system was open to the atmosphere, we were unable to measure gas evolution from the solution. However, visible gas production was observed as tiny bubbles of gas on the anode and cathode electrodes at and beyond 4.0 V. Gas evolution was not visually observed at 2.5 V and below, at which the overall potentials between cathode and anode were below 1.23 V and water hydrolysis was thermodynamically infeasible. Previous study has suggested that H_2 evolution rate increases as external applied potential increases {Sun, 2010}, indicating that at higher potential U(VI) ions may be prevented from approaching electrode surfaces by gas formation at the electrode surface and occupation of adsorption sites. A diminishing return on k_{obs} at higher external potential may due to combined impacts from above-mentioned factors.

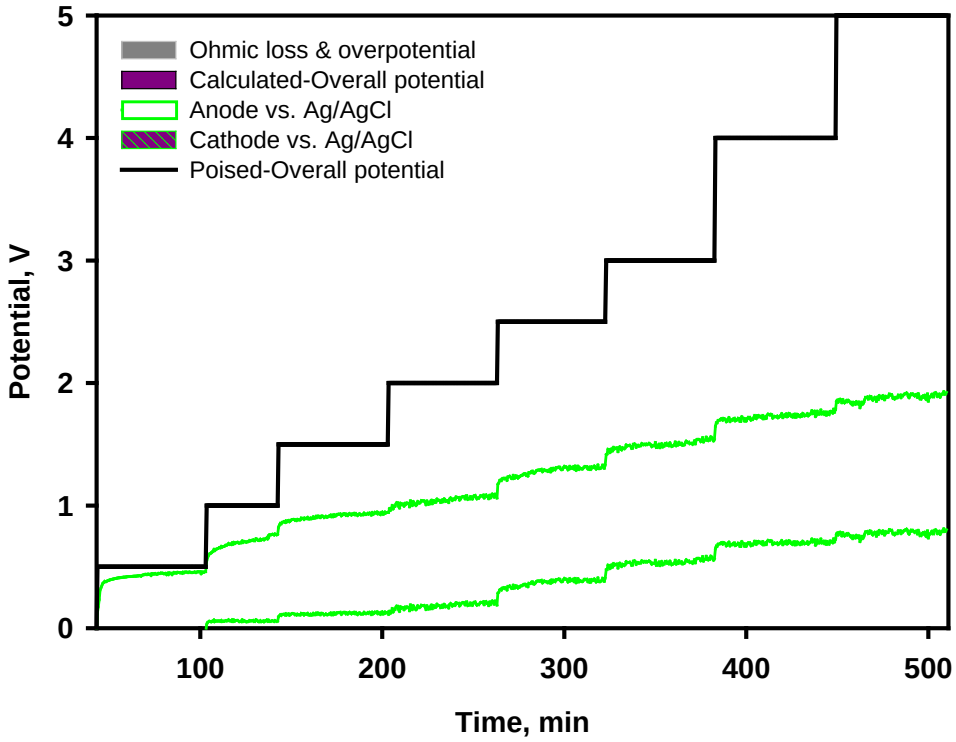

Figure 6. Potential distribution versus external potential change in pH 3, 150 μM U(VI) solution. The horizontal black line defines external potential applied. Area in purple (including the hatched area) shows the real potential between anode and cathode, gray area illustrates potential lost in ohmic resistance and overpotentials. Area between the green lines represents anode potential against Ag/AgCl, green line shaded area represents the absolute value of cathode potential against Ag/AgCl.

Influence of Initial U(VI) Concentration on Removal

The impact of U(VI) concentration on removal rates at acidic pH was examined through a range of concentrations between 1 μM and 200 μM. Rates were examined at an external potential of 2.5 V, the optimal potential determined in **Figure 5** from a removal rate and energy perspective. **Figure 7** shows that U(VI) was removed faster at lower concentrations. Although quantitatively more U(VI) was removed as initial concentration increased, the removal rate decreased by 72% and the fraction of U(VI) removed decreased to less than 50% as the initial concentration of U(VI) increased from 1 μM to 200 μM. A previous study on removal of Li^+ from aqueous solution with activated carbon also showed that the amount of lithium adsorbed increased with initial lithium concentration {Alfarra, 2002}. Possible reason is that as initial concentration decreases in bulk solution, ion flux decreases according to Equation 2. Each ion has access to larger surface area/more space in EDL and experiences less competition for adsorption site, resulting in faster adsorption/removal.

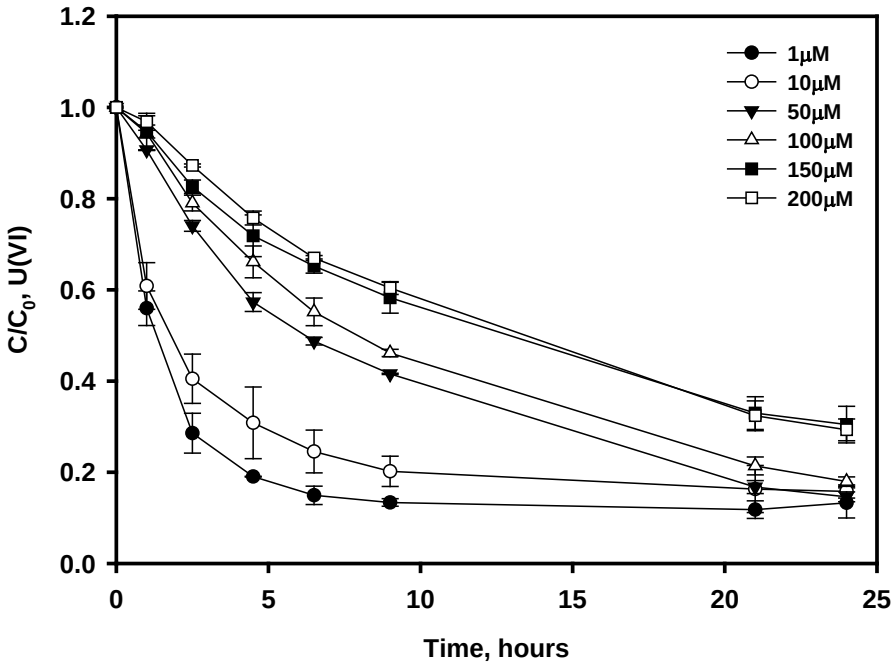

Figure 7. Removal of U(VI) changed with increasing initial concentration of U(VI) (1 μM, 10 μM, 50 μM, 100 μM, 150 μM, and 200 μM) at pH 3 and 2.5 V. The data markers report the average and range of duplicate experiments.

Influence of Other Cations on U(VI) Removal

Cationic groundwater constituents will move into the EDL and have the potential to occupy reactive sites on the electrode in a similar way to protons. In addition to low pH, groundwater at the FRC Area 3 exhibits high concentrations of cationic species which may compete with U(VI) during electrosorption. In particular, Al^{3+} is present in concentrations up to 180 mM {Brooks, 2001}. In order to examine the influence of cationic groundwater constituents on U(VI) removal, Al^{3+}, Mg^{2+}, and Na^{+} were amended to DI water containing 150 μM U(VI) in pH 3 solution. Diffusion coefficient of Al^{3+}, Mg^{2+}, and Na^{+} are all larger than that of UO_2^{2+} (**Table 1**), suggesting these cations migrate faster than UO_2^{2+}, the dominant U(VI) species at pH 3, in the same electric field.

Figure 8 shows that with 2.5 V external potential, the concentration of Al^{3+}, Mg^{2+}, ad Na^{+} ions had little influence on initial U(VI) removal rate (k_{obs}). However, no significant change in aqueous concentrations of Al^{3+}, Mg^{2+}, and Na^{+} was observed throughout the experiments at 2.5 V (data not shown), indicating there was either no removal of cations other than U(VI) occurred or that the removal of Al^{3+}, Mg^{2+}, and Na^{+} was too small to be observed under the conditions tested. There was little difference in the U(VI) removal rates for any of the aluminum, magnesium, or sodium concentrations examined. Although other cations had little impact on k_{obs} for U(VI) at 2.5 V, when the external potential was increased to 5.0 V, k_{obs} decreased with increasing concentrations of Al^{3+} or Mg^{2+} (**Figure 8**), but not Na^{+}; k_{obs} increased slightly with increasing concentrations of Na^{+} cations.

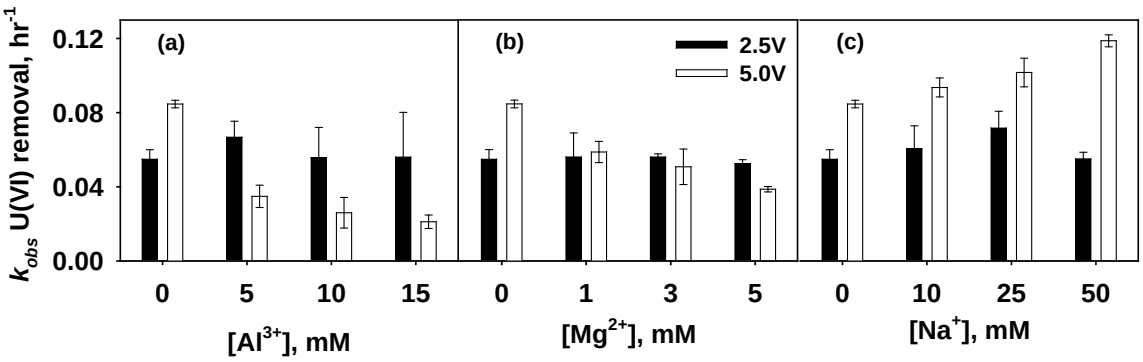

Figure 8. Initial removal rate (k_{obs}) of U(VI) from acidic water by electrodes at 2.5 V or 5.0 V of external potential in the presence of increasing concentrations of a) Al^{3+}, b) Mg^{2+}, and c) Na^{+}. The solutions initially contained 150 µM U(VI) at pH 3 and were examined over a 24 hr period. Error bars represent the average and standard deviation of triplicate reactors.

It is reasonable that higher Na^{+} concentration would decrease ohmic loss in the solution by increasing solution conductivity, and enhancing potential on electrode. An enhanced electrode potential will provide strongly electric field, and result in faster migration of ions in the solution, which may eventually result in an increase in U(VI) removal rate.

The decrease in k_{obs} with Al^{3+} or Mg^{2+} at 5.0 V, is likely the result of pH effects as OH^{-} may accumulate near the cathode as protons are depleted by electrolysis at 5.0 V (**Figure 6**). Even in acidic bulk solution, high pH (11-13) on cathode surface is easily obtained {Hansen, 1959}. 5 mM of Al^{3+} can precipitate out as $Al(OH)_3$ at pH beyond 4.2 ($logK_{sp}$=-31.62, {Benjamin, 2002) and 1 mM Mg^{2+} ions precipitates out as hydroxides at pH beyond 9.9 ($logK_{sp}$=-11.25, {Haynes, 2011-2012}). At the cathode, Al^{3+} and Mg^{2+} ions may precipitate out as hydroxides at 5.0 V; precipitates may cover the electrode surface, dissipate the potential, and provide less favorable conditions for U(VI) adsorption. The higher the concentration of Al^{3+} and Mg^{2+}, the more hydroxides will form at 5.0 V, causing less surface availability for U(VI) electrosorption and ultimately slower U(VI) removal rate. Although not qualified or quantified, white precipitates were observed on cathode during the 5.0 V experiments. Moreover, a decrease in Al^{3+} and Mg^{2+} concentration was also detected at 5.0 V at all studied concentrations (**Figure 9**). When power was turned off, white precipitates on cathode gradually disappeared, and removed Al^{3+} and Mg^{2+} were completely recovered, which further supports the hypothesis that U(VI) removal was hindered by the formation of aluminum and magnesium precipitates.

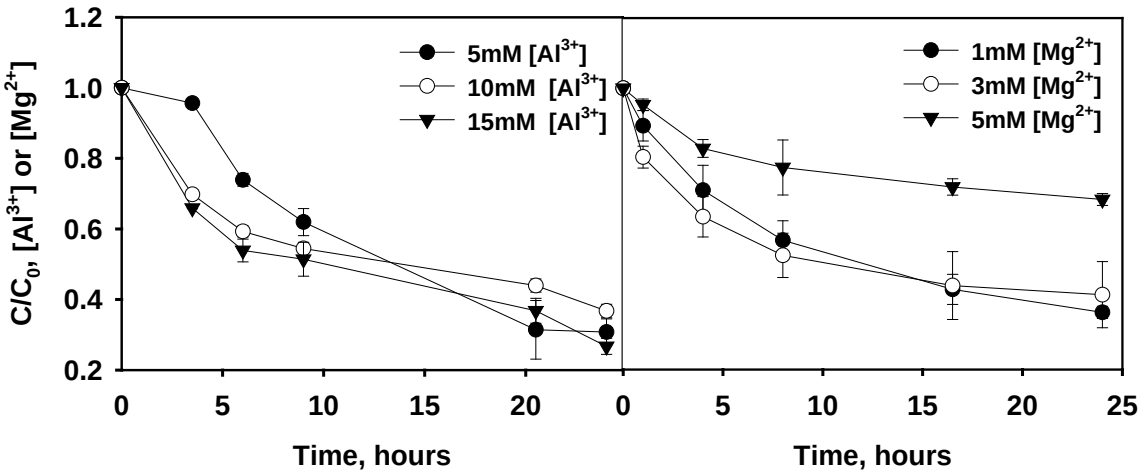

Figure 9. With the removal of U(VI) at 5.0 V, Al^{3+} and Mg^{2+} were also removed. Initial concentration of U(VI) was 150 µM. Error bars represent the average and standard deviation of triplicate reactors.

Influence of Ionic Strength on U(VI) Removal

Ionic strength of groundwater at Area 3 is around 0.2 M. Ionic strength influences ionic activity coefficient {Benjamin, 2002}, and Debye length and difference capacitance of electric double layer. Since ionic strength is an important term determining ionic activity, solution conductance, and electrode capacity, it may also impact U(VI) removal rate, as will be discussed below.

Removal of U(VI) was also fitted into first order kinetic reaction. The change of k_{obs} versus ionic strength was plotted in **Figure 10**. It was found that ionic strength did not have a significant impact on U(VI) removal as expected, suggesting removal of U(VI) is not limited by electrode capacity at 2.5 V. Possible reason is that removal of U(VI) by graphite electrode is considered to be a surface reaction. Although ionic strength impact electrosorption capacity of electrodes, initial removal rate should not be impacted when capacity is not a limiting factor. Influence of ionic strength at 2.0 V is expected to be similar to 2.5 V. Initial removal rates of U(VI) increased from 0.01 hr^{-1} at pH 2 to 0.06 hr^{-1} at pH 6 and 2.0 V (**Figure 2**). Since ionic strength did not influence U(IV) removal rate within 10^{-3} M to 10^{-1} M range, it could be concluded that increased concentration of protons has an detrimental impact on U(VI) removal rate, probably due to competition for absorption sites on electrodes or in the electric double layer.

Influence of Humic Acid on U(VI) Removal

Humic substances are derived from degradation of natural organic matter, and are ubiquitous in soil. Since they usually strongly bind to metals, and could reduce mobility of U(VI) in groundwater {Wan, 2011}, it is necessary to study potential effect of humic substances on U(VI) removal rate. Previous studied reported that Natural Organic Matters (NOM) could significantly reduce sorption capacity of carbon aerogel electrode {Gabelich, 2002}.

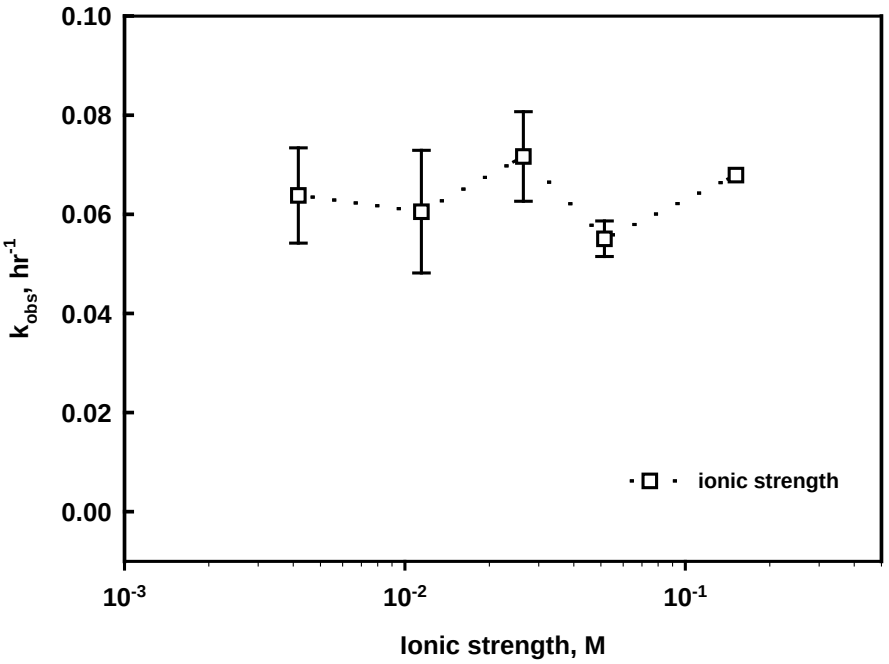

Figure 10. k_{obs} at different ionic strength at pH 3 with 150 µM U(VI) solution. Ionic strength of the solutions was adjusted by adding desired concentration of $NaNO_3$; external potential applied was 2.5 V. Error bar represents standard deviation from duplicate experiments.

Humic acids are large organic molecules, and it is highly impossible that humic acids can outcompete U(VI) for reaction sites on electrode. However, they may attach to the electrode surface by forming strong complexation with surface functional group, block reactive sites on electrode, and reduce available electrode surface area for U(VI) removal. Therefore, the influence of humic acid on U(VI) was also investigated at pH 3 and 2.5 V.

The relationship between U(VI) removal first order rate constant and concentration of humic acid was displayed in **Figure 11**. It suggests that humic acid within 25 mg/L did not have a significant impact on U(VI) removal as expected, suggesting presence of humic acid may not be a limiting factor of removal of U(VI) under practical conditions. Possible reasons are that: 1) U(VI) is removed before humic acid may interact with electrode, 2) humic acid (pK_{a1} = 4) should be mostly neutral at pH 3, and is not preferentially attracted to cathode and competes with U(VI). At common, environmentally-relevant concentrations of humic acids (below 25 mg/L), removal of U(VI) is not expected to be significantly impacted.

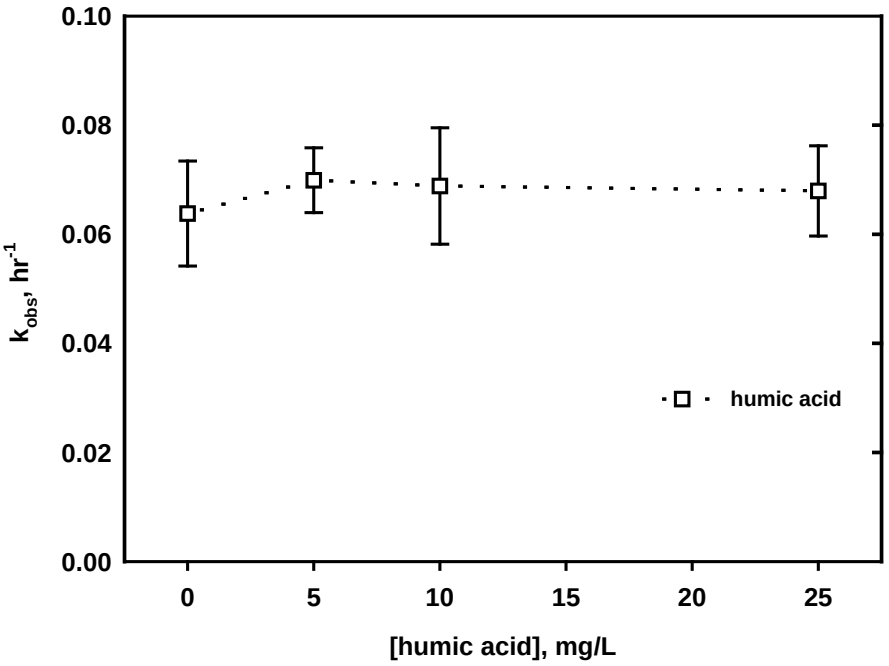

Figure 11. k_{obs} with different concentrations of humic acid at pH 3 with 150 µM U(VI) solution. External potential applied was 2.5 V. Error bar represents standard deviation from duplicate experiments.

Task 1: Summary and Discussion

An electrode-based U(VI) remediation method was applied to contaminated acidic subsurface. It was found that U(VI) removal can be achieved from acidic groundwater of Oak ridge, TN. We hypothesized that geochemical and remedial conditions may affect the removal and/or recovery of metals from the subsurface. Using 2-electrode system, we explored the impact of pH, externally applied potential, U(VI) concentration, potential competing cations, ionic strength and humic acid on the removal rates of U(VI) from aqueous solutions. The results show that initial U(VI) removal rates followed first-order reaction kinetics. The observed rate constant increased from 0.01 hr^{-1} at pH 2 to 0.06 hr^{-1} at pH 6, indicating a strong competition from protons. The fraction and rate of U(VI) recovery was also closely related to pH. These evidences, together with the results from potential monitoring on electrode, suggest that most of the U(VI) is probably electrosorbed by oppositely charged electrode, with the occurrence of surface complexation and/or ion exchange as well. The slower removal rates exhibited at lower pH were overcome by increasing the applied potential, but with diminishing returns. With a slight increase of external potential from 2.0 V to 2.5V, U(VI) removal rate almost doubled. The concentration of U(VI) was also found related to removal rate: U(VI) was removed faster at lower concentrations. At 2.5 V, presence of Al^{3+}, Mg^{2+}, and Na^{+} did not influence U(VI) removal, but showed different impacts on U(VI) removal at 5.0 V. It is highly possible that at 5.0 V, Al^{3+} or Mg^{2+} precipitated on the cathode via complexation with hydroxide ion, which decreased available electrode surface area and incurred a decline in U(VI) removal rate. This study demonstrates that electrodes may be employed for rapid removal and recovery of U(VI) across a broad spectrum of aqueous geochemical conditions.

Traditional bioremediation in FRC Area 3 requires removal of nitrate {Gu, 2005}, a common contaminant from nitric acid usage during uranium processing {Brooks, 2001}, since it is a competitive microbial electron acceptor greatly reduces U(VI) reduction rates {Istok, 2004; Edwards, 2007}. Neutralization of the groundwater is another prerequisite for biostimulation of U(VI) reduction to occur. Even after these pre-remedial steps, reduced uranium, or U(IV), is still vulnerable to various environmental factors, like oxygen, calcium, and carbonate/bicarbonate. Electrode-based removal of U(VI), however, despite of influences from geochemical conditions, could eliminate pretreatment of groundwater since optimal operation condition could be achieved via adjusting controllable electrochemical parameters such as externally applied potential. Most importantly, bioremediation of metals does not allow for simple recovery of the immobile metals from the contaminated site, which is distinctively different from organic chemical biodegradation. The principal advantage of an electrode-based remediation approach for metals lies in the localization of contaminant stabilization on an electrode surface, enabling permanent restoration through the removal of metal from the subsurface and recovery outside the contaminated site.

Task 2: Impact of Aqueous Geochemical and Operational Conditions on Tc Removal

The objectives of this research are to: a) demonstrate pertechnetate removal and recovery using graphite electrodes, and b) determine the impact of environmental conditions on removal rates and extents. Experiments were designed to evaluate the feasibility of Tc remediation of Tc from Area 3 groundwater at Oak Ridge National Laboratory. A manuscript has been prepared that is based on findings from Task 2. The most recent draft is appended to the report as Manuscript 2.

Influence of Applied Potential on Tc Removal

Removal of pertechnetate from solution containing 40 nCi/L NH_4TcO_4 at pH 3, a concentration level commonly observed at Area 3, was first studied at different applied external potential. Removal of ^{99}Tc was strongly influenced by external potential. **Figure 12** illustrates a predictable trend that as potential increased, removal of pertechnetate became faster. Little removal was observed at 0-1.0 V. As potential increased to 1.5 V, about 50% of ^{99}Tc was removed after 24 hours. A further potential increase to 2.0 V resulted in 79.8% removal within 8 hours, and 88.6% removal was achieved within 8 hours at 2.5 V. A similar trend was observed for the electrode-based removal of U(VI) described in Task 1. Increasing the applied potential changes the potential distribution in the EDL by enhancing cathodic potential {Bard, 2001}. As the potential gradient between cathode and bulk solution increases, ions are expected to migrate faster towards the electrodes according to Equation 2. Therefore a faster reaction on the electrode is also expected. The impact of potential is similar to what has been reported for pertechnetate removal with anodically polarized magnetite {Farrell, 1999}. However, beyond 2.5 V, the benefit of additional potential diminished and no significant difference in removal rate or extent was observed for pertechnetate removal at 2.5-5.0 V.

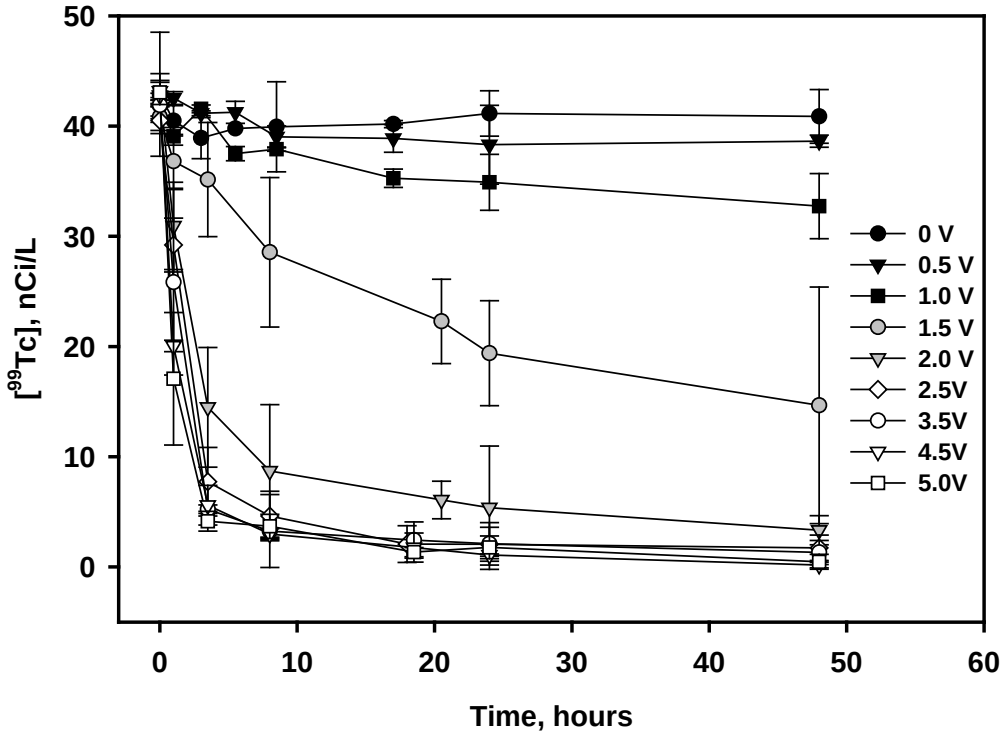

Figure 12. Removal of Tc(VII) from pH 3, 40 nCi/L Tc(VII) solution at different external potentials. The data markers represent the average and range of duplicate experiments.

Observed pertechnetate removal rates were calculated by fitting concentration versus time into first order kinetic equation. **Figure 13** shows that removal rate reached a plateau at 2.5-5.0 V. The highest k_{obs} was around 0.3 hr^{-1}, which is three orders of magnitude higher than what has been reported for pertechnetate removal with adsorbed Fe(II) at similar concentration {Cui, 1996}. The removal may be limited by electron-transfer on electrode surface to reduce Tc(VII), or affected by hydrogen evolution on cathode at higher potentials. Based on this result, 2.5 V was selected as the optimal applied potential for future Tc removal studies.

Since diminishing return on external potential above 2.5V was observed for Tc removal, another experiment was performed to measure potential of anode and cathode versus Ag/AgCl electrode (0.20 V versus standard hydrogen electrode) by a stepwise increase of the externally applied potential from 0 V to 5.0 V, as was done previously for U and shown in **Figure 6**. It was found that at 1.5 V, potential of cathode stabilized at around -0.078 V versus Ag/AgCl, or 0.122 V versus SHE, while overall potential between the electrode did not exceed 1.0 V, which is not sufficient for water electrolysis.

The reduction potential of Tc(VII) to Tc(IV) is 0.343 V versus standard hydrogen electrode (SHE) at pH 3. Therefore, Tc reduction is feasible with an external potential at 1.5 V and it is possible that electroreduction of Tc was the principle mechanism of removal. As externally applied potential continued to increase from 2.5 V to 5.0 V, same as what has been shown in **Figure 6**, cathode potential did not increase dramatically. However, real potential between anode and cathode exceeded 1.23 V, the threshold potential for water hydrolysis {Benjamin, 2002}.

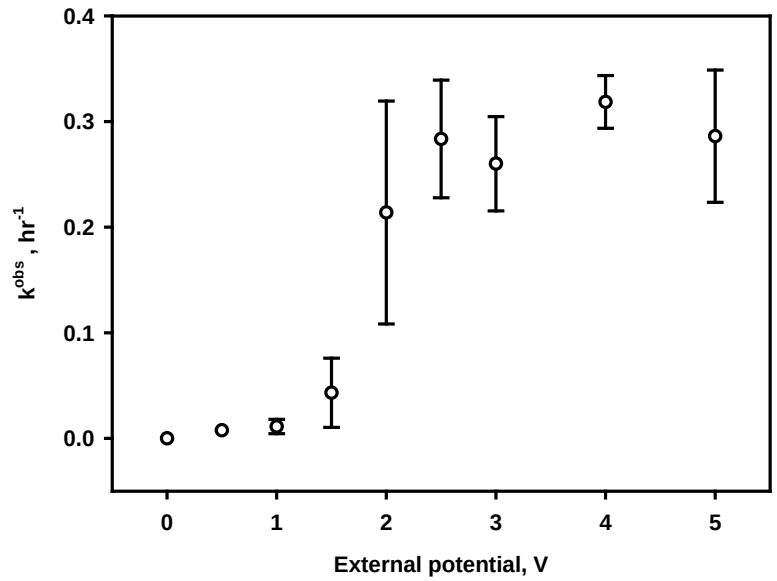

Figure 13. Change of first order rate constant with external potentials from pH 3, 40 nCi/L Tc(VII) solution.

Figure 14 shows that currents began to increase at potential beyond 2.0 V, which further suggests that side reactions, likely water hydrolysis occurred. As applied potential was partial used in side reactions, less electrons were available for Tc reduction. Moreover, pertechnetate may be prevented from approaching electrode surfaces by gas formation at the electrode surface and getting reduced. Therefore, it is not surprising that pertechnetate removal did not become faster as potential exceed 2.5 V.

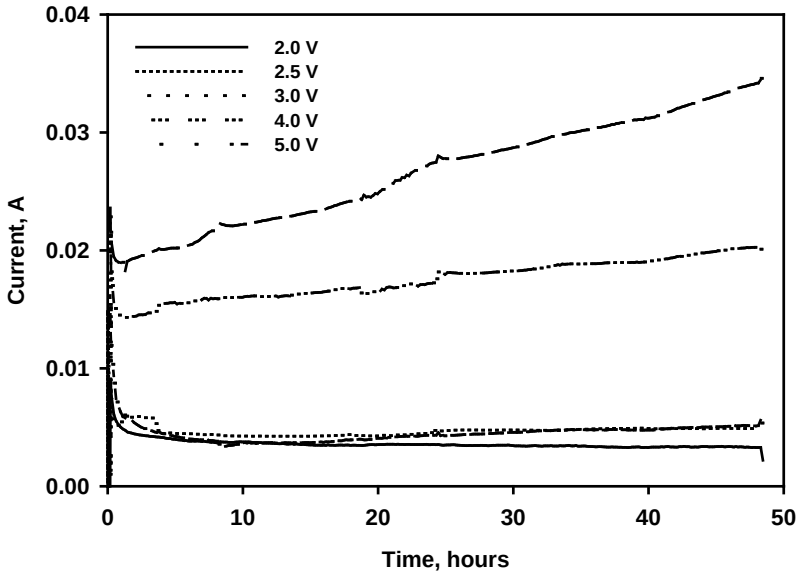

Figure 14. Change of current versus time during the removal of Tc(VII) at varied external potentials from pH 3, 40 nCi/L Tc(VII) solution.

Tc Recovery after Removal at Different Potentials

The ability to recover Tc from the electrodes following removal is a chief advantage of the electrode based approach. It is therefore important to understand on which electrode the Tc was recovered and what is the most optimal way to recover. Recovery of Tc from the electrodes was examined after 48 hours of pertechnetate removal shown in **Figure 12**. The anode and cathode were taken out from the reactors and directly put into separate containers with polarity removed. They were rinsed with buffer reagents for Tc recovery. The results of the recovery experiments are shown in Table 2. Regeneration of the electrodes and recovery of Tc were performed as described below.

Pertechnetate exist as $Tc(VII)O_4^-$ even under acidic conditions, which favors anodic migration. Tc(VII) is the most oxidized form of Tc and anode is an oxidizing electrode. No interactions other than electrosorption could be expected between Tc(VII) and anode. If $Tc(VII)O_4^-$ is electrosorbed by anode, as suggested by recovery of electrosorbed $U(VI)O_2^{2+}$ from cathode, removing poise from the electrodes will cause the recovery of Tc(VII) from electrode since the anode losses electrostatic force to attract and trap Tc(VII) in the double layer.

If Tc was recovered from cathode, it should be reduced because as an anion, the only possible reason for cathodic Tc recovery is the reduction of Tc(VII) on cathode. If all Tc(VII) ($10^{-7.4}$ M) was reduced to Tc(IV) oxides and adsorbed on the electrode surface as postulated by other researchers {Lawson, 1984}, it may be recovered via re-solubilization of Tc(IV) or re-oxidation to Tc(VII). Re-solubilized Tc(IV) should be no higher than $10^{-8.4}$ M according to its solubility{Rard, 1999}:

$$TcO_2 \cdot 1.6H_2O_{(s)} \rightleftharpoons 0.6H_2O_{(l)} + TcO(OH)_{2(aq)}, \text{ pK=-8.4} \qquad \text{Equation 3}$$

Solubilization of Tc(IV) with water is considered to be slow at anaerobic condition {Fredrickson, 2004}. However, according to a recent study, in carbonate media, Tc(IV) exists as an electrically neutral aqueous species, $TcCO_3(OH)_2$, at pH 3 and E_H between +0.2 V and –0.4 V {Alliot, 2009}. The same Tc species at pH 3 was reported by another group of researchers, but between E_H value of +0.4V and -0.17V {Wildung, 2004}. Therefore, rinsing the electrodes with carbonate media is probably an effective way of solubilizing Tc. Tc may also return to the solution via re-oxidation. Previous studies have already shown that re-oxidization of Tc(IV) by air is a major contribution to Tc rembolization {Burke, 2006; McBeth, 2007}. In order to determine which electrode played a major role in Tc removal, a 50 mM Na_2CO_3 solution was used to clean the electrodes along with ultrasonic cleansing. Since the experiments were run at open-to-atmosphere condition, it is expected that most reduced Tc(IV) can be re-oxidized and/or re-mobilized during this cleansing process.

The electrodes were cleaned 5x, for 20 minutes in an ultrasonic bath. Washing solutions were collected and assayed for Tc to calculate a mass balance on Tc. As shown in **Table 2**, no obvious trend was observed in terms of the amount of Tc recovered from anode and cathode at different potentials. Although total recovered Tc is far less than the amount initially introduced, most recovered Tc was from cathode. Tc recovered from anode is almost negligible.

If Tc(VII) is electrosorbed onto anode, the recovery is expected to be fast, as observed in U

recovery. Therefore, the results suggest that anode had little interaction with Tc during the removal; otherwise, Tc should recover immediately from the anode to the solution if it were removed via electrosorption.

Therefore, Tc(VII) should be reduced on the cathode during the removal. The reason why Tc(VII), an anion, was reduced on cathode may be explained as follows. On the cathode side, although electromigration favors the collection of cations near the cathode, the cathodic electric double layer dominated by cations also contain small amount of counterions ($Tc(VII)O_4^-$, OH^- in this case). When cathode potential favors Tc(VII) reduction, Tc(VII) can accept electrons and be removed from the cathode. As Tc(VII) continues to be removed, electric charge in the electric double layer became unbalanced, so does Tc(VII) concentration gradient. Therefore, more Tc(VII) enters the cathodic electric double layer to the re-balance the equilibrium, and gets further reduced by the cathode.

Since remaining Tc concentration in bulk solution was low and no precipitate was observed, it is hypothesized that un-recovered Tc residual remained on cathode. 33.5%-56.5% recovery of total Tc demonstrates that some reduced Tc was not easily re-mobilized by these recovery methods.

Table 2. Mass balance (%) on recovery of ^{99}Tc from solutions after 48 hours of removal. Total amount of ^{99}Tc introduced was 6 nCi (defined as 100%). Electrodes were ultrasonically cleaned in 50mM Na_2CO_3 solution for 5 times, with 20 minutes each. Data are average of duplicate samples.

Potential V	Anode (%)	Cathode (%)	Total on electrodes (%)	Total in solution (%)	Sum (%)
2.0	0.68	47.83	48.50	8.00	56.50
3.0	5.33	25.17	30.33	3.17	33.50
4.0	0.30	39.00	39.33	0.43	39.83
5.0	0.57	38.50	39.17	1.13	40.17

Influence of Unbuffered pH on Tc Removal and Recovery

Reduction of Tc(VII) to insoluble Tc(IV) involves both electrons and protons {Rard, 1999}, as shown below:

$$TcO_4^- + 4H^+ + 3e \rightleftarrows 0.4H_2O_{(l)} + TcO_2 \cdot 1.6H_2O_{(s)} \qquad \text{Equation 4}$$

Therefore, pH is also expected to influence Tc removal with poised electrodes, and a group of experiments were conducted to investigate the impact from pH. To ensure the conductivity of solution at neutral pH, 0.1 M $NaNO_3$ was added to all studied pH conditions as supporting electrolyte. No buffer reagent was amended. As shown in **Figure 15a**, unbuffered pH had no significant impact on pertechnetate removal at 2.5 V. 38.6%-68.6% of total Tc was removed within the first 1 hour of reaction. Majority of the removal was completed within the first 5 hours. During the removal process, pH of the solutions all shifted towards neutral (**Figure 15b**), especially for alkaline solutions, which indicates that water hydrolysis or some other side reactions probably occurred under these conditions. Since Tc was poorly recovered by simple extraction from electrodes, recovery process of this experiment was initiated by reversing the polarity of the electrodes, so that reduced Tc may be re-oxidized on the former cathode. After 24 hours of removal, polarity of anode and cathode was immediately reversed and maintained for 1 hour for solutions with pH 2-9. Percentage of recovered Tc within 1 hour ranged between 52.4% and 85.9%, but had little correlation with pH. Comparing Tc recovery with Tc removal within

the first 1 hour of reaction, it was found that recovery process was slightly faster than removal within studied pH range.

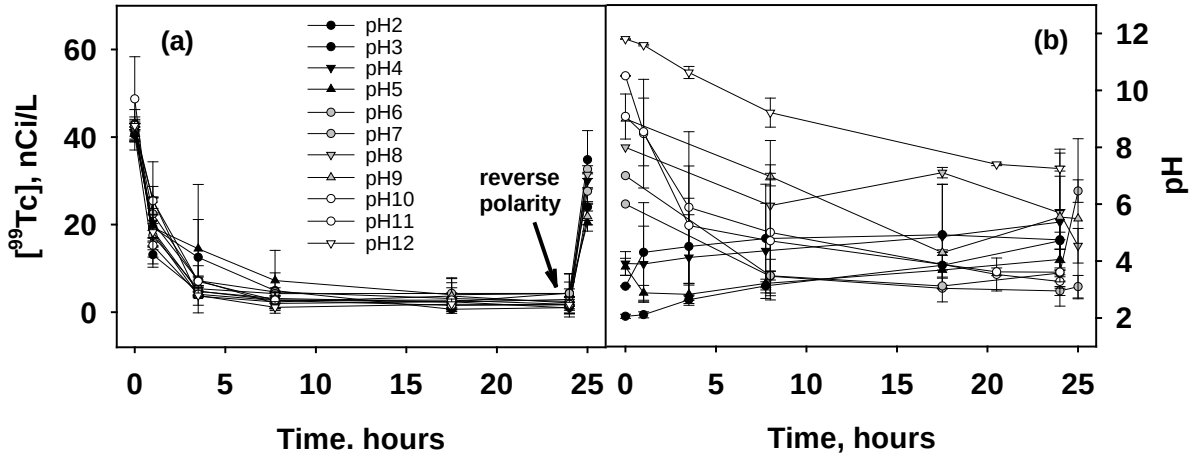

Figure 15 (a) Removal of Tc(VII) from unbuffered 40 nCi/L Tc(VII) solution at 2.5 V at different pHs. 0.1 M $NaNO_3$ was added to the solutions as supporting electrolyte. Recovery of Tc was performed by reversing potential at hour 24 for 1 hour. (b) pH change in unbuffered solutions during Tc(VII) removal.

Table 3 Mass balance (%) on recovery of ^{99}Tc from solutions after 24 hours of reaction and 1 hour of polarity reverse (pH 6-9). Total amount of ^{99}Tc introduced was 6 nCi. Electrodes were ultrasonically cleaned in 50mM Na_2CO_3 solution for 5 times, with 20 minutes each. Data are average of duplicate samples.

pH	Anode	Cathode	Total on electrodes	Total in solution	Sum	Note
6	23.67	7.00	30.67	77.83	108.50	With 1 hr polarity reverse
7	21.50	6.67	28.33	65.83	94.00	
8	32.50	8.33	41.33	74.83	115.67	
9	41.17	9.17	50.50	52.17	102.50	
10	4.17	86.67	90.83	4.00	94.83	Without polarity reverse
11	2.33	76.83	79.17	4.33	83.50	
12	1.60	76.17	77.83	4.00	81.83	

After the polarity was reversed for 1 hour, electrodes were cleaned with 50 mM Na_2CO_3 solution. Mass balance of Tc recovery for pH 6-9 solutions was listed in **Table 3**. Reversing the polarity changes the anode potential to a cathodic potential. Therefore it is not surprising that most of the recovered Tc came from the former anode. About 94% to 116% of Tc was recovered, which is significantly higher than the recovery observed when only poise removal and no reverse polarity was used for Tc recovery (shown in **Table 2**). Therefore, reverse polarity for a short period of time may be a useful pretreatment step for regenerating the electrodes and recovering Tc from the groundwater. Electrodes from pH 10-12 solutions were directly rinsed with 50 mM Na_2CO_3 solution after 24 hours of reaction. **Table 3** shows that recovery of Tc from these electrodes pH 10-12 was not as high as process with polarity reversed. However, 81.8%-94.8%

recovery at 2.5 V and pH 10-12 was still much higher than the recovery at pH 3 and 2.5 V. pH may to be an important factor during the recovery. Since the system was not buffered, the influence of pH may be interfered by side reactions. Therefore, another group of tests were conducted to examine the influence of pH in buffered systems.

Influence of Buffered pH on Tc Removal and Recovery

Pertechnetate was removed faster under buffered basic conditions (**Figure 16**), demonstrating that, as with U(VI), pertechnetate removal rate is also influenced by pH. A possible reason for the discrepancy between **Figure 15a and 16** is that, in an unbuffered system, pH in close proximity of electrode may be different from in bulk solution due to the occurrence of side reactions such as hydrogen evolution. Comparing pH 2-12 solutions at a specific time during the removal, the difference in their pHs near the electrodes may be not as significant as that in the bulk solutions. From this perspective, the removal of pertechnetate proceeded at similar rate in the unbuffered systems. However, in buffered systems change of pH was controlled in a narrow range. Therefore, dissociation of buffer reagent can maintain a high proton concentration at acidic condition, and provide strong competition with pertechnetate for reactive sites on the electrode and electrons when at a sufficient potential for electrolysis. Under basic conditions, consumption of H^+ was controlled by buffer and hydrogen production was expected to slow down and electrode surface should be more accessible to pertechnetate, resulting in relative faster removal at higher pH.

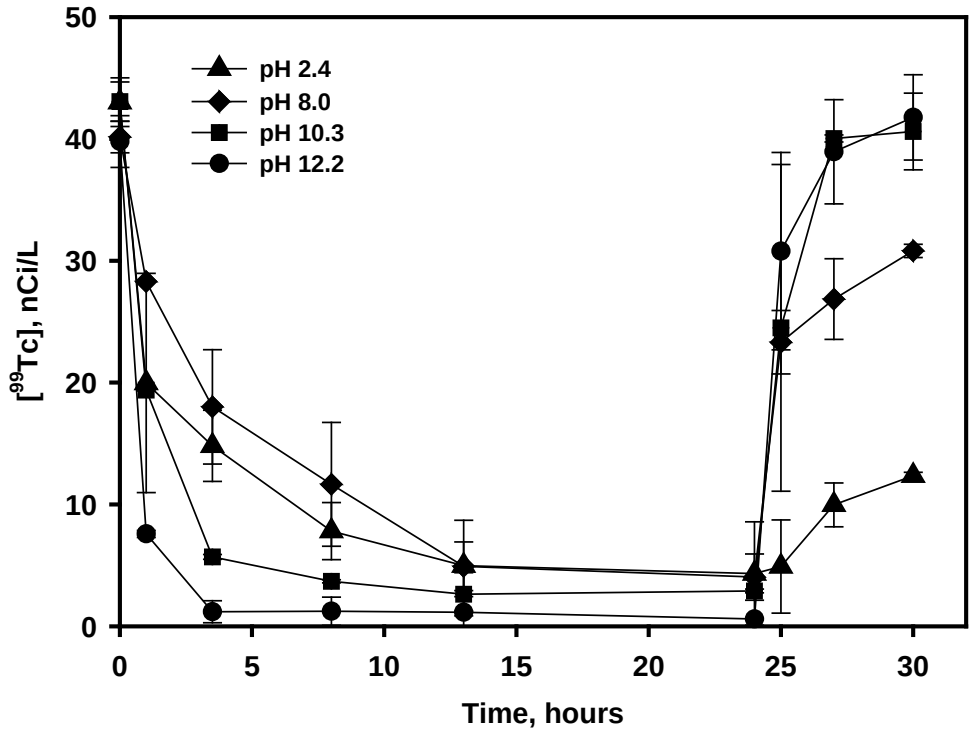

Figure 16. Removal of Tc(VII) from buffered 40 nCi/L Tc(VII) solution at 2.5 V at selected pHs. Power was removed after 24 hours.

The recovery of Tc from buffered systems began directly following removal of the external

potential. Tc concentration in the bulk solutions was monitored for 5 additional hours. It was found that almost all Tc was recovered at pH 10.3 and 12.2 after 5 hours, whereas only 79.5% and 30.2% was achieved at pH 8.0 and 2.4, respectively. This may be related to complexation of reduced Tc with buffer ligands (carbonate or phosphate) at higher pH {Rard, 1999; Alliot, 2009}.

Tc Removal with Repeated Addition

A semi-continuous removal of pertechnetate was conducted at pH 3 and 2.5 V. The result was plotted in **Figure 17**. Two additional pertechnetate spikes were added from stock solution to the reactor after technetium concentration in bulk solution stabilized at a low concentration. Technetium was quickly removed from the solution at all three spikes. No significant decrease in either removal rate or extent was observed. This finding further supports the conclusion that Tc was reduced rather than merely electrosorbed. In an electro-reduction process, ideally the electrode is expected to have infinite capacity, as long as sufficient potential is provided, conductivity of the electrode does not decrease, and electrode is not covered by non-conductive precipitates. In an electrosorption process, the electrode has a limited capacity; as more ions are sorbed, the electrode could accommodate less ions, resulting in declining removal rate and extent after each additional spike. This hypothesis for electrosorption is discussed more in Task 4, below.

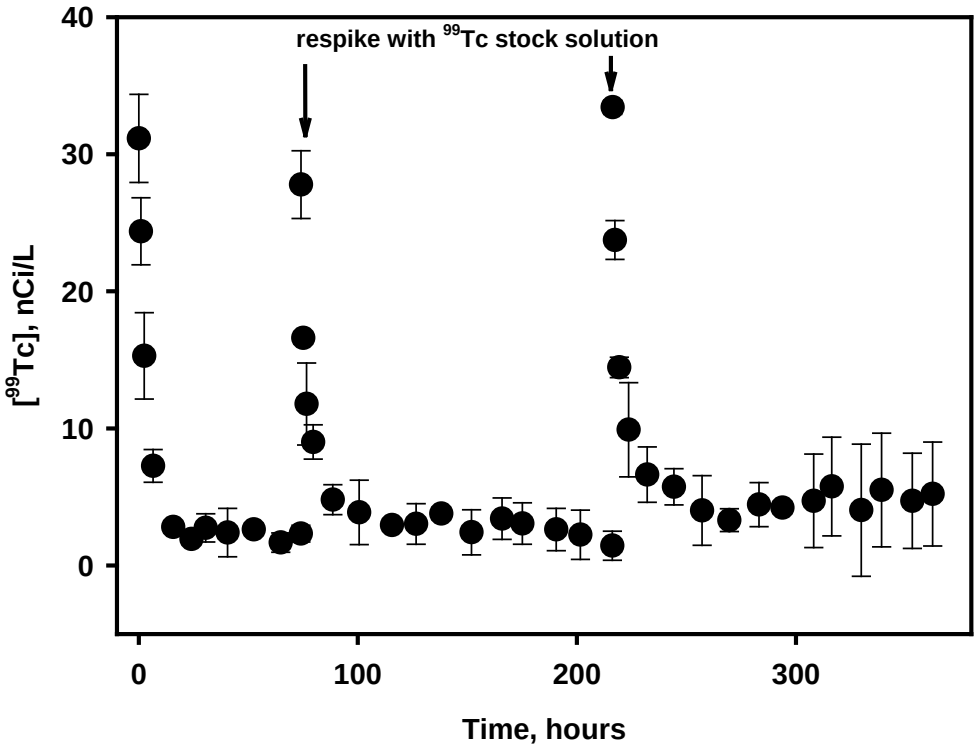

Figure 17. Semi-continuous removal of Tc(VII) at pH 3 and 2.5 V. The data markers represent the average and range of duplicate experiments.

Influence of Ionic Strength on Tc Removal

As discussed in above in Task 1, ionic strength is an important term determining ionic activity, solution conductance, and electrode capacity. However, ionic strength is found to have little

impact on U(VI) removal rate. Tc removal in solutions with different ionic strength was also studied. It was found that same as U(VI) removal, Tc removal rate is not influenced by a change in electrode capacity, or, not affected by ionic strength within 10^{-3} to 10^{-1} M range (**Figure 18**). Since Tc removal in this study is considered an electroreduction process, which has little relationship with electrode capacity, this result indicates that Tc removal is more vulnerable to influential factors that directly interact with electrode or affect electron transfer or distribution. Ionic strength, in this case, is not a factor of concern.

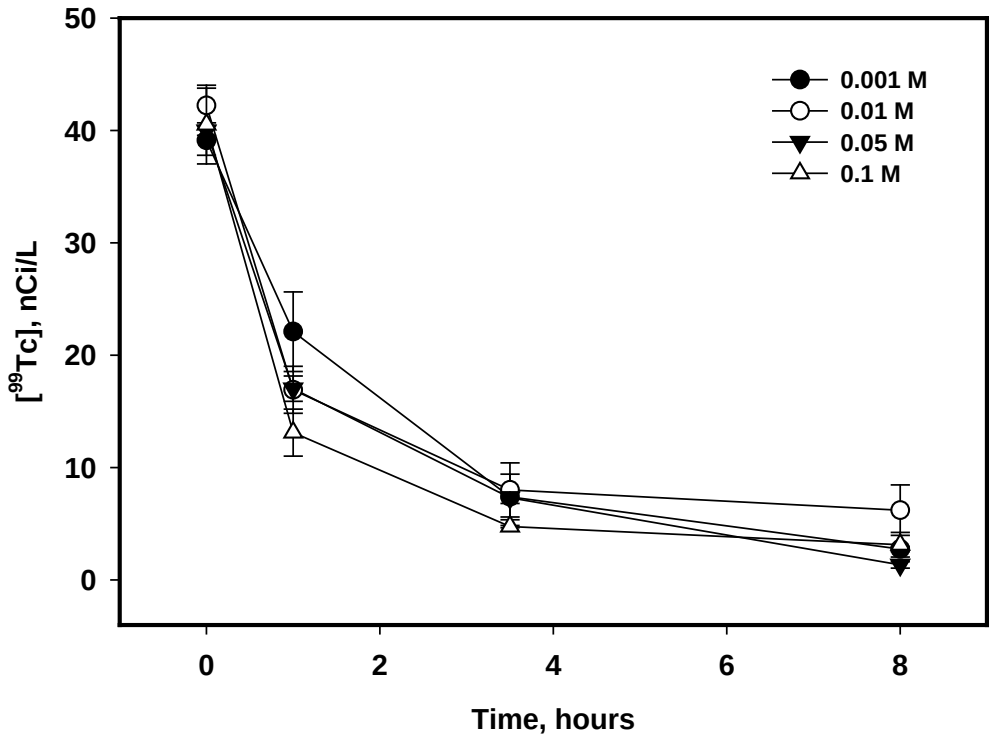

Figure 18. Removal of Tc with different ionic strength at pH 3 with 150 μM U(VI) solution. Ionic strength of the solutions was adjusted by adding desired concentration of $NaNO_3$; external potential applied was 2.5 V. Error bar represents standard deviation from duplicate experiments.

Influence of Humic Acid on Tc Removal

Another factor that may influence pertechnetate removal is the presence of humic acid. Previous studies on interaction between technetium and humic substances mostly support for a limited binding for both Tc(VII) and Tc(IV) {Icenhower, 2008}. Even with soil containing organic matter as high as 12%, obvious change in solubility of Tc(IV) was not observed {Maset, 2006}. However, a recent study revealed that humic substances could increase mobility of Tc(IV) in groundwater by forming strong complex at acidic pH {Boggs, 2011}. Humic acid was added in concentrations between 5 and 25 mg/L, which are considered environmentally relevant concentrations, to study whether humic acid can affect pertechnetate removal with electrode-based method. Humic acid had no impact on Tc removal at pH 3 and 0.1 M ionic strength (**Figure 19**). Similar to the influence of humic acid on U removal (**Figure 11**), this result also indicates that humic acid is probably not a factor of concern for pertechnetate removal with

electrodes within out studied concentration.

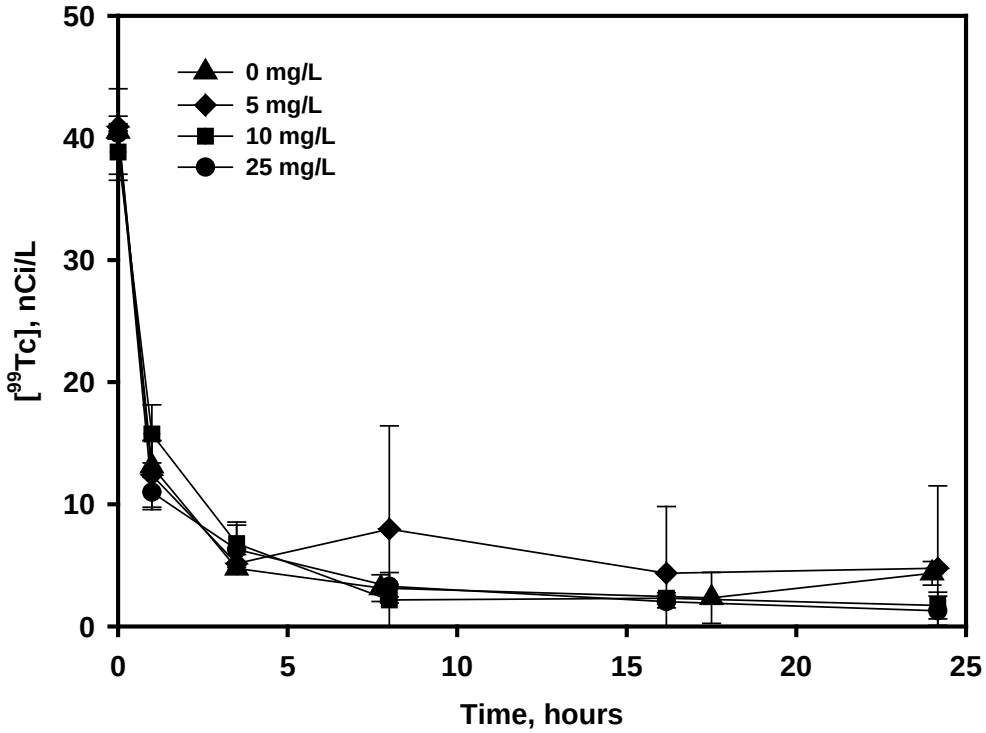

Figure 19. Removal of Tc(VII) from 40 nCi/L Tc(VII) solution at 2.5 V and pH 3 with different concentration of humic acid. 0.1 M $NaNO_3$ was added as supporting electrolyte. Power was removed after 24 hours. The data markers represent the average and range of duplicate experiments.

Task 2: Summary and Discussion

Technetium was effectively removed from buffer solutions using poised graphite electrodes. Removal of pertechnetate could occur at potential as low as 1.5 V. Observed removal rate increased with higher externally applied potential. The highest k_{obs} was around 0.3 hr^{-1}, but this rate is about two times lower than removal from anodically polarized magnetite {Farrell, 1999}. Farrell and coworkers postulated that Tc was removed by anodic sorption and reduction on magnetite anodes {Farrell, 1999}. However, since they also used carbon as a cathode and applied similar potentials across their electrode system, we think it may also be possible that Tc in their system was reduced on the cathode. No improvement in observed removal rate constant was observed as potential continued to increase beyond 2.5 V, probably due to the occurrence of side reactions. Removal of technetium was greatly affected by pH in a buffered system. Basic condition seemed to be more favorable for both technetium removal and recovery. Humic acid is considered to be a factor that may re-mobilize technetium in subsurface; however, it did not have evident impact on technetium removal within our studied range. Recovery of removed technetium can be achieved simply by removing the poise on electrodes. But technetium was found to return to bulk solution faster at more alkaline pH. Reversing polarity of electrodes followed by carbonate rinsing was an effective and efficient way to remove any technetium attached to the electrode surface and regenerate the electrodes.

Although Tc(IV) is the most important technetium species at reducing condition, this study does not exclude the possibility of pertechnetate reduction to more reduced form, such as Tc(III). It does not affect the key findings of this study that technetium removal and recovery could be quickly achieved using graphite electrodes, and that electrodes could be easily regenerated and reused. Electro-based removal and recovery of technetium with cost-effective graphite electrodes can be possibly applied to contamination situations requiring quick response and permanent elimination.

Task 3: Area 3 Site Water Remediation

The objective of this research is to determine whether electrode-based remedial approach is a feasible option for removal of U and Tc from Area 3 groundwater. Although we may eventually decide to publish findings from Task 3, there is no draft of a manuscript as of yet.

Potentiostat-poised Batch Reactors With CEM

This study was conducted to evaluate whether removal and recovery of U and Tc could be achieved with Area 3 groundwater. A cation exchange membrane (CEM) was placed between working and counter chambers to study the removal from both chambers separately. A controlled system was utilized to eliminate possible interference and provide constant potential (-0.6 V versus Ag/AgCl) on working electrode using a potentiostat. Anaerobic gas mixture of 80 N_2 : 20 CO_2 was bubbled into the reactors.

Figure 20 shows that the Nafion® membrane completely prevented U(VI) from being removed from counter chamber (anodic). Fitting U removal within 1 day of reaction yielded a k_{obs} of 0.1 hr^{-1}. 97% of U removal was achieved 4 days after the experiment started. U gradually returned to the bulk solution within 7 days after poise was removed, the highest recovery achieved was 89.0%. The reactor also demonstrated similar U(VI) removal ability upon re-poise after the recovery. However, only 67% recovery of U(VI) was achieved at the second recovery. No additional U(VI) returned to bulk solution after reactor became aerobic, suggesting uranium residuals were likely strongly associated with electrode.

Concentration of Tc was monitored for a shorter period of time than U. **Figure 21** also shows that no Tc removal was observed from counter chamber (anodic), which is consistent with the finding in Task 3 (above) that Tc was preferentially removed by cathode instead of anode. Fitting Tc removal within 1 day of reaction yielded a k_{obs} of 0.048 hr^{-1}. Over 85% of Tc was removed within 3 days, and did not return to bulk solution as long as the electrodes were still poised. After poise was removed, almost all removed Tc was recovered within 3 days. It is hypothesized that recovery of Tc in this experiment was more likely associated with dissolution, since CO_2 was bubbled into the reactors in excessive concentration while no oxidant was amended into the system.

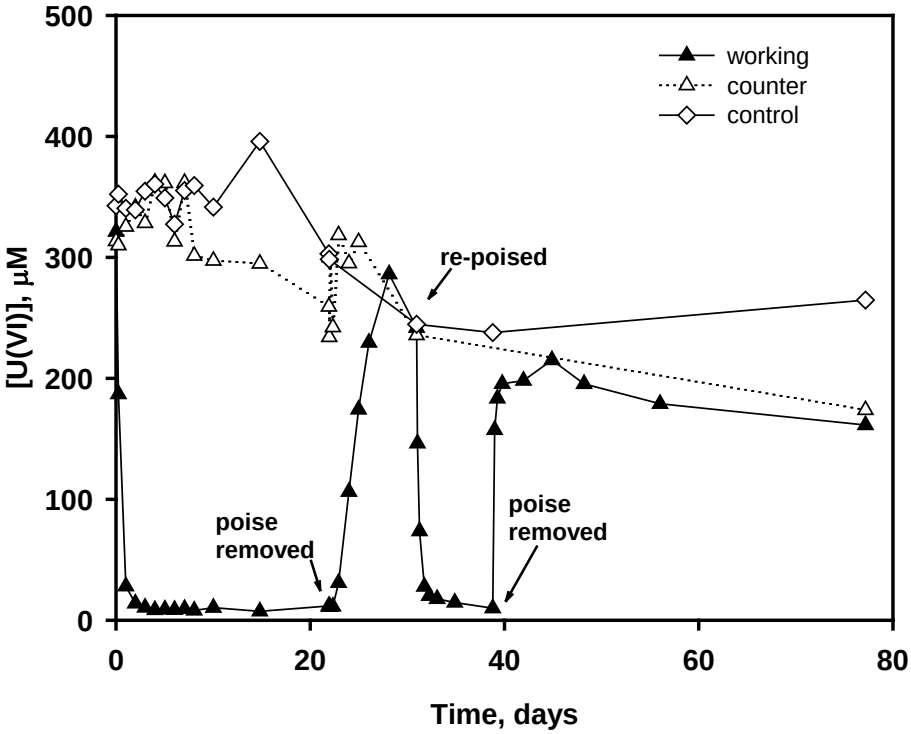

Figure 20. Change of U(VI) concentration in reactors over 78 days. This experiment was operated with continuous bubbling with anaerobic gas mixture 80:20 N_2:CO_2. Poise was removed on day 22 and added back on day 31. On day 39 the poise was removed again. Anaerobic gas mixture stopped on days 56, and reactor turned aerobic by exposing headspace to atmosphere.

It was found that anion concentrations, especially nitrate and sulfate dropped slightly during the process (**Figure 22**), but the change was far less significant than U and Tc removal. Since nitrate and sulfate concentration also drop slightly in control reactor, it is possible that they are removed biotically. **Figure 20-22** suggest that U and Tc can be removed in Area 3 site water under anaerobic condition, no pretreatment with pH or nitrate was necessary. Majority of the contaminants was removed within 3 days from the cathodic chamber. After the poise was removed, both U and Tc returned quickly.

Due to the existence of CEM, working electrode was only responsible for U and Tc removal in the 200 mL chamber. Another experiment was conducted to study U and Tc removal without CEM in the potentiostat poised system. Additional spike of U was also amended after a certain period of operation to evaluate the stability and performance of the reactors in a longer term, as will be discussed in detail below.

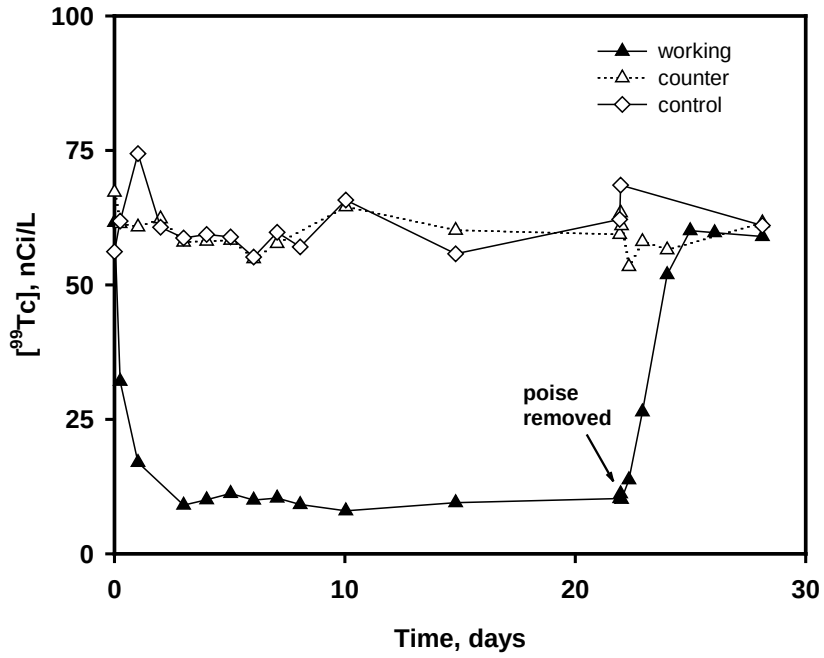

Figure 21. Change of ^{99}Tc concentration in reactors over 28 days. This experiment was operated with continuous bubbling with anaerobic gas mixture 80:20 N_2:CO_2. Poise was removed on day 22.

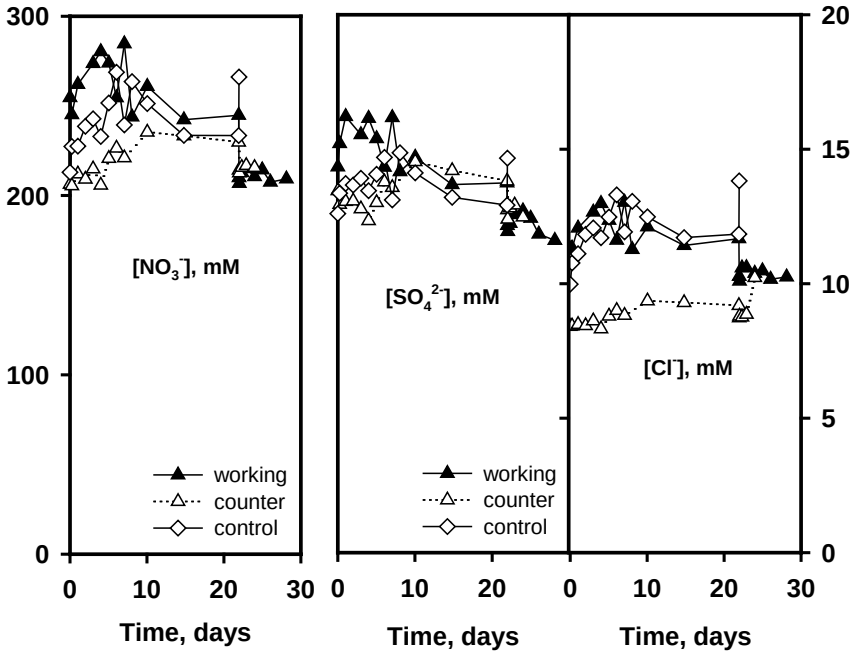

Figure 22. Change of anion concentrations in reactors over 28 days. This experiment was operated with continuous bubbling with anaerobic gas mixture 80:20 N_2:CO_2. Poise was removed on day 22.

Potentiostat-poised Batch Reactors Without CEM

Comparing U and Tc removal in Task 3 (anaerobic conditions) with that in Task 1 and Task 3 (aerobic conditions), it is hypothesized that oxygen concentration did not seem to be an influential factor in electrode-based U and Tc removal, therefore, anaerobic gas was not bubbled into the reactors in this experiment. Working electrode was poised at -0.5 V versus Ag/AgCl.

It was found that U was removed slower in the system without CEM (**Figure 23a**), the initial U removal rate dropped to 0.020 hr^{-1} compared with the reaction with CEM. It is also lower than U removal k_{obs} in synthetic solution at 2.5 V (0.06 hr^{-1}, **Figure 5**). Concentration was stabilized after 10 days of operation. Based on our previous assumptions, for the initial spike which contains groundwater from Area 3, Y-axis in **Figure 23b**, total radioactivity subtracting the radioactivity of ^{238}U, is assumed to be ^{99}Tc concentration. Tc was removed about the same rate as in the system without CEM; initial k_{obs} was 0.056 hr^{-1}. But this rate is significantly lower than that in synthetic solutions at 2.5 V (0.28 hr^{-1}, **Figure 15**). Over 81% of total Tc was removed when stabilization was reached after 3 days of reaction. Uranyl acetate stock solution was added into the two experimental reactors on day 29. Sample radioactivity excluding ^{238}U also hiked as U concentration, suggesting our commercially purchased uranyl acetate reagent may also contain some other radionuclides, probably other isotopes of U. Both U and radioactivity were removed slower during the respike. Since -0.5 vs. Ag/AgCl is not thermodynamically favorable for reduction of U(VI) to U(IV) {Xu, 2000}, U removal is probably still an electrosorption process (as has been discussed in Task 1). Therefore, a gradual slowdown of U removal rate is expected for semi-continuous removal via additional spikes, since the electrode capacity decreases as more U is removed. Electrode sorption capacity will be further discussed in Task 4. In a system containing both U and Tc, and they are both removed from cathode, availability of the electrode is expected to decrease as more U and Tc were transferred from solution to the electrode surface. Decline in removal rates for both U and radioactivity at the second spike was probably caused by lower availability, therefore lower reactivity, of the cathode.

Poise of electrodes was removed at day 160. Both U and radioactivity returned to the solution immediately, although not to a full extent, which was consistent to what have been observed and discussed in Tasks 1 and 2. pH in experimental reactors dropped immediately after the poise, but not in the control reactor (**Figure 23c**). Although there is no CEM between the working and counter chambers, since the samples were taken from sampling port on cathode side, this sharp decline in pH may be related to movement of protons towards cathode after poise. pH of all three reactors increased gradually over the term of removal, suggesting the consumption of protons may not only attributed to electrochemical reactions. However, pH barely went beyond 4.0 after 250 days of reaction, which again indicates that the groundwater has a large buffer capacity.

H_2 and O_2 level was measured in the headspace to monitor potential side reactions occurred in the reactor, and examine possible influence on U and Tc removal. **Figure 24a** shows that the amount of H_2 in the two experimental reactors was not identical; suggesting hydrogen evolution rate in the two reactors was different. But this difference did not cause a significant difference in U and Tc removal rate in the two reactors. It was observed in reactor 1 that the amount of H_2 increased sharply immediately after the reaction began as well as after the respike. It is worth noting that in reactor 1, H_2 level in counter chamber headspace was higher than that in working

chamber. Since there is no membrane between working and counter chambers, hydrogen generated from the working chamber should be able to diffuse to the counter chamber through the bulk solution. Therefore, concentration in both headspaces was supposed to be the same. The lower mass of H_2 in cathodic headspace indicates consumption of hydrogen in cathodic chamber, possibly related to U and Tc removal.

The amount of O_2 dropped quickly after poise (**Figure 23b**). O_2 level was remained low in both working and counter chambers of the two reactors; suggesting O_2 generation may not occur during the removal. It only bounced back after the reactors were exposed to the atmosphere along with poise removal. The concentration of CO_2 in the headspace was much higher than that in the atmosphere. High CO_2 level in the reactor was probably attributed to dissolution of carbonate minerals in the soil to the acidic groundwater upon the mixing, which may also be partially responsible for the slight increase in pH during the operation (**Figure 23c**).

Flow-Through Reactors

The previous two sections discussed U and Tc removal in batch reactors. This experiments investigates the performance of flow-through reactors. A peristaltic pump was used to help circulate groundwater between the two chambers. The batch reactors employed a potentiostat system with which potential on working electrode can remain stable despite of any change in the counter chamber. In practical application, a potentiostat needs to be replaced by a power supply to reduce the cost and facilitate the operation. Therefore, the potentiostat was replaced by power supply in this test. Before the operation, potential distribution on cathode and anode was investigated with Area 3 groundwater for better understanding of potential on both electrode and to help determine the applied potential for reaction. As illustrated in **Figure 25**, ohmic loss was significantly reduced compared with the synthetic pH 3 U or Tc solutions (**Figure 6** and **Figure 13**) due to higher ionic strength in the groundwater (about 0.24 M). Cathode potential was also higher than in the synthetic solutions. Since cathode potential remained relatively stable at 2.0 V - 3.0 V overall potential, 2.5 V was selected to be the operational potential in this test.

It was found that U and Tc concentration both decreased rapidly when electrodes were poised at 2.5 V (**Figure 26**). Both U and Tc removal was found to be slightly faster than what has been observed in the potentiostat system with CEM; initial U removal rate was 0.025 hr^{-1} and k_{obs} for Tc was 0.074 hr^{-1}. Potential of anode, cathode and control electrode versus Ag/AgCl was closely monitored. Cathode potential was stabilized between -0.55 V to -0.60 V versus Ag/AgCl during the reaction, which indicates that a power supply system can also provide stable poise to the electrode in operation with real site conditions. Current in the reactor dropped rapidly within the first day after electrodes were poised, then gradually declined, probably due to a fast consumption of electrons at the beginning of the process.

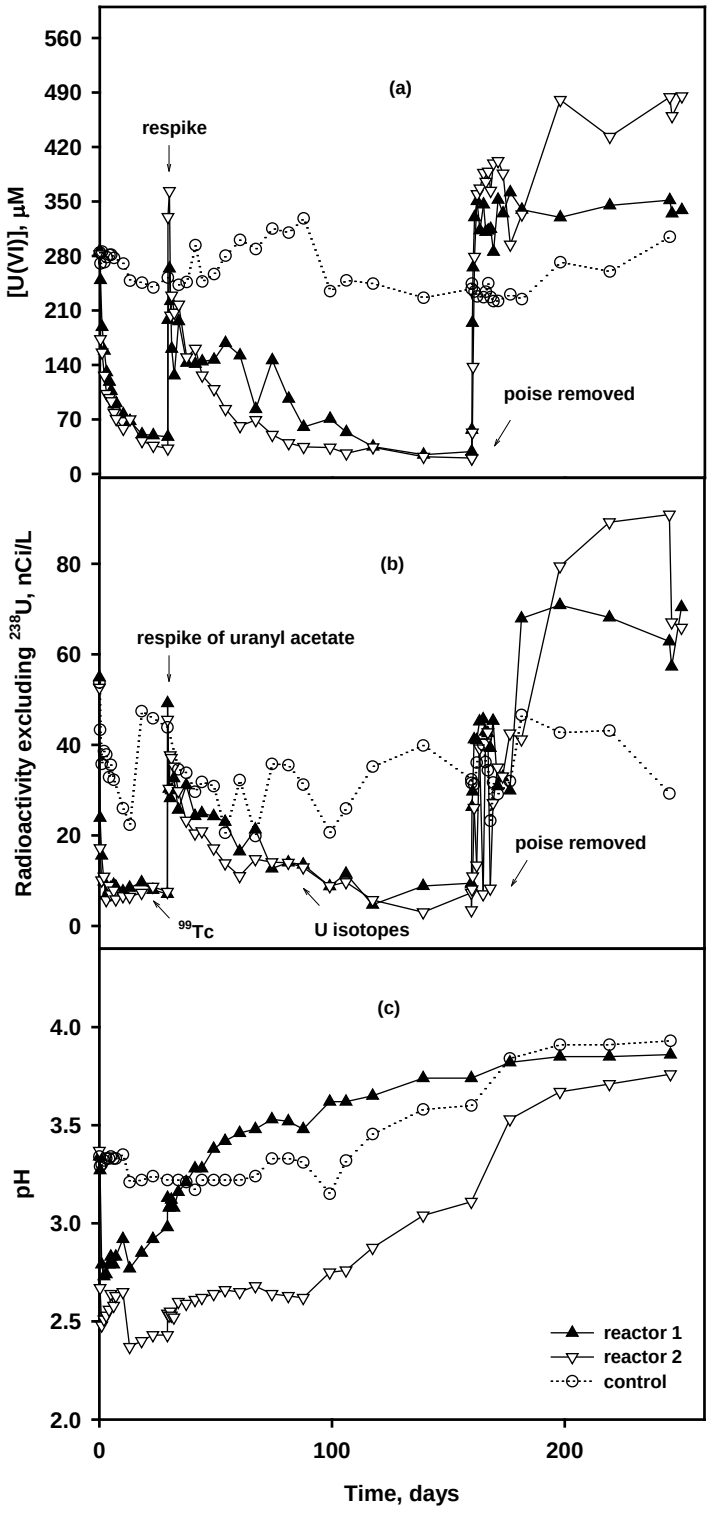

Figure 23. Change of (a) [U(VI)] (b) [^{99}Tc] and (c) pH in reactors over 250 days. Additional U(VI) was spiked into the experimental reactors on day 29. Poise was removed on day 160. Reactor 1 and 2 are two identical replicates.

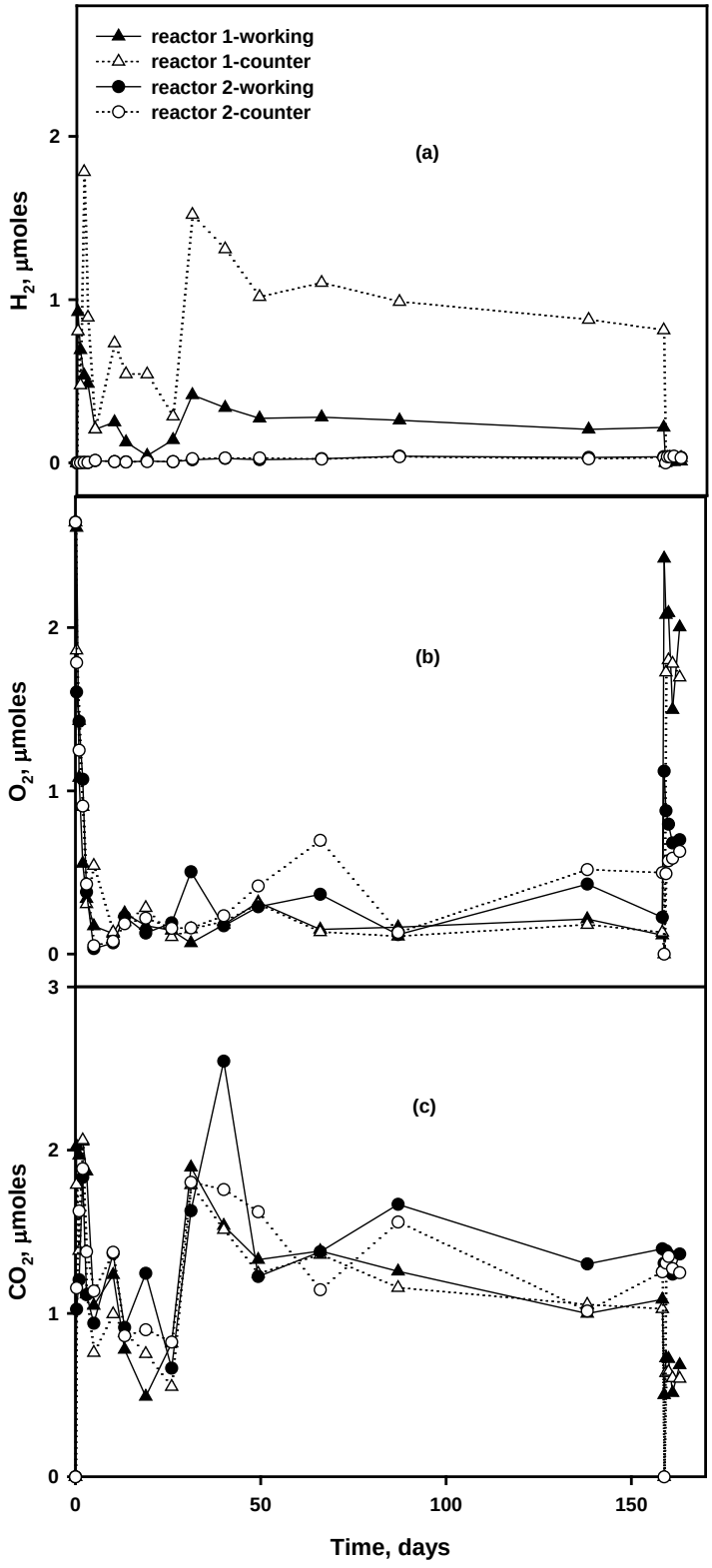

Figure 24. Amount of (a) H_2 (b) O_2 and (c) CO_2 in the headspace over 160 days. Additional U(VI) was spiked into the experimental reactors on day 29. Poise was removed on day 160.

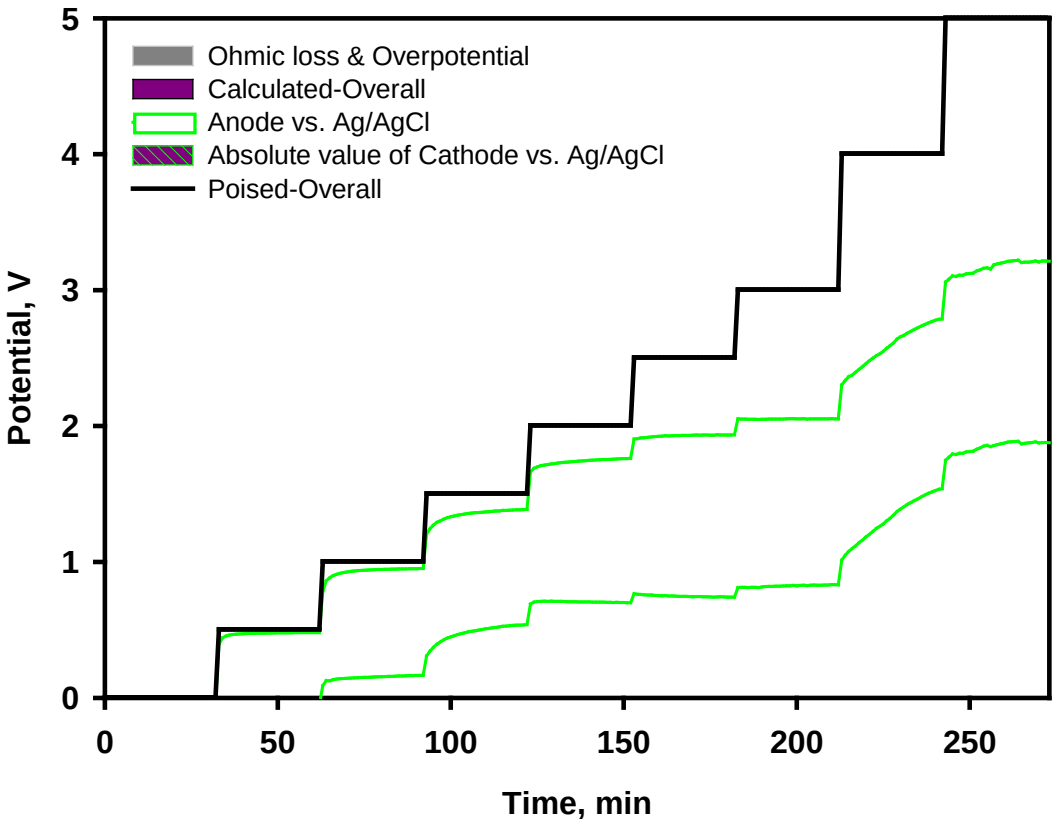

Figure 25. Potential distribution versus external potential change in Area 3 groundwater. The horizontal black line defines external potential applied. Gray area illustrates potential lost in ohmic resistance and overpotentials. Area between the green lines represents anode potential against Ag/AgCl, green line shaded area represents the absolute value of cathode potential against Ag/AgCl. Area in purple (including the hatched area) shows the real potential between anode and cathode.

Similar to what has been observed in potentiostat system (**Figure 22**), nitrate concentration also decreased slightly, but to a lesser extent. Therefore, the decrease in nitrate concentration is not considered significant given its high initial concentration. Sulfate concentration remained stable throughout 16 days of operation. Although nitrate is a more favorable electron acceptor than U(VI) and sulfate being a potential electron competitor during stimulated *in situ* bioremediation, the presence of nitrate and sulfate did not seem to be a factor of concern for electrode-based U and Tc removal in Area 3 groundwater.

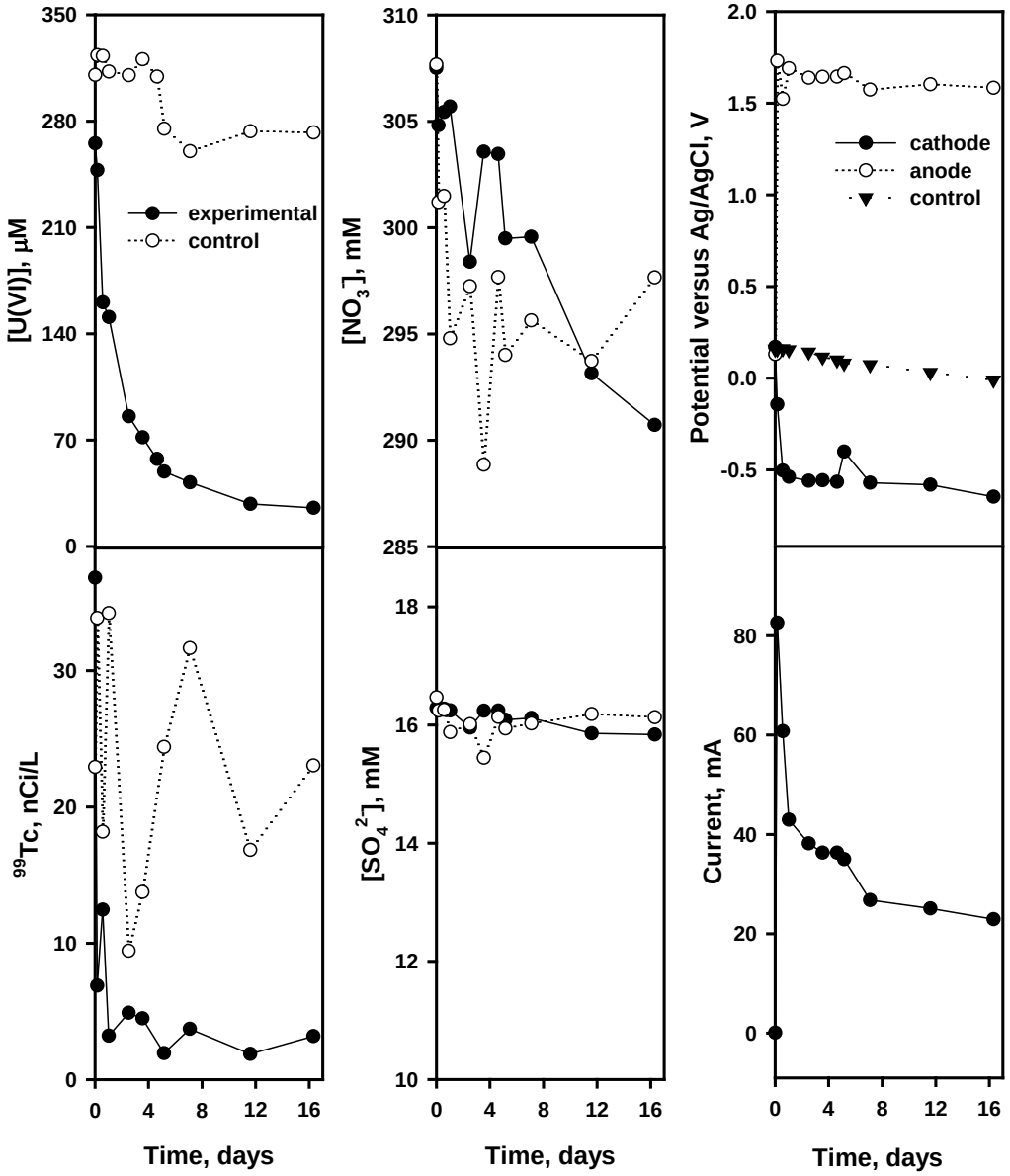

Figure 26. U, ^{99}Tc, NO_3^-, and SO_4^{2-} concentrations, potential of electrodes and current in experimental reactor over 16 days of operation.

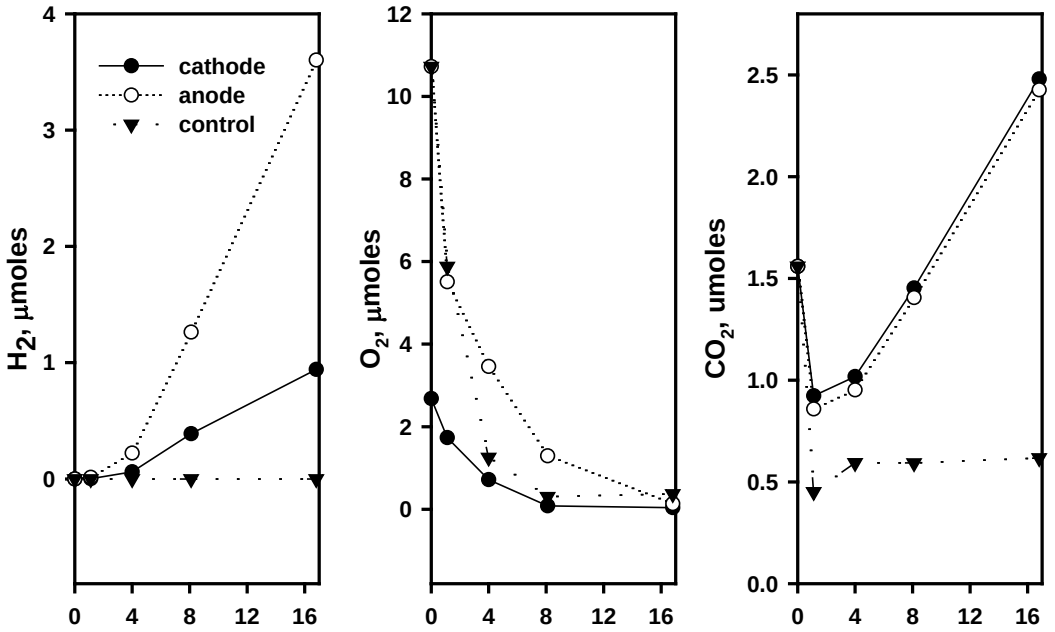

Figure 27. Molar mass of H_2, O_2, and CO_2 in headspace of each reactor over 16 days.

Unlike in the potentiostat system, significant hydrogen evolution was only observed after majority of U and Tc was removed. But H_2 level in counter chamber was higher than in working chamber, which is same as previously discovered in **Figure 24a**. Oxygen was consumed rapidly in all three reactors (**Figure 27**), which is similar to what was observed in potentiostat system (**Figure 24b**). CO_2 level was also high in counter and working chambers. In general, performance of flow-through reactor powered by a power supply is consistent with the performance of batch reactors poised by potentiostats. It suggests electrode-based U and Tc removal in Area 3 groundwater is repeatable and future field-scale implement can be operated with simple power supplies. Nitrate or other potential inhibitors and clogging agents are not necessarily need to be pretreated.

Task 3: Summary and Discussion

This study explored the application of electrode-based technique to real Area 3 site groundwater, with low pH (~3) and high concentration of nitrate (~300 mM). Removal and recovery of U and Tc in a potentiostat-controlled system with CEM clearly suggested the effectiveness of electrode-based technique with complex real site geochemical condition. U and Tc were removed simultaneously from the working (cathodic) chamber. Even under anaerobic condition, U and Tc returned to the bulk solution rapidly after poise removal. In batch reactors without CEM, U removal was observed in both the initial and repeated spike. Although both U and Tc initial removal rates were lower than those in reactor with CEM, probably due to the doubling of solution volume. U and Tc removal was also achieved at 2.5 V applied potential in a simple power supply system, with cathode and anode potentials remained stable throughout.

In all three tests, U and Tc were removed simultaneously within 3-7 days of operation from Area 3 soil and groundwater mixture; although the rates were lower than from synthetic solutions. The existence of nitrate and sulfate did not hinder U and Tc treatment, neither was significant removal of nitrate and sulfate observed. This finding verifies one of the major advantages of

electrode-based remediation over bioremediation – no pretreatment of nitrate is necessary. Other potential inhibitors (such as sulfate) and clogging agents (such as Al) were also not removed prior to the reactions. In contaminated groundwater with acidic pH and high concentration of nitrate, removing U and Tc with poised electrodes may be a better alternative to bioremediation. The results of U and Tc removal with batch and flow-through reactors will provide valuable information for future pilot scale tests, such as power system selection, reactor selection, and operational duration control.

Task 4: Electrode Capacity and Mathematical Model

The objective of this study was to evaluate electrode capacity and develop and verify a mathematical kinetic model for U(VI) removal from aqueous solution. A manuscript has been prepared that is based on findings from task 4. The most recent draft is appended to the report as Manuscript 3.

Graphite Carbon Electrode Capacity for U(VI) Removal at pH 3

Figure 28 illustrates U(VI) removal with time with several additional spikes. The solution initially contained 150 μM U(VI), which was quickly removed after the electrodes were poised at 2.5 V. When less than 5% removal could be observed over 12 hours, more U(VI) was added from a uranyl acetate stock solution to increase U(VI) concentration back to ~150 μM. The re-spike was repeated for 9 times. Not only was U(VI) removed slower each following spike, U(VI) residual concentration was also higher at the end of each following spike. Percentage of U(VI) removed further decline after 6th spike, and only ~10% U(VI) removal can be achieved thereafter. This trend indicates that individual capacity for U(VI) removal at each spike decreased after each addition, and electrode adsorption capacity does exist at a defined condition. This decreased capacity for removal was partially overcome by increasing the applied potential. At the 9th spike, when U(VI) concentration was stabilized, external potential was slightly increased by 0.5 V to 3.0 V. Continuous U(VI) removal was observed. However, no more U(VI) removal was observed at the 10th spike with external potential remained 3.0 V. It is also consistent with electric double layer theory that increase of electrode capacity can be achieved by increasing potential.

The last data point in each spike was re-calculated in order to correlate the amount of U(VI) removed (C_s) with that remained in the bulk solution (C_w). C_w is the molar mass of U(VI) in the solution and was calculated by multiplying concentration with solution volume (500 mL). C_s represents U(VI) molar mass on the electrode surface, and was calculated cumulatively by adding the mass difference between initial and final U(VI) molar mass in the solution after each spike. Here C_w = [L], Cs = [LX] in Langmuir isotherm. C_s was plotted versus C_w in **Figure** 29. Fitting of the all nine spikes at 2.5 V yields a Langmuir equation:

$$\frac{C_w}{C_s} = 0.063 + 0.0036 C_w \qquad \text{Equation 5}$$

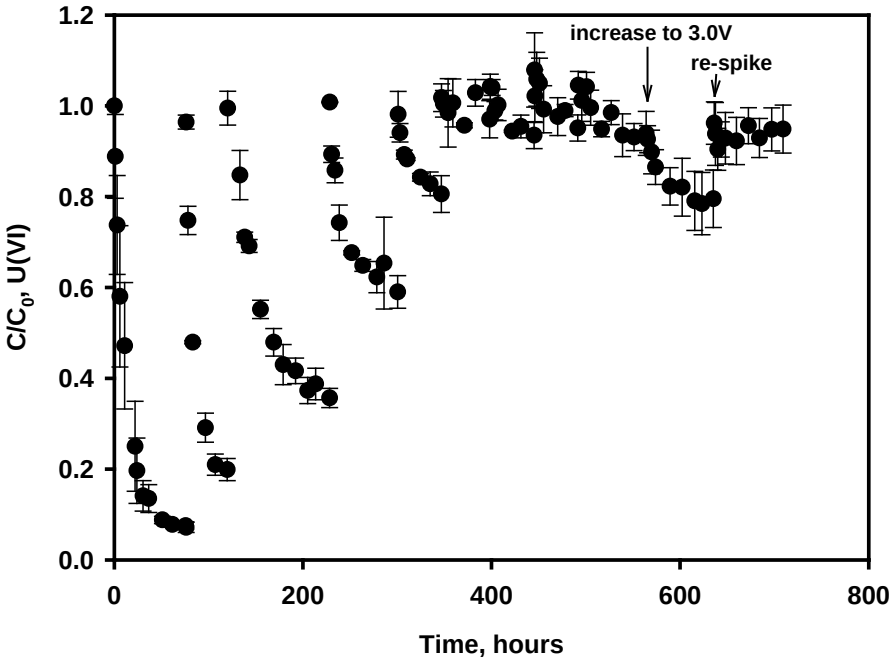

Figure 28. Semi-continuous removal of U(VI) with graphite electrodes at 2.5 V initially. Additional U(VI) stock solution was added to the reactor after U(VI) concentration stabilized. Each increase in normalized concentration to ~1.0 represents a spike of uranium acetate stock solution. Nine additional spikes were added before overall potential was increased to 3.0 V. Final spike was added at 3.0 V after more U(VI) was removed at higher potential. The data markers represent the average and range of triplicate experiments.

According to the constants defined in Eq. 6.7 and Langmuir equation displayed as Eq. 5.4, $1/X_T$ equals to 0.0036, and $1/(kX_T)$ equals to 0.063. Therefore, total electrode capacity X_T = 277.78 μM, and rate constant k = 0.0572. However, some artifact may effect the final two points on the isotherm curve, as the electrosorption was approaching electrode maximal capacity; these data did not fit well into the equation. Considering only the first 7 spikes, the Langmuir equation is:

$$\frac{C_w}{C_s} = 0.0595 + 0.0038C_w \qquad \text{Equation 6}$$

with X_T = 263.16 μM and k = 0.0638. Therefore, capacity of graphite electrodes for U(VI) removal at 2.5 V is 263.16 μmoles of U(VI) under our studied condition. The blue curve is the fitting to Langmuir equation. It suggests that the Langmuir isotherm model is appropriate to explain equilibrated electrosorption of U(VI).

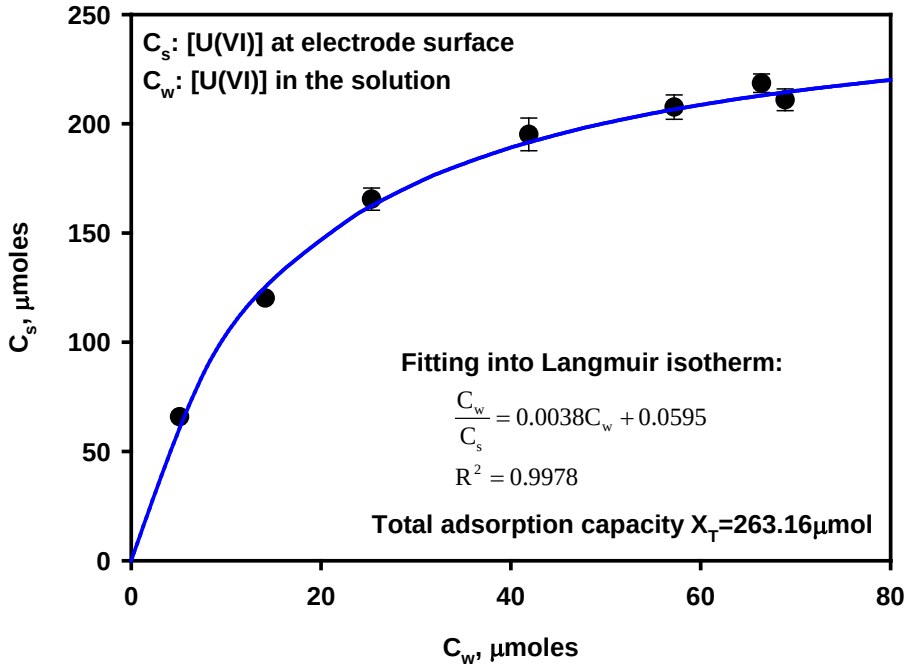

Figure 29. Concentration of U(VI) in the solution against that on the electrode surface. *C_s* is U(VI) concentration on the electrode surface, and was calculated cumulatively from the difference between initial and final concentrations during each spike. *C_w* is U(VI) concentration in the solution and was directly measured. The blue curve is the fitting curve of Langmuir isotherm.

Surface Area of Graphite Calculated from Electrode Capacity

Maximum capacity of the electrode was estimated to be ~263 μmol according to Langmuir isotherm fitting. Using the single layer adsorption assumption of Langmuir isotherm, electrode surface area available for 263 μmol uranyl ions can be estimated as follows. A conceptual depicture of a single UO_2^{2+} adsorbed onto negatively charged cathode is shown in **Figure 30**. The dimensions of the uranyl ion are indicated. Since U is the one positively atom of the charged compound, the figure illustrates the scenario in which the U atom is in direct with electrode surface and face inwards.

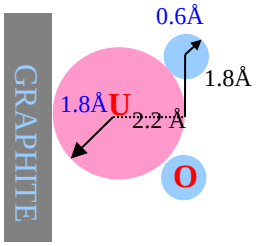

Figure 30. Dimensions of UO_2^{2+} ion and attachment of the ion to graphite. Data were obtained from reference {Burns, 1999}.

Radius of oxygen ion is about 0.6 Å, radius of uranium ion is about 1.8 Å. Considering the largest projected rectangular area on electrode, one uranyl molecule can occupy $[(1.8+0.6)*2]*[1.8*2]=1.7*10^{-17}$ m^2 on electrode surface according to the dimensions indicated in **Figure 30**. 263 μmol of uranyl ions equals to $263*6.02*10^{23} = 1.6*10^{20}$ ions. As suggested by Langmuir isotherm, uranyl ions covered electrode via single layer adsorption. 263 μmol uranyl ions will need a surface area of $1.6*10^{20}*1.7*10^{-17}$ m^2 = 2720 m^2. Average weight of graphite rod electrode used is 63 g. Therefore, specific surface area of the electrode, estimated from the U sorption capacity was **43.2m^2/g**. This is about an order of magnitude higher than the specific surface area of this graphite usually reported (~4 m^2/g) {Kinoshita, 1988}, and 3 times higher the surface area of commercial graphite powders (10 m^2/g) {Kinoshita, 1988}. This result suggests that additional adsorption capacity may have been created inside the electric double layer during electrosorption, resulting in larger electrode capacity than that was defined by gas adsorption measurement.

Mathematical Kinetic Model for U(VI) Removal

Results from Task 1 demonstrated that the roles of pH, external potential, and initial U(VI) concentration are important factors that determine kinetic rate of U(VI) removal. Electrode surface area is another crucial parameter for electrode-based remediation system design. Maslennikov and coworkers, used an S/V ratio to address the importance of electrode surface area; where S is reactive electrode surface area, and V is volume of aqueous solution {Farrell, 1999 #11; Maslennikov, 1998}. At given conditions, metal removal rate constant is considered to be proportional to S/V ratio {Farrell, 1999}. An increase in S/V ratio caused faster Tc(VII) removal by electrodes {Maslennikov, 1998}. S/V ratio is considered to be proportional to first-order Tc removal rate by electrodes {Farrell, 1999}. However, since concentration of ions varies in different groundwater and metal ions directly interact with electrodes during electrode-based removal, the term S/V ratio could not predict a change in removal rate when initial concentration varies. For example, although U(VI) removal was found to fit first-order kinetics best under the conditions tested, it obviously also varied with initial U(VI) concentration (**Figure 7**), suggesting U(VI) removal reaction is not a strict first order reaction. It should be more accurate to consider the amount or molar mass of targeted ions instead of solution volume. Therefore we normalize the surface area to the molar mass of the contaminant to create an S/m ratio, where S is reactive electrode surface area and m is the total molar mass of studied ions at the beginning of the experiments. This will better address the importance of electrode surface area per mole of ions. If we arbitrarily define 1 S/m united as batch reactor with one anode and one cathode and 150 μM U(VI) at 500 mL solution, **Figure 7** can be converted to a k_{obs}-S/m curve, as shown in **Figure 6**. It suggests a great impact from S/m on k_{obs}. A possible reason is that when pH remains constant, electrode surface area per U(VI) ion increases with higher S/m, offering U(VI) higher chance of be absorbed while chance of H^+ being absorbed remains the same.

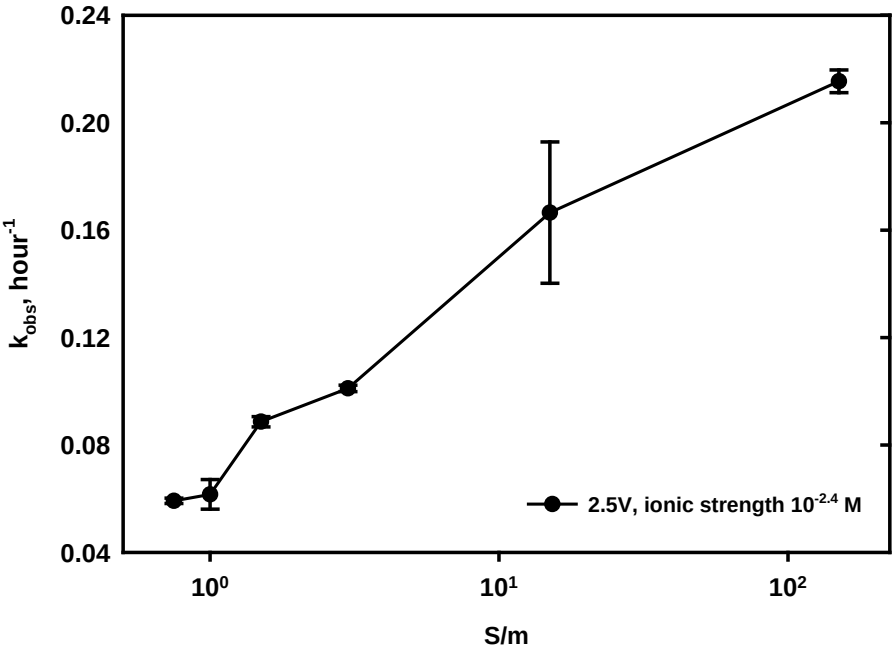

Figure 31. Impact of S/m ratio on initial removal rates (k_{obs}) of U(VI). S/m ratio of a system with two graphite electrodes and 500 mL 150 µM U(VI) solution is arbitrarily defined as 1 S/m. The external potential was 2.5 V and starting concentration of U(VI) was 150 µM at pH 3. The data markers represent the average and range of duplicates.

As has been suggested by **Figure 28**, the overall rate of U(VI) removal diminished as the system was approaching the maximal adsorption capacity. Since both ionic strength and external potential influence electric double layer capacity, differential capacitance of electric double layer per unit area, C_d, is another important determinant of U(VI) removal rate. When ionic strength and potential are constant, differential capacitance of the electric double layer is also constant for defined electrolyte solution.

It should be noted that according to traditional electric double layer theory, the average U(VI) concentration in the diffusion layer is expected to be lower than that in the bulk solution, therefore the amount of U(VI) inside the diffusion layer is not considered significant compared with that trapped inside the electric double layer during the removal. In other words, U(VI) electrosorption is primarily attributed to double layer adsorption. As for the contribution of mass transfer in the diffusion layer, prior research has shown that UO_2^{2+} requires 24 seconds to move across a diffusion layer as thick as 10^{-2} cm according to the following equation {Socolofsky, 2005}:

$$t_d = \frac{L^2}{D} \qquad \text{Equation 7}$$

where t_d is the diffusion time, L is the diffusion distance and D is diffusion coefficient of a

certain ion. The diffusion coefficient of UO_2^{2+} (dominant U(VI) species at pH 3 is 0.426×10^{-5} cm^2/s (**Table 1**). Comparing with the time for U(VI) removal (hours), mass transfer of U(VI) in diffusion layer is not considered a rate limiting step for U(VI) electrosorption, instead, electric double layer processes play the vital role. Although charging of electric double layer is generally a fast process, previous researchers also revealed a slow-charging phenomena with graphite and other types of electrode {Oren, 1985}, which may be related to up to hours of U(VI) removal in this study.

Therefore, the factors that are considered closely related to k_{obs} are pH, double layer potential (included in C_d term), ionic strength (included in C_d), and S/m ratio. It has to be mentioned again that since U(VI) initial concentration is included in S/m term, U(VI) removal reaction is actually not a strict first-order reaction.

Model Development

Assuming that initial U(VI) removal rate obeys first-order kinetics, k_{obs} could be interpreted by a combined effect of S/m, C_d, and $[H^+]$, where C_dS/m represents the theoretical vacancy per ion, $[H^+]$ represents the influence of a competing ion. k_{obs} expression is:

$$k_{obs} = c_1 f(pH) g(C_d \frac{S}{m}) \qquad \text{Equation 8}$$

where c_1 is an unknown constant, $f(pH)$ is the function related to pH, and $g(C_d \frac{S}{m})$ is the function for S/m and C_d. As a reminder, in this study, S/m ratio of a system with two graphite electrodes and 500 mL 150 μM U(VI) solution is arbitrarily defined as 1. Parameters for C_d calculation are listed in Table 4, below:

Table 4. Parameters used for C_d estimation

x_H	0.4 nm	z	2
ε_0	8.85419×10^{-12} F/m	R	8.314
ε	5 for Helmholtz layers 80 for diffuse layer	T	298 K
F	96485 C/mol	φ_H	-

The only parameter that is undetermined for C_d estimation is the potential of diffuse layer, φ_H, or the potential on the outer Helmholtz layer in relative to bulk solution. In our previous experiments, potential on electrode versus Ag/AgCl was measured at different external potentials to address the potential distribution in the solution. However, since the reference electrode can not be placed several nanometers away from the electrode surface, and overpotentials cannot be accurately defined, cathode potential measured is still not as negative as the real φ_H. A group of experiments were done to measure potential distribution as well as current and conductance of solutions at different ionic strength and external potential (data not shown). Ohmic loss was calculated from measured current, conductance and estimated electrode distance to solution cross section area ratio (0.1 cm^{-1}) (**Table 5**). Assuming potential (other than ohmic loss) is distributed evenly between the two identical graphite electrodes; cathode potential on electrode surface (φ_s) can be estimated by dividing this potential value by 2. Then potential at about 0.4 nm from electrode surface can be estimated from $\varphi_H = \varphi_s e^{-x/\lambda}$, where x is the distance from electrode surface and λ is Debye length {Bard, 2001}. φ_H and C_d can then be estimated, and the results for

two selected applied potential, 2.0 V and 2.5 V, were listed in **Table 5**. It shows that the Debye length is large with more diluted solution (lower ionic strength) and solution conductance increases with ionic strength. The results suggest that at ionic strength ranging from 10^{-3} M to 0.24 M, capacity of electric double layer does not change dramatically at 2.0 V and 2.5 V; only with a slight increase from 9.1 to 11.1μF/cm^2. Therefore, within our studied range, S/m is expected to be more influential on k_{obs} since C_d remained stable at a wide range of ionic strength. The next step is to develop k_{obs} equations related to pH and S/m.

Table 5. φ_H and C_d estimation at various ionic strength conditions with 2.0 V and 2.5 V externally applied potential. Measured cathode potential is converted versus SHE (Ag/AgCl is 200mV versus SHE)

	Ionic strength	10^{-3} M	$10^{-2.5}$ M	$10^{-1.6}$ M	0.24 M
	Conductance (mS/cm)	0.47	0.6	2	12
	$x_H/\varepsilon\varepsilon_0$	9.04	9.04	9.04	9.04
	λ (nm)	9.71	5.46	1.94	0.63
2.0 V	Measured cathode potential (V)	0.08	-0.01	-0.2	-0.5
	Current (A)	0.007	0.01	0.013	0.046
	Ohmic loss (V)	1.489	1.667	0.650	0.383
	φ_s (V)	-0.255	-0.167	-0.675	-0.808
	φ_H (V)	**-0.245**	**-0.155**	**-0.549**	**-0.427**
	C_d (μF/cm^2)	**9.1**	**9.1***	**11.1**	**11.1**
2.5 V	Measured cathode potential (V)	0.07	-0.2	-0.52	-0.66
	Current (A)	0.01	0.011	0.023	0.089
	Ohmic loss (V)	2.128	1.833	1.150	0.742
	φ_s (V)	-0.186	-0.333	-0.675	-0.879
	φ_H (V)	**-0.178**	**-0.309**	**-0.549**	**-0.464**
	C_d (μF/cm^2)	**2.8**	**11**	**11.1**	**11.1**

*calculated as 2.2 μF/cm^2, which should be an error caused by experimental artifacts since theoretically C_d increases with ionic strength at given potential. Therefore 9.1 μF/cm^2 was used instead as its minimum possible value.

Removal of 10 μM U(VI) from 500 mL solution (15 S/m unit) was compared with that of 150 μM U(VI) from **Figure 2** (1 S/m unit) and plotted together in **Figure 32.** It shows that k_{obs} is higher at 15 S/m at acidic pH. Assuming C_d remains unchanged, Linear fitting of the two k_{obs} versus pH curve in **Figure 32** yields the relationship between k_{obs} and pH at two different S/m ratios, as listed in **Table 6**. Linear fitting of k_{obs}-S/m curve in **Figure 31** generates another equation defining k_{obs} with S/m, shown as the third equation in **Table 6**.

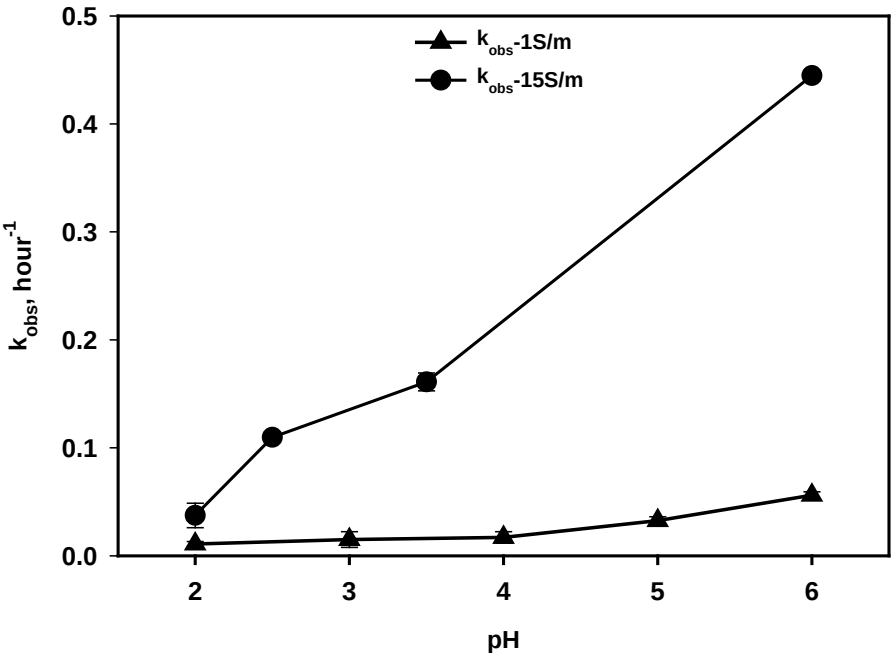

Figure 32. k_{obs} at different pHs with two tested S/m ratios (initial U(VI) concentration were 10 μM and 150 μM, respectively) at 2.0 V, with ionic strength of each condition calculated and plotted versus the Y-axis on the right. Error bar represents standard deviation from duplicates.

Table 6 Fitting results of k_{obs}-pH and k_{obs}-S/m

Factor	Fitting equation	S/m	pH	Potential	Ionic strength
pH	k_{obs} = 0.0996(pH-1.61) R^2=0.9870	15	-	2.0 V	10^{-2} -10^{-5} M
pH	k_{obs} = 0.0108(pH-1.56) R^2=0.8472	1	-	2.0 V	10^{-2} -10^{-5} M
S/m	k_{obs} = 0.0306[ln(S/m) + 2.25] R^2 = 0.9812	-	3	2.5 V	$10^{-2.4}$ M

For a condition with defined potential and ionic strength, C_d is constant. Therefore C_d is included in the constant in the k_{obs}-S/m equation. According to **Table 5**, C_d for the k_{obs}-S/m equation is 11 μF/cm^2. Therefore, k_{obs}-S/m equation can be rewritten as k_{obs} = 0.0306 ln(0.85C_dS/m). From the hypothesized k_{obs} formula, $c_1 f$(pH) = 0.0306. Using either (pH-1.61) or (pH-1.56) as f(pH), and we could eventually get c_1 = 0.022. The k_{obs} equation can be put as:

$$k_{obs} = 0.022(pH - 1.6)\ln(0.85 C_d \frac{S}{m}) \qquad \text{Equation 9}$$

where unit of k_{obs} is hour^{-1}, unit of C_d is μF/cm^2, and unit of S/m is cm^2/mol.

Model Verification

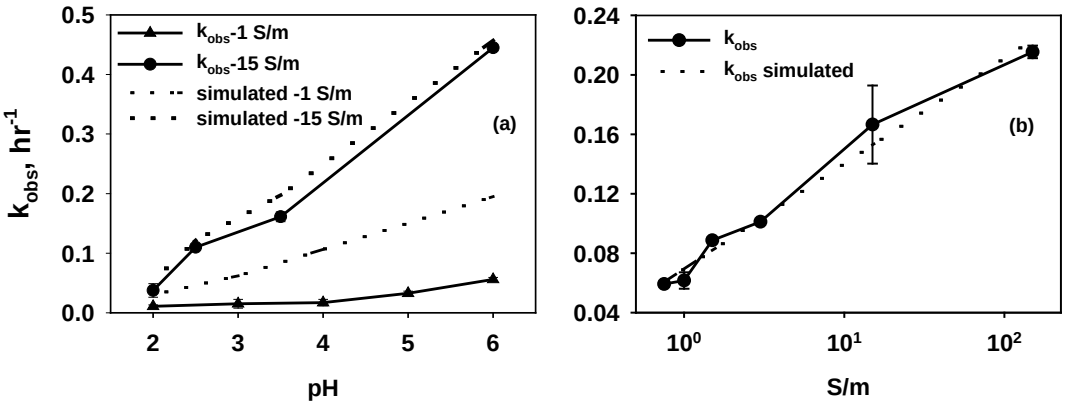

Figure 33. Modeling fitting of k_{obs} change with pH (a) and S/m ratio (b). Dashed lines represents modeling results; solid symbols and lines were experimental results.

Bring the Eq. 6.11 back to conditions examined in **Figure 31 and Figure 32**, with C_d calculated as 9.1 μF/cm^2 and 11.1μF/cm^2 respectively, comparison of experimental results and model simulation results is shown in **Figure 33**. The model successfully predicts k_{obs} change with pH at 15 S/m ratio, but not so well at 1 S/m. It was found that the simulated results tend to overestimate k_{obs} by 65%-253% with 1 S/m scenario at high pHs. Since ionic strength of solutions at pH 5 and 6 was actually two orders of magnitude lower than our lowest studied condition, 10^{-3} M, it is likely that the assumption of constant C_d caused the discrepancy since the actual C_d is expected to be lower at ionic strength lower than 10^{-3} M. When S/m ratio is as high as 15, the large value reduces the error introduced by the higher value of C_d. Therefore, the model equation is more effective in predicting k_{obs} in our studied ionic strength range (10^{-3} – 0.24 M) than in ionic strength below 10^{-3} M.

The model equation also explains the finding form Task 1 that ionic strength did not influence U(VI) removal rate at pH 3 (**Figure 10**), since C_d only changes in a narrow range at ionic strength between 10^{-3} M and 10^{-1} M. Another experiment was performed with changes both in S/m ratio and ionic strength. The results as well as its fitting curve are shown in **Figure 33a**. It appears that the model does not predict the change in rate constant as expected. It underestimates rate constant at low pH. However, the pH of the bulk solution was not constant throughout the adsorption reaction (**Figure 34b**). Unlike U(VI) removal from lower ionic strength and constant pH (data not shown), when ionic strength was as high as 0.1 M, the solution pH all converged on a value of 4, which suggests the occurrence of side reactions. Treatment of Area 3 groundwater with ionic strength of 0.24 M with electrodes poised at 2.5 V reported evolution of hydrogen during U removal (**Figure 27**). For ionic strength as high as 0.1 M, low ohmic loss probably causes a high φ_s value. The synergic effect of increased S/m and φ_s may result in more complicated situations, and lessen the impact of pH on U(VI) removal, causing significant deviation from the observed results. Another reason for model failure in predicting trend in **Figure 33a** is that the pH value incorporated in the model equation for verification was not real solution pH but rather initial pH. Therefore, the model seems to be

more suitable for prediction of k_{obs} with simple electrosorption process without the occurrence of side reactions such as electrolysis.

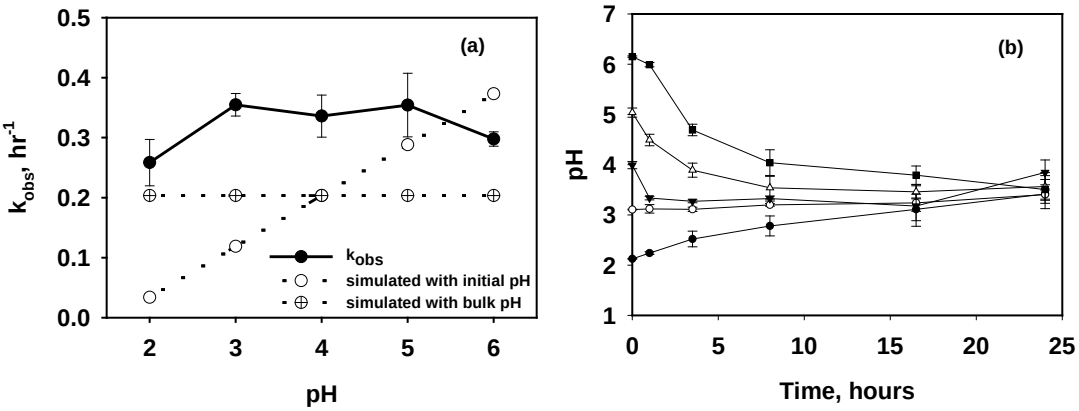

Figure 34 (a) k_{obs} at different pHs at ionic strength of 0.1 M. Ionic strength of each pH condition is plotted as vertical bar versus Y-axis on the right. The external potential is 2.5 V, and S/m ratio is 5. Open symbols and dashed lines represents modeling results; solid symbols and lines were experimental results. (b) Shift of solution pH with time during the removal. The data markers represent the average and range of duplicate experiments.

Task 4: Summary and Discussion

The extent and kinetics of electrosorption of U(VI) on graphite electrodes has not been investigated before. Models for predicting electrosorption of metals under environmental conditions must also include terms for aqueous geochemical conditions. The model presented here includes influence of potential, ionic strength, molar mass of adsorbate, and pH that was not considered in previous kinetic reaction models.

A semi-continuous study of U removal on graphite electrodes shows that U(VI) can be removed repeatedly as solution U(VI) concentration stabilized and additional U(VI) was spiked. However, stabilized U(VI) concentration by the end of each spike gradually increased, suggesting electrosorption of U(VI) was also limited by a capacity. When little U(VI) removal was observed with the 9th spike, externally applied potential was adjusted from 2.5 V to 3.0 V. U(VI) was continued to be remove after this slight increase of potential, but stopped at the second spike. Calculating U(VI) concentration on electrode surface versus in the bulk solution shows that the removal fits well with Langmuir isotherm. Maximum electrosorption capacity is 263.16 μmol for U(VI), which required a specific surface area of 43.2 m^2/g theoretically.

References

Alfarra, A.; Frackowiak, E.; Beguin, F. Mechanism of lithium electrosorption by activated carbons. *Electrochim. Acta* 2002, *47* (10), 1545-1553.

Alliot, I.; Alliot, C.; Vitorge, P.; Fattahi, M. Speciation of technetium(IV) in bicarbonate media. *Environ. Sci. Technol.* 2009, *43* (24), 9174-9182.

Bard, A. J.; Faulkner, L. R. *Electrochemical methods: fundamentals and applications*; John Wiley & Sons, Inc.: New York, 2001.

Benjamin, M. M. *Water Chemistry*; McGraw Hill: New York, 2002.

Boggs, M. A.; Minton, T.; Dong, W. M.; Lomasney, S.; Islam, M. R.; Gu, B. H.; Wall, N. A. Interactions of Tc(IV) with humic substances. *Environ. Sci. Technol.* 2011, *45* (7), 2718-2724.

Brooks, S. C. *Waste characteristics of the former S-3 ponds and outline of uranium chemistry relevant to NABIR Field Research Center studies*; Oak Ridge National Laboratory: Oak Ridge, TN, 2001.

Burke, I. T.; Boothman, C.; Lloyd, J. R.; Livens, F. R.; Charnock, J. M.; McBeth, J. M.; Mortimer, R. J. G.; Morris, K. Reoxidation behavior of technetium, iron, and sulfur in estuarine sediments. *Environ. Sci. Technol.* 2006, *40* (11), 3529-3535.

Burns, P. C. a. F., R., Eds. *Uranium: Mineralogy, Geochemistry and the Environment*; Mineralogical Society of America: Washington D.C., 1999.

Cui, D. Q.; Eriksen, T. E. Reduction of pertechnetate by ferrous iron in solution: Influence of sorbed and precipitated Fe(II). *Environ. Sci. Technol.* 1996, *30* (7), 2259-2262.

Edwards, L.; Kusel, K.; Drake, H.; Kostka, J. E. Electron flow in acidic subsurface sediments co-contaminated with nitrate and uranium. *Geochim. Cosmochim. Acta* 2007, *71* (3), 643-654.

Farmer, J. C.; Bahowick, S. M.; Harrar, J. E.; Fix, D. V.; Martinelli, R. E.; Vu, A. K.; Carroll, K. L. Electrosorption of chromium ions on carbon aerogel electrodes as a means of remediating ground water. *Energ. Fuel* 1997, *11* (2), 337-347.

Farrell, J.; Bostick, W. D.; Jarabek, R. J.; Fiedor, J. N. Electrosorption and reduction of pertechnetate by anodically polarized magnetite. *Environ. Sci. Technol.* 1999, *33* (8), 1244-1249.

Fredrickson, J. K.; Zachara, J. M.; Kennedy, D. W.; Kukkadapu, R. K.; McKinley, J. P.; Heald, S. M.; Liu, C. X.; Plymale, A. E. In *Reduction of TcO_4^- by sediment-associated biogenic Fe(II)*, 2004; Pergamon-Elsevier Science Ltd: 2004; pp 3171-3187.

Gabelich, C. J.; Tran, T. D.; Suffet, I. H. Electrosorption of inorganic salts from aqueous solution using carbon aerogels. *Environ. Sci. Technol.* 2002, *36* (13), 3010-3019.

Gregory, K. B.; Lovley, D. R. Remediation and recovery of uranium from contaminated subsurface environments with electrodes. *Environ. Sci. Technol.* 2005, *39* (22), 8943-8947.

Gu, B. H.; Wu, W. M.; Ginder-Vogel, M. A.; Yan, H.; Fields, M. W.; Zhou, J.; Fendorf, S.; Criddle, C. S.; Jardine, P. M. Bioreduction of uranium in a contaminated soil column. *Environ. Sci. Technol.* 2005, *39* (13), 4841-4847.

Hansen, P. G. The conditions for electrodeposition of insoluble hydroxides at a cathode surface - a theoretical investigation. *J. Inorg. Nucl. Chem.* 1959, *12* (1-2), 30-37.

Haynes, W. M.; Lide, D. R., Eds. *Solubility product constants*; CRC Press: 2011-2012.

Icenhower, J. P.; Martin, W. J.; Qafoku, N. P.; Zachara, J. M. *The geochemistry of technetium: A summary of the behavior of an artificial element in the natural environment*; U.S. Department of Energy: Richland, WA, December 2008.

Istok, J. D.; Senko, J. M.; Krumholz, L. R.; Watson, D.; Bogle, M. A.; Peacock, A.; Chang, Y. J.; White, D. C. *In situ* bioreduction of technetium and uranium in a nitrate-contaminated aquifer. *Environ. Sci. Technol.* 2004, *38* (2), 468-475.

Kinoshita, K. *Carbon: electrochemical and physicochemical properties*; Wiley-Interscience: 1988.

Lawson, B. L.; Scheifers, S. M.; Pinkerton, T. C. The Electrochemical reduction of pertechnetate at carbon electrodes in aqueous non-complexing acid-media. *J. Electroanal. Chem.* 1984, *177* (1-2), 167-181.

Maset, E. R.; Sidhu, S. H.; Fisher, A.; Heydon, A.; Worsfold, P. J.; Cartwright, A. J.; Keith-Roach, M. J. Effect of organic co-contaminants on technetium and rhenium speciation and solubility under reducing conditions. *Environ. Sci. Technol.* 2006, *40* (17), 5472-5477.

Maslennikov, A.; Masson, M.; Peretroukhine, V.; Lecomte, M. Technetium electrodeposition from aqueous formate solutions: Electrolysis kinetics and material balance study. *Radiochim. Acta* 1998, *83* (1), 31-37.

McBeth, J. M.; Lear, G.; Lloyd, J. R.; Livens, F. R.; Morris, K.; Burke, I. T. Technetium reduction and reoxidation in aquifer sediments. *Geomicrobiol. J.* 2007, *24* (3-4), 189-197.

Newman, J.; Thomas-Alyea, K. E. *Electrochemical systems*; Wiley Interscience: Hoboken, NJ, 2004.

Oren, Y.; Soffer, A. The electrical double layer of carbon and graphite electrodes : Part II. Fast and slow charging processes. *J. Electroanal. Chem.* 1985, *186* (1-2), 63-77.

Seron, A.; Benaddi, H.; Beguin, F.; Frackowiak, E.; Bretelle, J. L.; Thiry, M. C.; Bandosz, T. J.; Jagiello, J.; Schwarz, J. A. Sorption and desorption of lithium ions from activated carbons. *Carbon* 1996, *34* (4), 481-487.

Rard, J. A.; Rand, M. H.; Anderegg, G.; Wanner, H. *Chemical thermodynamics of technetium*; Elsevier Science: Amsterdam, The Netherlands, 1999.

Socolofsky, S. A.; Jirka, G. H. Advective diffusion equation. In *Special topics in mixing and*

transport processes in the environment; Eds.; College Station, TX, 2005.

Sun, M.; Yan, F.; Zhang, R. L.; Reible, D. D.; Lowry, G. V.; Gregory, K. B. Redox control and hydrogen production in sediment caps using carbon cloth electrodes. *Environ. Sci. Technol.* 2010, *44* (21), 8209-8215.

Wan, J. M.; Dong, W. M.; Tokunaga, T. K. Method to attenuate U(VI) mobility in acidic waste plumes using humic acids. *Environ. Sci. Technol.* 2011, *45* (6), 2331-2337.

Wildung, R. E.; Li, S. W.; Murray, C. J.; Krupka, K. M.; Xie, Y.; Hess, N. J.; Roden, E. E. In *Technetium reduction in sediments of a shallow aquifer exhibiting dissimilatory iron reduction potential*, 2004; Elsevier Science Bv: 2004; pp 151-162.

Ying, T. Y.; Yang, K. L.; Yiacoumi, S.; Tsouris, C. Electrosorption of ions from aqueous solutions by nanostructured carbon aerogel. *J. Colloid Interface Sci.* 2002, *250* (1), 18-27.

Xu, Y.; Zondlo, J. W.; Finklea, H. O.; Brennsteiner, A. Electrosorption of uranium on carbon fibers as a means of environmental remediation. *Fuel Process. Technol.* 2000, *68* (3), 189-208.

Output from Research

Manuscripts

Juan Peng and Kelvin B. Gregory (Submitted) Geochemical Conditions Affecting the Removal and Recovery of Uranium from Acidic Solutions Using Electrodes.

Juan Peng, Fei Lian, and Kelvin B. Gregory (in Preparation) Removal and Recovery of Pertechnetate from Acidic Solutions with Graphite Electrodes

Juan Peng and Kelvin B. Gregory (in Preparation) Equilibrium Isotherm and Kinetic Model for U(VI) Electrosorption by Graphite Electrodes

Presentations and Invited Seminars

Kelvin B. Gregory. Advancing Environmental and Biotechnology using Electrodes: CDI and Bromide Removal from Oil and Gas Brines. DeNora Industries 1st Annual Research Symposia. November 14, 2012.

Kelvin B. Gregory Bacterial Respiration in Electrochemical Cells for Renewable Energy and Micron-scale Sensing. International Conference on Re-Newable Energy, Baru Sahib, India. May 5-6, 2012.

Kelvin B. Gregory and Juan Peng. Remediation and recovery of uranium and technetium from contaminated groundwater using graphite electrodes. American Chemical Society Pacifichem 2010. Honolulu HI. December 2010.

Juan Peng and Kelvin B. Gregory. Geochemical Conditions Affecting Electrode-based Removal of Uranium 238th ACS National Meeting & Exposition. Washington, D.C. August 16-20, 2009.

Juan Peng and Kelvin B. Gregory. Electrode-based Remediation of Uranium(VI) from Acidic Subsurfaces. HydroGeoLogic, Inc., Reston, VA. August 2009.

Kelvin B. Gregory. Prokaryote Power: Electrode Technology for Energy and the Environment, Department of Energy, National Energy Technology Laboratory. Pittsburgh, PA. April 2009.

Kelvin B. Gregory. Batteries and Bioremediation: Electrode Technology for Energy and the Environment. Environmental Engineering and the Environmental Molecular Science Institute, The Ohio State University, Columbus, OH. January 2009.

Appendix

The appendix contains the submitted manuscript for Task 1 and the draft manuscripts from Tasks 2 and 4.

Geochemical Conditions Affecting the Removal and Recovery of Uranium from Acidic Solutions Using Electrodes

*Juan Peng and Kelvin B. Gregory**

***Corresponding Author: Department of Civil and Environmental Engineering, Carnegie Mellon University, 5000 Forbes Ave, Pittsburgh, PA 15213, Phone: (412)268-9811; Fax: (412)268-7813; E-mail: kelvin@cmu.edu**

ABTRACT

Polarized electrodes emplaced in the subsurface have emerged as a potential strategy for *in situ* bioremediation, removal, and recovery of metal contaminants from groundwater. Little is known, however, about the influence of geochemical and design conditions that may affect the removal and recovery of metals from the subsurface. Using a 2-electrode system, the removal rates of U(VI) were determined with respect to the impact of pH, applied potential, and other cations. Initial removal rates of U(VI) were approximately first-order and increased from 0.01 hr^{-1} at pH 2 to 0.06 hr^{-1} at pH 6. The slower removal rates exhibited at lower pH were overcome by increasing the applied potential, but with diminishing returns at above 2.5 V. The presence of Al^{3+}, Mg^{2+}, or Na^{+} did not influence U(VI) removal at 2.5 V. However, at 5.0 V, Al^{3+} and Mg^{2+} decreased removal rates while Na^{+} increased removal rates. Initial U(VI) recovery rate was also pH-dependent. This study demonstrates that electrodes may be employed for rapid removal and recovery of U(VI) across a broad spectrum of aqueous geochemical conditions. The results presented may guide the selection and design of an electrode-based remedial approach for metals.

INTRODUCTION

Electrode-based bioremediation may be an alternative approach for *in situ* mitigation of contaminated sediments [1] and groundwater [2]. In brief, polarized electrodes are emplaced in sediment or groundwater to establish desirable redox gradients for remediation [1] and serve as the electron donor [2-6] or acceptor [1] for bacteria that participate in contaminant transformation. If sufficient potential is applied, the target contaminant may be reduced at the cathode or oxidized at the anode. The key advantage of an electrode-based approach lies in the ability to adjust the voltage between the electrodes and readily change the rate of supply and redox potential of the desired electron donor or acceptor.

During electrode-based bioremediation of uranium, a rapid abiotic removal of U(VI) is followed by the microbially-mediated reduction to U(IV) [2]. The abiotic removal mechanism is the deionization of the solution through entrapment of metal ions in the electrical double layer and is only stable as long as potential is applied between the electrodes [2]. The subsequent biological reduction of uranium results in uranium species which are stable on the electrode in the absence of applied potential and until reoxidized [2]. Regardless of the removal mechanism, the principal advantage of an electrode-based bioremediation approach for uranium (and other metals) lies in the localization of contaminant from the groundwater to an electrode surface where it may be easily recovered [2] and creates opportunity for complete and permanent mitigation of risk associated with subsurface metals contamination.

Although electrode-based technique is a promising technology for remediation of metals, the underlying principles which govern removal and recovery rates from environmental media are poorly understood. For example, pH controls speciation of metal ions, and may also affect electrode surface functional groups. It was found that initial solution pH is a crucial factor for electrochemical sorption of Li^+ [7]. When multiple cationic species are present,

competition may exist and the cations can be selectively removed by the electrodes. Proposed explanations include differences in hydrated ionic radii [8], electric charge a cation carries [9], and initial ion concentration [10].

The experiments described herein were designed to assess some of the unique subsurface conditions encountered in the groundwater near the S-3 waste disposal area at the U.S. DOE Y-12 site in Oak Ridge, TN. This legacy site exhibits high concentrations of radionuclide contaminants in a heterogeneous system that is buffered at a low pH (pH < 4) [11]. Groundwater immediately downgradient of the S-3 disposal area, also has high concentrations of nitrate (~100 mM), and metal cations such as magnesium and aluminum (~8 mM and ~20 mM, respectively). Pretreatments are needed to adjust the geochemical conditions before applying *in situ* biorestoration [12, 13], which complicates remedial design and implementation. In this geochemical environment, an electrode-based remedial approach may be an ideal solution. Experiments described below define the impacts of pH and other common cations in groundwater that influence the abiotic removal and recovery of U(VI) on polarized electrodes.

MATERIALS AND METHODS

U(VI) Removal and Recovery from Site Water. Contaminated soil and groundwater were collected from the U.S. Department of Energy Field Research Center (FRC) S-3 area. The pH of the groundwater sample was 3.3 and the initial U(VI) concentration was 280 μM. The glass, dual-chamber reactors and graphite electrodes were described previously [2, 3]. 5 g of soil and 200 mL of groundwater was transferred to each sterilized chamber. Duplicate chambers were stirred on a multi-position stir plate (Variomag Poly 15, Thermo Scientific) at 300 rpm. Experimental reactors contained a potentiostat-poised (AMEL2049, Milan, Italy) graphite electrode (working) at a potential of -0.5 V versus Ag/AgCl (reference). Both

working and counter chambers were closed to the atmosphere. Experiments were initiated by the establishment of potential at the working electrode. Control reactors were prepared identically but not connected to a potentiostat. Aqueous samples were removed over time intervals for analysis. Recovery of uranium from the experimental reactors was initiated by removing power from the working electrodes.

U(VI) Removal and Recovery in Synthetic Groundwater. Uranium was amended to reactors from an aqueous stock solution of uranium acetate (Electron Microscopy Sciences, Hatfield, PA) in deionized water and pH adjusted as needed with 1 M HCl. Batch, 2-electrode experiments were performed in covered, 600 mL beakers containing 500 mL of medium. Electrodes were cylindrical graphite rods (Graphite Engineering & Sales, Co., Greenville, MI) with a diameter of 2.54 cm and length of 7.62 cm. The electrodes were connected to each lead via neoprene-coated cables (Teledyne Impulse, San Diego, CA). The electrodes were connected to the power supply by neoprene-coated cables and connectors (Teledyne Impulse, San Diego, CA) affixed with silver epoxy (Epoxy Technology, Billerica, MA). External potential between the electrodes was established using an Agilent E3620A power supply (Englewood, CO). Duplicate or triplicate reactors were stirred at 300 rpm. Experiments were initiated by establishing electrical potential between the anode and cathode electrodes with power supplies. Recovery of U(VI) was initiated by removing power from the electrodes.

Analytical Methods. Uranium was measured using a kinetic phosphorescence analyzer (KPA). In brief, 100 μL of unfiltered sample was removed from reactors with a pipetter and diluted as necessary to meet the high-range calibration of the KPA (0-20 μM), complexed with 1.5 mL of Uraplex®, and let stand for 5 minutes prior to analysis with KPA instrument (KPA-11, Chemchek Instruments, Richland, WA). Aluminum, magnesium and sodium were measured using atomic adsorption spectrometry (GBC908, GBC Scientific Equipment LLC,

Hampshire, IL). Samples were diluted in 2% nitric acid prior to measurement. Aluminum concentrations were determined in a nitrous oxide-acetylene flame with an acetylene flow rate of 2.0 L/min and nitrous oxide flow rate 10.0 L/min. Spectroscopy was performed at 396.2 nm with a slit opening of 0.5 nm. Magnesium and sodium were measured with an air-acetylene flame with an acetylene flow rates of 2.0 L/min and 10.0 L/min, respectively. Spectroscopy was examined with slit opening of 0.5 nm at a wavelength of 204.2 nm and 330.2 nm, respectively. Potential at the cathode and anode versus standard reference electrode was performed using Ag/AgCl reference electrodes and monitoring potential using a multimeter (Keithley Instruments, Cleveland, OH).

RESULTS AND DISCUSSION

Removal and Recovery of U(VI) from Site Water. The extraction of U(VI) from FRC Area 3 site water using electrodes was examined using a 3-electrode, potentiostat-poised reactor. This reactor was identical to previous studies by the authors [2]. The application of electric potential at the working electrode (-0.5 V vs Ag/AgCl) initiated the rapid removal of U(VI) from a slurry of low pH sediment and groundwater from the FRC Area 3 site (Fig. 1). 86% of the initial U(VI) was removed after 29 days. No U(VI) removal occurred in the control reactors that lacked external potential. On day 29, U(VI) was respiked into the reactors from an aqueous stock solution of uranium acetate to achieve a concentration of 310 μM. On day 88, 86% of the respiked U(VI) had been removed and over the next 71 days, very little additional U(VI) was removed. Although the initial U(VI) removal rates (over the first 48 hours) were similar for both removal of endogenous uranium and spikes uranium, the overall removal rate for the respike was slower and may represent limiting reactive sites on the working electrode.

Recovery of U(VI) from the electrodes began immediately following the removal of potential

from the working electrode on day 159. 52% of removed U(VI) returned to solution within 24 hours. The remaining U(VI) returned solution over the next 85 days. The average recovery of U(VI) was 68.0% on day 244 and no further U(VI) returned to solution.

The rapid removal and recovery of uranium from the low pH groundwater on polarized electrodes was consistent with entrapment of uranium ions in the electrical double layer at the electrode reported previously using circumneutral pH solutions [2, 14]. These studies further suggested that reduction of U(VI) to U(IV) in groundwater solutions by a graphite electrode poised at -0.5 V vs. Ag/AgCl was not a significant source of abiotic removal [2] and was also insignificant for potentials ranging from -0.45 V to -0.9 V versus Ag/AgCl electrode [14]. Theoretically, reduction of U(VI) to U(IV) requires a working electrode potential of ~-0.6 V vs. Ag/AgCl. The potential further decreases to -0.70 V for reduction of 280 μM U(VI) to U(IV) ($UO_{2(s)}$) at pH 3. Therefore, the removal and recovery of U(VI) may be attributed to charging/discharging of the electric double layer (EDL) around cathode [15, 16] or cationic adsorption/desorption [7].

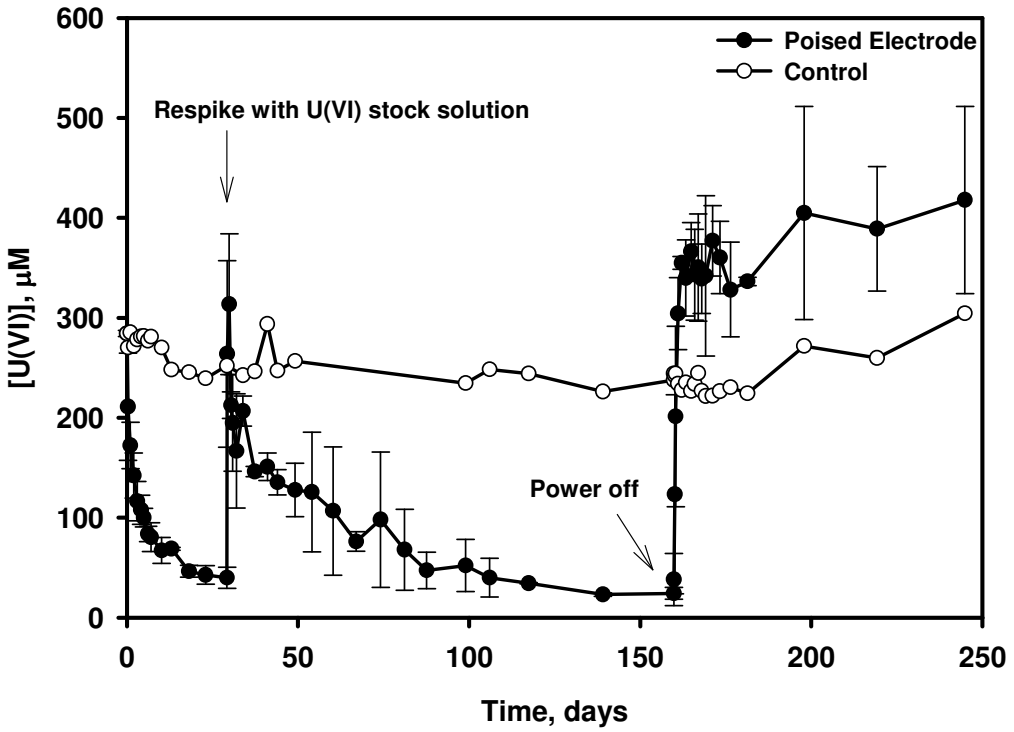

Figure 1. Removal and recovery of U(VI) in batch incubations of uranium-contaminated sediment and groundwater slurries. The working electrode was poised at -0.5 V (vs a Ag/AgCl reference) via a potentiostat. After 29 days, U(VI) was respiked. Power was turned off on day 159. Error bars represent the average and standard deviation of duplicate reactors.

The total fraction of U(VI) removed from the FRC Area 3 site samples was similar to previous studies examining removal of U(VI) from a biological growth media using electrodes [2]. However, the rates of removal were much lower from the FRC Area 3 samples despite nearly identical reactors and electrode materials. For example, only 39% of the initial U(VI) was removed within 1 day from the FRC Area 3 samples whereas 99.0% of removal was observed from the media samples [2]. The difference in U(VI) removal rates between the two samples was likely the result of differences between the aqueous constituents of the media between the two studies. For example, the initial U(VI) concentration, pH, concentrations of other dissolved cations as well as ionic strength at FRC Area 3 are all higher than in Gregory *et al*'s study [2]. The more concentrated conditions may

have the effect of blocking reactive sites on the electrode and greatly slowing the rates of adsorption and ion exchange with U(VI) at the electrode surface.

Influence of pH on U(VI) Removal. The impact of pH on the initial removal rate of U(VI) (k_{obs}) was examined in a 2-electrode system using pH adjusted water between pH 2 and 6 (Fig. 2). Initial removal rates were approximated using first order kinetics. The rates were dependent on pH, increasing from 0.01 hr^{-1} to 0.06 hr^{-1} as pH increased from 2 to 6 (Fig. 2). The pH dependence of U(VI) removal on carbon-based electrodes has previously been attributed to the rapid charging of the EDL by protons at low pH [14].

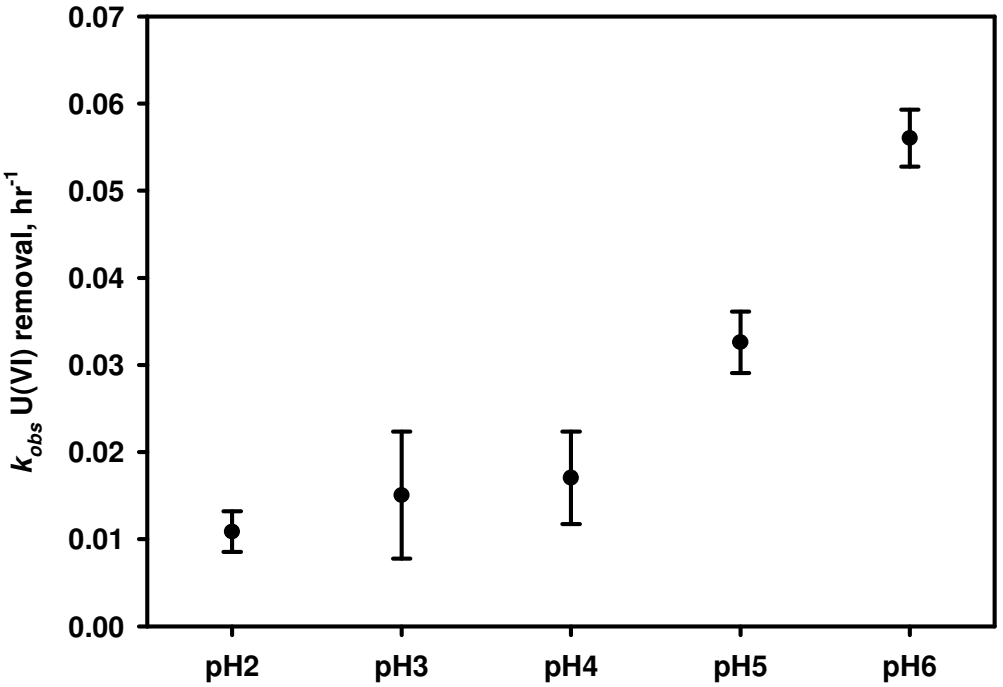

Figure 2. Impact of solution pH on initial removal rates (k_{obs}) of U(VI). Initial removal rates were approximately first order (Fig. S1). The external potential was 2.0 V and starting concentration of U(VI), 150 μM. Error bars represent the average and standard deviation of duplicate reactors.

However, the pH dependence may also arise from differences in the mobility of the predominant uranium species at each pH as well. For example, at pH 2, over 90% of U(VI) is expected to exist as free UO_2^{2+}. As the pH increases, the fraction of UO_2^{2+} decreases and the predominant species changes to $(UO_2)_2(OH)_2^{2+}$ and at pH 5-6 $(UO_2)_3(OH)_5^{+}$ becomes the dominant species (Fig. S2). Mobility is a factor that indicates how fast a given species can move in an electric field, which is determined according to Equation 1 [17]:

$$u_i = \frac{|z_i|e}{6\pi\eta r_i} \quad (1)$$

Where u_i is the mobility (m^2/ s•V) of species *i* in an electric field, z_i is the charge of species *i*, e is electronic charge (1.602×10^{-19} coulombs), η is the viscosity of the solution (g/m•s), and r_i is the radius of species *i* (m). Equation 1 predicts that UO_2^{2+} has higher mobility than either $(UO_2)_2(OH)_2^{2+}$ or $(UO_2)_3(OH)_5^{+}$ in electric field, due to the charge it carries and its relatively smaller ionic radius. Mobility of H^+ (3.63×10^{-3} cm^2/s•V) is about eleven times higher than that of UO_2^{2+}(3.32×10^{-4} cm^2/s•V) in diluted solution (Table S2). With the estimated mobility, the net flux of a particular species in the EDL may be estimated by Equation 2 [18]:

$$J_i = -u_i c_i \nabla\Phi - D_i \nabla c_i \quad (2)$$

where J_i is the net flux of a charged ion in an electric field (mol/m^2s) (convection is not considered near the electrode surface). The first group of terms on the right hand side of Equation 2 accounts for ionic migration, where, c_i is the concentration of species *i* (mol/m^3), $\nabla\Phi$ is the potential gradient (V/m). The second group of terms accounts for diffusion, where D_i is the diffusion coefficient of species *i* (m^2/s) ($D_i = \frac{u_i RT}{|z_i|F}$, where z_i is the charge of species *i*, u_i is the mobility of species *i*, F is Faraday's constant, R is universal gas constant, and T is absolute temperature) and ∇c_i is the concentration gradient of species *i*

(mol/m^4). For example, although carrying the same charge, flux of $(UO_2)_2(OH)_2^{2+}$ should be smaller than that of UO_2^{2+} (Eq. 1) since mobility (u_i) of $(UO_2)_2(OH)_2^{2+}$ is lower assuming potential gradient remain the same and diffusion flux is negligible in a well-mixed solution. At higher pH, $(UO_2)_2(OH)_2^{2+}$ or $(UO_2)_3(OH)_5^{+}$ are the dominant U(VI) species, since they both have lower mobility than UO_2^{2+}, U(VI) species do not move faster at higher pH than at lower pH according to Equation 2. Assuming ions reaching the electrode surface first will have the priority to be electrosorbed, the analyses above clearly suggests that U(VI) speciation is not the reason for increase of U(VI) removal at high pH, since U(VI) species move faster at lower pH at an electric field. More importantly, analyzing flux of H^+ and U(VI) species helps understand the role H^+ plays during U(VI) removal.

At low pH, both uranium cations and protons move towards the electric double layer and cathode. Protons have a higher mobility, and migration flux of protons is 73 times of that of UO_2^{2+} ions at pH 3 with 150 μM U(VI). Therefore protons move faster than U(VI) cations and enter the electric double layer earlier than uranium. The accumulation of protons will dissipate charge at the electrode surface, limiting its ability to hold uranium. As pH continues to increase, protons gradually lose advantage in flux. An increase of pH from 3 to 6 will decrease migration flux of protons by 3 orders of magnitude. Since ionic radius of $(UO_2)_2(OH)_2^{2+}$ or $(UO_2)_3(OH)_5^{+}$ are unknown, it is hard to compare flux of protons with that of U(VI) species at pH beyond 4. However, when pH exceeds 3.8, concentration of protons is no longer larger than U(VI), suggesting that the impact of proton "competition" for the electrical double layer lessens at pH beyond 4, and gives rise to faster removal rates for uranium.

In addition to reducing the effect of competition for the EDL between protons and uranium, increasing pH may deprotonate acidic surface functional groups on graphite such as carboxyl

groups (pK_a=3~8), and provide a negative charge to the electrode surface [19]. Cationic U(VI) species may form complexes with negatively charged functional groups [7], and contribute to faster U(VI) removal. Although surface complexation and electrostatic interactions in the EDL may be contribute to U(VI) removal, U(VI) could not outcompete H^+ under either circumstances at lower pH due to disadvantages in concentration and flux. Lower pH increases the impact of proton competition as well as decreases available surface functional groups where U(VI) may adsorb. Regardless of the mechanism, the aggregate impact greatly decreases U(VI) removal rate.

Similar impacts of pH were reported for the electrosorption of Li^+ onto activated carbons [7] as well as chemisorption of Cd(II), Pb(II), Hg(II) Cu(II), Ni(II), Mn(II) and Zn(II) onto carbon aerogel [20]. These previous studies show that the fraction of cations sorbed was low at lower pH, and increased with pH. These phenomena could be explained with the complexation change of heavy metal ion species with surface functional group at different pHs, suggesting that in our study, both U(VI) speciation and surface complexation may be important determinants of U(VI) removal rates.

Influence of Applied Potential on U(VI) Removal. The calculations above show that removal rates of uranium are adversely impacted by competition with faster moving and higher concentration protons in the EDL. However, the flux of ions through the EDL is also partially determined by the external potential gradient at the electrode (Eq. 2). Moreover, increasing the external potential will also change the potential distribution in the EDL by enhancing cathodic potential and increase the capacity of EDL [17]. The impact of applied potential between the electrodes on the removal rates of uranium and its ability to overcome the detrimental impacts of low pH were examined through step-wise adjustment of potential and calculation of initial removal rates (Fig. 3). No appreciable increase in k_{obs} was observed as the potential was adjusted from 0.5 V to 1.5 V. However, between 1.5 V and

2.5 V, k_{obs} increased from 0.15 hr^{-1} to 0.67 hr^{-1}. The rate observed at pH 3 with an external potential of 2.5 V was similar to the rate at 0.5 V and pH 6, indicating that the adverse impact of low pH in the field may be overcome by increasing the externally applied potential at the electrodes [21-23]. However, the benefit of increased potential on uranium removal rate diminished above 2.5 V.

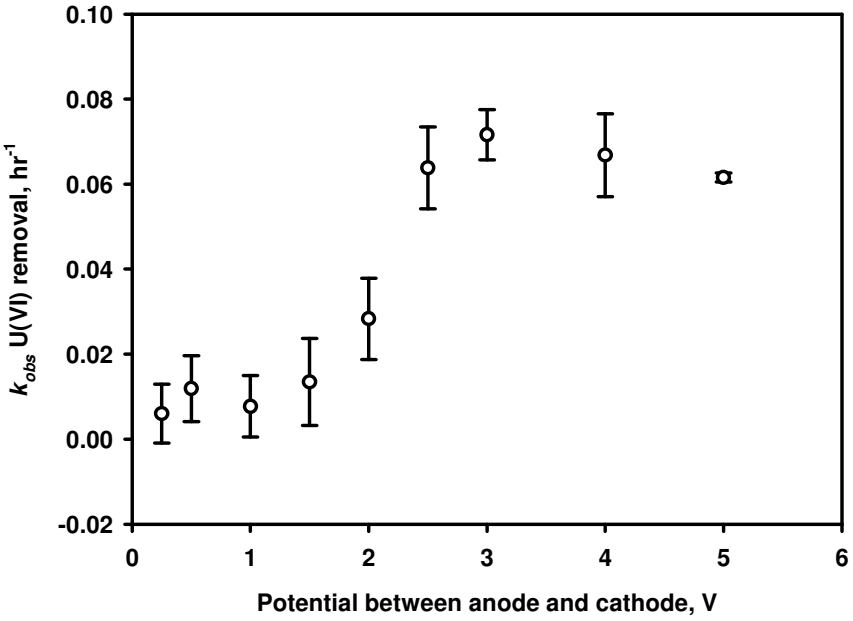

Figure 3. k_{obs} for U(VI) removal from pH 3 water with increasing applied potentials. Initial U(VI) concentration was 150 μM. Error bars represent the average and standard deviation of duplicate reactors.

This diminishing return on the applied potential was examined by measuring the potential of the anode and cathode independently during stepwise adjustments. Figure 4 shows that the absolute value of cathode potential against Ag/AgCl increased by over 80% with external potential increased from 2.0 V and 2.5 V, but by smaller percentages as the external potential was increased beyond 2.5 V. This is consistent with the observed doubling of k_{obs} between 2.0 V to 2.5 V, and the plateau of k_{obs} beyond 2.5 V as shown in Figure 3. Due to low conductivity of the solution, large ohmic loss greatly reduced potential difference between cathode and anode. Significant reduction of U(VI) to U(IV) was not observed when

working electrode was poised at -0.9 V versus Ag/AgCl electrode [14], which suggests that diminishing return should not be attributed to U(VI) reduction to U(IV). The reactors were open to the atmosphere, so gas evolution was not measured, however, visible gas production was observed as tiny bubbles of gas on the anode and cathode electrodes at and beyond 4.0 V. Gas evolution was not visually observed at 2.5 V and below, at which the overall potentials between cathode and anode were below 1.23 V and water hydrolysis was thermodynamically infeasible. Previous study has suggested that H_2 evolution rate increases as external applied potential increases [1], indicating that at higher potential U(VI) ions may be prevented from approaching electrode surfaces by gas formation at the electrode surface and occupation of adsorption sites. The diminishing return on k_{obs} with increasing potential beyond 2.5 V in our system was likely a combination result of gas evolution and increasing overpotentials.

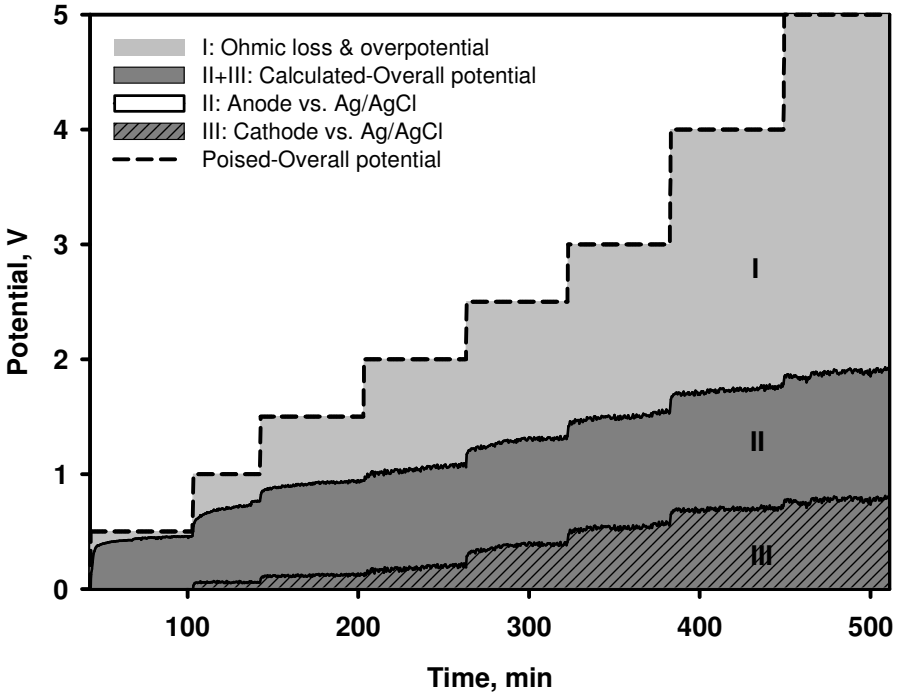

Figure 4. Potential distribution versus external potential change in pH 3, 150 □M U(VI) solution. The dashed line defines the stepwise adjustment of external potential applied. The light gray area (Area I) is potential lost in ohmic resistance and overpotentials. The dark gray area (Area II and the hatched Area III) defines the measured potential between anode and cathode. The dark gray Area II represents anode potential versus Ag/AgCl while the hatched Area III represents the absolute value of cathode potential against Ag/AgCl..

Influence of Other Cations. Cationic groundwater constituents will also move into the EDL and have the potential to occupy reactive sites and compete with U(VI) for reactive sites on the electrode. The impact of concentration of cations with different valence on the removal rates of U(VI) was explored in 2-electrode reactors. The concentrations of individual cations, Al^{3+}, Mg^{2+}, and Na^{+} were varied over ranges representative of those observed in Area 3 groundwater. Initial U(VI) concentration was 150 μM and the pH was 3. All were added as salts with chloride. The diffusion coefficient of all three ions is larger than that of UO_2^{2+} , the dominant U(VI) species at pH 3 (Table S1). According to Equation 1, suggesting Al^{3+}, Mg^{2+}, and Na^{+} should migrate faster than UO_2^{2+} in the same electric field.

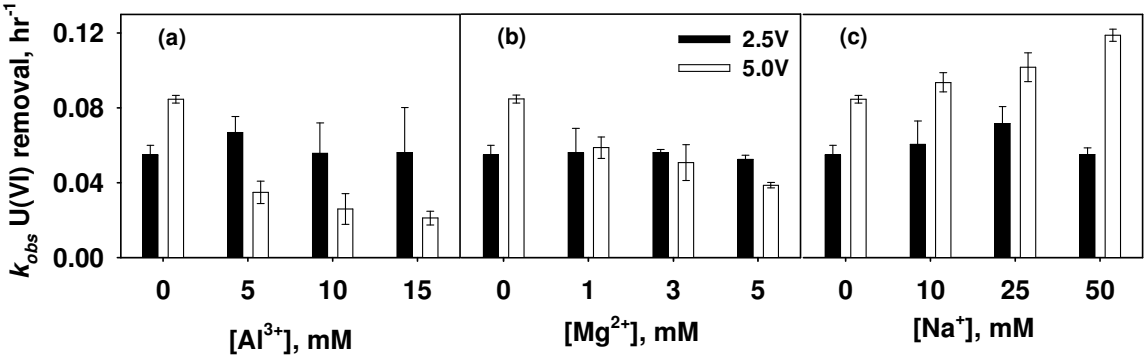

Figure 5. Initial removal rate (k_{obs}) of U(VI) from acidic water by electrodes at 2.5 V or 5.0 V of external potential at the presence of increasing concentrations of a) Al^{3+}, b) Mg^{2+}, and c) Na^{+}. The solutions initially contained 150 μM U(VI) at pH 3 and were examined over a 24-hour period. Error bars represent the average and standard deviation of triplicate reactors.

With 2.5 V external potential, the concentration of Al^{3+}, Mg^{2+}, ad Na^{+} ions had little influence on initial U(VI) removal rate (k_{obs}). No significant change in aqueous concentrations of Al^{3+}, Mg^{2+}, and Na^{+} was observed throughout the experiments at 2.5 V (data not shown), indicating there was either no removal of cations other than U(VI) occurred or that the

removal of Al^{3+}, Mg^{2+}, and Na^{+} was too small to be observed under the conditions tested. There was little difference in the U(VI) removal rates for any of the aluminum, magnesium, or sodium concentrations examined. Although other cations had no impact on k_{obs} for U(VI) at 2.5 V, when the external potential was increased to 5.0 V, k_{obs} decreased with increasing concentrations of Al^{3+} or Mg^{2+}, but not Na^{+}; k_{obs} increased slightly with increasing concentrations of Na^{+} cations. It is reasonable that higher Na^{+} concentration would decrease ohmic loss in the solution by increasing solution conductivity and enhancing potential between the electrodes and result in faster migration of ions in the solution.

The decrease in k_{obs} with Al^{3+} or Mg^{2+} at 5.0 V, is likely the result of pH effects as OH^{-} may accumulate near the cathode as protons are depleted by electrolysis at 5.0 V (Fig. 4). Even in acidic bulk solution, high pH (11-13) on cathode surface is easily obtained [24]. 5 mM of Al^{3+} can precipitate out as $Al(OH)_3$ at pH beyond 4.2 ($logK_{sp}$=-31.62 [25]) and 1 mM Mg^{2+} ions precipitates out as hydroxides at pH beyond 9.9 ($logK_{sp}$=-11.25 [26]). The higher the concentration of Al^{3+} and Mg^{2+} ions are, the more hydroxides will form at 5.0 V, causing less surface availability for U(VI) electrosorption and ultimately slower U(VI) removal rate. Although not qualified or quantified, white precipitates were observed on cathode during the 5.0 V experiments. Moreover, a decrease in Al^{3+} and Mg^{2+} concentration was also detected at 5.0 V at all studied concentrations (Fig. S4). When power was turned off, white precipitates on cathode gradually disappeared, and removed Al^{3+} and Mg^{2+} were completely recovered, which supports the hypothesis for the formation of aluminum and magnesium precipitates.

Influence of pH on U(VI) Recovery. After 240 hours of removal at 2.0 V with 150 μM U(VI) solution at pH 2-6 with synthetic groundwater, poise was removed from the electrodes to determine the impact of pH on the recovery of U(VI). Initial recovery was approximately zero-order for all pH. Over 50% of total U(VI) returned to the solution within 10 hours at

all pH evaluated in the study (data not shown). Additional U(VI) was recovered slowly afterwards. Figure 6 shows that pH is as important in U(VI) recovery process as it is in U(VI) removal; up to pH 5, initial uranium recovery rates decreased. The pH-dependence for uranium recovery is likely related to U(VI) speciation with pH and complexation phenomena. As discussed previously, at higher pH the dominant U(VI) species is $(UO_2)_2(OH)_2^{2+}$ or $(UO_2)_3(OH)_5^{+}$. These species have lower diffusion coefficients than UO_2^{2+} and may diffuse back to bulk solution at slower rate. However, at pH 6, initial k_{obs} for recovery of uranium in solution increased over that at pH 5. With all other conditions unchanged, carbonate speciation may contribute to this phenomenon. As pH approaches 6, more carbonate species exist as HCO_3^- instead of $H_2CO_{3(aq)}$ than at pH 5. Naturally dissolved HCO_3^- and CO_3^{2-} in pH 6 solution are about 501 μM and 0.025 μM, respectively. Dominant U(VI) species at pH 6, $(UO_2)_3(OH)_5^{+}$, may react with HCO_3^- or CO_3^{2-} and speed up U(VI) recovery by forming uncharged species such as $UO_2(CO_3)_{(aq)}$, $UO_2(OH)_{2(aq)}$, and other more mobile species [27].

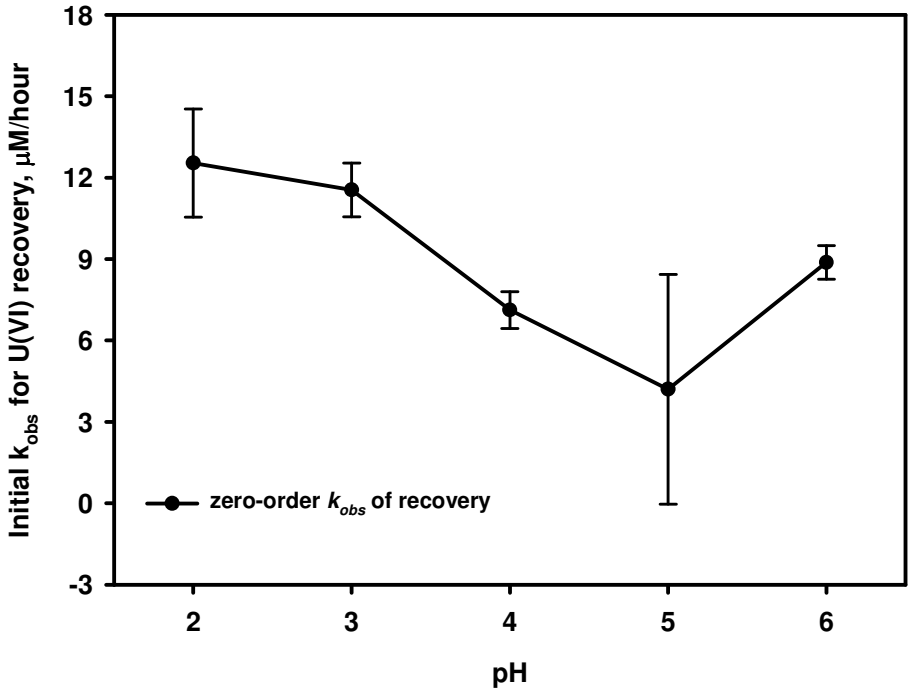

Figure 6. Initial recovery rate of removed U(VI) varies with pH. Recovery of U(VI) is a zero-order reaction during the beginning of the recovery, and k_{obs} was calculated from

zero-order linear fitting. Error bars represent the standard deviation of duplicate reactors.

Implications for Electrode-based U(VI) Removal. The findings presented here demonstrate that an electrode-based remedial approach utilizing low external potentials may be feasible for the removal and recovery of uranium from the low pH groundwater in FRC Area 3. Moreover, the data show that uranium may be removed and recovered from water across a broad range of aqueous geochemical conditions. Although low pH and the presence of aluminum or magnesium slow U(VI) removal rates, the application of higher electrode potentials overcomes this removal rate loss. Bioremediation studies in FRC Area 3 show that uranium removal is optimal with pretreatment of groundwater for nitrate removal [12] as it is a competitive electron acceptor for bacteria and may reduce U(VI) reduction rates [28, 29]. Neutralization of the groundwater is another prerequisite for biostimulation of U(VI) reduction to occur. After these pretreatment steps, uranium that has been reductively precipitated is still vulnerable to environmental factors that may remobilize the metal, such as oxygen [30, 31] and carbonate/bicarbonate [12, 32, 33]. Electrode-based remediation of U(VI) may simplify the remedial approach and offer the opportunity to remove the contaminant from the subsurface permanently by extracting uranium from the electrodes *in situ* or temporarily removing the electrodes to the surface for recovery. Moreover, electrode potential is readily adjustable, in real-time for changing subsurface geochemical conditions. The results suggest that an electrode-based remedial approach may be also suitable for a broad range of dissolved metals contaminants.

ACKNOWLEDGEMENTS

This material is based upon work supported by the Department of Energy, Biological and Environmental Research. Environmental Remediation Science Program under award DE-PS02-07ER07-18

Supporting Information. Linear fitting of U(VI) removal first-order kinetics, U(VI)

speciation distribution as a function of pH, Values of radii, mobility and diffusion coefficients of major ions, and Al^{3+} and Mg^{2+} removal at 5.0 V. This material is available free of charge via the Internet at http://pubs.acs.org.

REFERENCES

(1) Sun, M.; Yan, F.; Zhang, R. L.; Reible, D. D.; Lowry, G. V.; Gregory, K. B. Redox control and hydrogen production in sediment caps using carbon cloth electrodes. *Environ. Sci. Technol.* **2010**, *44* (21), 8209-8215.

(2) Gregory, K. B.; Lovley, D. R. Remediation and recovery of uranium from contaminated subsurface environments with electrodes. *Environ. Sci. Technol.* **2005**, *39* (22), 8943-8947.

(3) Gregory, K. B.; Bond, D. R.; Lovley, D. R. Graphite electrodes as electron donors for anaerobic respiration. *Environ. Microbiol.* **2004**, *6* (6), 596-604.

(4) Strycharz, S. M.; Woodard, T. L.; Johnson, J. P.; Nevin, K. P.; Sanford, R. A.; Loffler, F. E.; Lovley, D. R. Graphite electrode as a sole electron donor for reductive dechlorination of tetrachlorethene by *Geobacter lovleyi*. *Appl. Environ. Microbiol.* **2008**, *74* (19), 5943-5947.

(5) Aulenta, F.; Canosa, A.; Reale, P.; Rossetti, S.; Panero, S.; Majone, M. Microbial reductive dechlorination of trichloroethene to ethene with electrodes serving as electron donors without the external addition of redox mediators. *Biotechnol. Bioeng.* **2009**, *103* (1), 85-91.

(6) Thrash, J. C.; Van Trump, J. I.; Weber, K. A.; Miller, E.; Achenbach, L. A.; Coates, J. D. Electrochemical stimulation of microbial perchlorate reduction. *Environ. Sci. Technol.* **2007**, *41* (5), 1740-1746.

(7) Alfarra, A.; Frackowiak, E.; Beguin, F. Mechanism of lithium electrosorption by activated carbons. *Electrochim. Acta* **2002**, *47* (10), 1545-1553.

(8) Gabelich, C. J.; Tran, T. D.; Suffet, I. H. Electrosorption of inorganic salts from aqueous solution using carbon aerogels. *Environ. Sci. Technol.* **2002**, *36* (13), 3010-3019.

(9) Gao, Y.; Pan, L. K.; Li, H. B.; Zhang, Y. P.; Zhang, Z. J.; Chen, Y. W.; Sun, Z. Electrosorption behavior of cations with carbon nanotubes and carbon nanofibres composite film electrodes. *Thin Solid Films* **2009**, *517* (5), 1616-1619.

(10) Xu, P.; Drewes, J. E.; Heil, D.; Wang, G. Treatment of brackish produced water using carbon aerogel-based capacitive deionization technology. *Water Res.* **2008**, *42* (10-11), 2605-2617.

(11) Gu, B. H.; Brooks, S. C.; Roh, Y.; Jardine, P. M. Geochemical reactions and dynamics during titration of a contaminated groundwater with high uranium, aluminum, and calcium. *Geochim. Cosmochim. Acta* **2003**, *67* (15), 2749-2761.

(12) Zhou, P.; Gu, B. H. Extraction of oxidized and reduced forms of uranium from contaminated soils: Effects of carbonate concentration and pH. *Environ. Sci. Technol.* **2005**, *39* (12), 4435-4440.

(13) Wu, W. M.; Carley, J.; Fienen, M.; Mehlhorn, T.; Lowe, K.; Nyman, J.; Luo, J.; Gentile, M. E.; Rajan, R.; Wagner, D.; Hickey, R. F.; Gu, B. H.; Watson, D.; Cirpka, O. A.; Kitanidis,

P. K.; Jardine, P. M.; Criddle, C. S. Pilot-scale *in situ* bioremediation of uranium in a highly contaminated aquifer. 1. Conditioning of a treatment zone. *Environ. Sci. Technol.* **2006**, *40* (12), 3978-3985.

(14) Xu, Y.; Zondlo, J. W.; Finklea, H. O.; Brennsteiner, A. Electrosorption of uranium on carbon fibers as a means of environmental remediation. *Fuel Process. Technol.* **2000**, *68* (3), 189-208.

(15) Farmer, J. C.; Bahowick, S. M.; Harrar, J. E.; Fix, D. V.; Martinelli, R. E.; Vu, A. K.; Carroll, K. L. Electrosorption of chromium ions on carbon aerogel electrodes as a means of remediating ground water. *Energy Fuels* **1997**, *11* (2), 337-347.

(16) Ying, T. Y.; Yang, K. L.; Yiacoumi, S.; Tsouris, C. Electrosorption of ions from aqueous solutions by nanostructured carbon aerogel. *J. Colloid Interface Sci.* **2002**, *250* (1), 18-27.

(17) Bard, A. J.; Faulkner, L. R. *Electrochemical methods: fundamentals and applications*; John Wiley & Sons, Inc.: New York, 2001.

(18) Newman, J.; Thomas-Alyea, K. E. *Electrochemical systems*; Wiley Interscience: Hoboken, NJ, 2004.

(19) Seron, A.; Benaddi, H.; Beguin, F.; Frackowiak, E.; Bretelle, J. L.; Thiry, M. C.; Bandosz, T. J.; Jagiello, J.; Schwarz, J. A. Sorption and desorption of lithium ions from activated carbons. *Carbon* **1996**, *34* (4), 481-487.

(20) Meena, A. K.; Mishra, G. K.; Rai, P. K.; Rajagopal, C.; Nagar, P. N. Removal of heavy metal ions from aqueous solutions using carbon aerogel as an adsorbent. *J. Hazard. Mater.* **2005**, *122* (1-2), 161-170.

(21) Farmer, J. C.; Fix, D. V.; Mack, G. V.; Pekala, R. W.; Poco, J. F. Capacitive deionization of NaCl and $NaNO_3$ solutions with carbon aerogel electrodes. *J. Electrochem. Soc.* **1996**, *143* (1), 159-169.

(22) Farmer, J. C.; Fix, D. V.; Mack, G. V.; Pekala, R. W.; Poco, J. F. Capacitive deionization of NH_4ClO_4 solutions with carbon aerogel electrodes. *J. Appl. Electrochem.* **1996**, *26* (10), 1007-1018.

(23) Wang, S.; Wang, D. Z.; Ji, L. J.; Gong, Q. M.; Zhu, Y. F.; Liang, J. Equilibrium and kinetic studies on the removal of NaCl from aqueous solutions by electrosorption on carbon nanotube electrodes. *Sep. Purif. Technol.* **2007**, *58* (1), 12-16.

(24) Hansen, P. G. The conditions for electrodeposition of insoluble hydroxides at a cathode surface - a theoretical investigation. *J. Inorg. Nucl. Chem.* **1959**, *12* (1-2), 30-37.

(25) Benjamin, M. M. *Water chemistry*; McGraw Hill: New York, 2002.

(26) Haynes, W. M.; Lide, D. R., Eds. *Solubility product constants*; CRC Press: 2011-2012.

(27) Suzuki, Y.; Banfield, J. F. Geomicrobiology of uranium. In *Uranium: mineralogy, geochemistry and the environment*; Burns, P. C.; Finch, R., Eds.; Mineralogical Society of America: Washington D.C., 1999.

(28) Istok, J. D.; Senko, J. M.; Krumholz, L. R.; Watson, D.; Bogle, M. A.; Peacock, A.; Chang, Y. J.; White, D. C. *In situ* bioreduction of technetium and uranium in a nitrate-contaminated aquifer. *Environ. Sci. Technol.* **2004**, *38* (2), 468-475.

(29) Edwards, L.; Kusel, K.; Drake, H.; Kostka, J. E. Electron flow in acidic subsurface sediments co-contaminated with nitrate and uranium. *Geochim. Cosmochim. Acta* **2007**, *71* (3), 643-654.

(30) Wu, W. M.; Carley, J.; Luo, J.; Ginder-Vogel, M. A.; Cardenas, E.; Leigh, M. B.; Hwang, C. C.; Kelly, S. D.; Ruan, C. M.; Wu, L. Y.; Van Nostrand, J.; Gentry, T.; Lowe, K.; Mehlhorn, T.; Carroll, S.; Luo, W. S.; Fields, M. W.; Gu, B. H.; Watson, D.; Kemner, K. M.; Marsh, T.; Tiedje, J.; Zhou, J. Z.; Fendorf, S.; Kitanidis, P. K.; Jardine, P. M.; Criddle, C. S. *In situ* bioreduction of uranium (VI) to submicromolar levels and reoxidation by dissolved oxygen. *Environ. Sci. Technol.* **2007**, *41* (16), 5716-5723.

(31) Moon, H. S.; Komlos, J.; Jaffe, P. R. Uranium reoxidation in previously bioreduced sediment by dissolved oxygen and nitrate. *Environ. Sci. Technol.* **2007**, *41* (13), 4587-4592.

(32) Wan, J. M.; Tokunaga, T. K.; Brodie, E.; Wang, Z. M.; Zheng, Z. P.; Herman, D.; Hazen, T. C.; Firestone, M. K.; Sutton, S. R. Reoxidation of bioreduced uranium under reducing conditions. *Environ. Sci. Technol.* **2005**, *39* (16), 6162-6169.

(33) Noubactep, C.; Meinrath, G.; Dietrich, P.; Merkel, B. Mitigating uranium in groundwater: Prospects and limitations. *Environ. Sci. Technol.* **2003**, *37* (18), 4304-4308.

TOC-Art

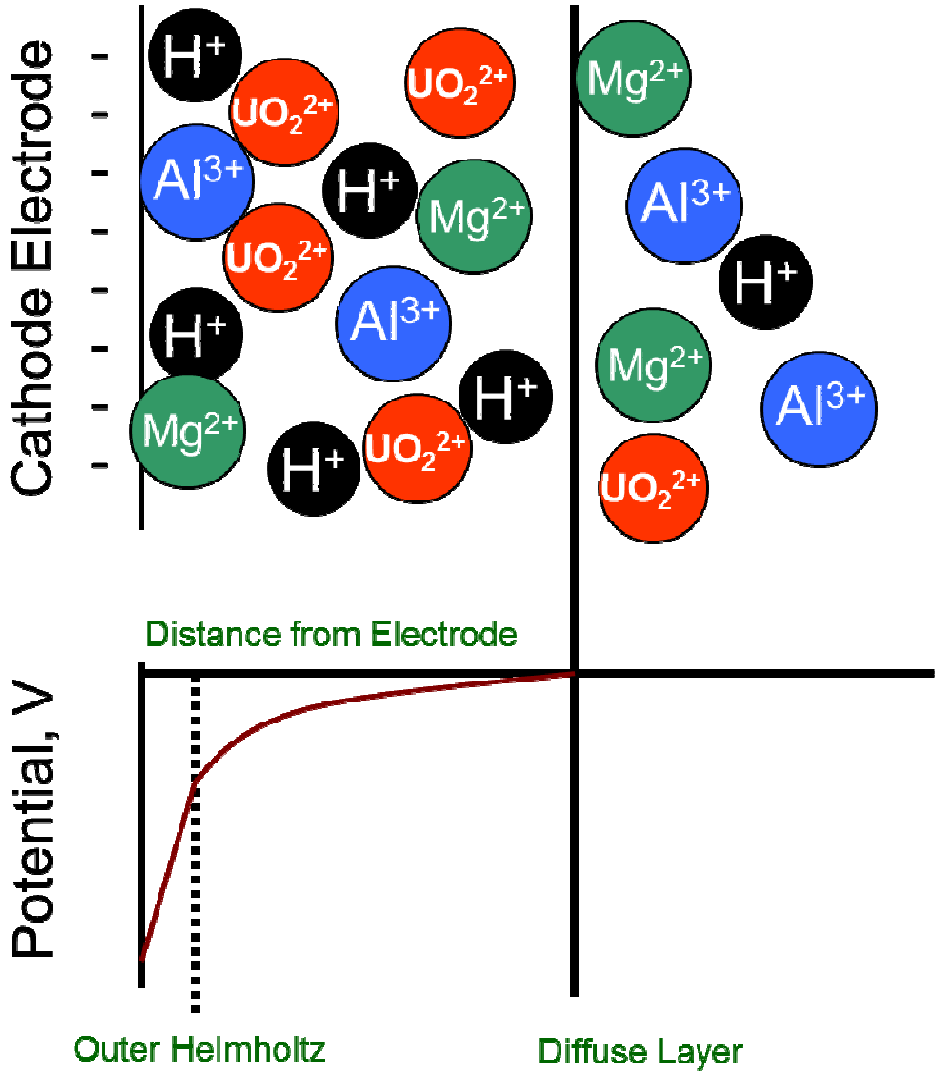
Cathode Electrode
H+
UO2 2+
Al3+
Mg2+
Distance from Electrode
Potential, V
Outer Helmholtz
Diffuse Layer

Removal and Recovery of Pertechnetate from Acidic Solutions with Graphite Electrodes

4.1 ABSTRACT

Electrode-stimulated bioremediation is an alternative approach for control, removal, and recovery of soluble uranium (UO_2^{2+}) cations from groundwater. In the case of uranium, contaminant cations become entrapped in the electrical double layer prior to bacterial reduction and stabilization of uranium on the electrode surface. Pertechnetate, a common co-contaminant with uranium is predominantly found as the TcO_4^- anion. Experiments were performed to explore the potential for removal and recovery of pertechnetate from water using polarized graphite electrodes and determine the effect of common and variable environmental factors (pH, applied potential, and organic matter) for operational consideration. Experiments show that pertechnetate may be removed with an externally-applied potential as low as 1.5 V. The observed removal rate for technetium increased with higher externally applied potential, but with diminishing returns above 2.5 V. Technetium was readily recovered in solution after removing the external potential. The extent of technetium removal and recovery was also found to be strongly related to pH. Technetium was removed and recovered faster and to a greater extent with higher pH. The finding that Tc was mainly recovered from the cathode suggests that the primary removal mechanism was electroreduction at the electrode surface at 2.5 V. Ionic strength and humic acid did not exhibit an impact on technetium removal rates over the range of conditions studied. Results show that technetium is readily removed and recovered from contaminated groundwater and that electrode-based remediation may be a potential solution for permanent restoration of radionuclide contaminated subsurfaces.

4.2 INTRODUCTION

As a fission production of uranium, technetium is one of the major contaminants in several Department of Energy sites, such as Oak Ridge National Laboratory and the Paducah Gaseous Diffusion Plant. ^{99}Tc is the most common technetium isotope, with a half life of 2.14×10^5 years [1]. In aqueous systems, technetium primarily exists as pertechnetate, or $Tc(VII)O_4^-$, the most oxidized species. Pertechnetate has poor affinity to sediments [2], soil, and bacteria [3]. Its high mobility and toxicity after ingestion makes it a contaminant of great concern for both environmental and human health. *In situ* remediation of Tc is primarily carried out by reductive immobilization. This process involves stimulating the biotic or abiotic reduction of Tc(VII) to Tc(IV), which has much lower solubility. Reduction of Tc also increases its adsorption onto soil by three orders of magnitude [4].

Abiotic reduction of pertechnetate for environmental restoration is encouraged through the introduction of bulk chemical reductant into the subsurface. This is usually achieved through construction of a permeable reactive barrier (PRB) in the path of groundwater flow and back-filling with reductant. Bulk reductants for abiotic reductive immobilization include zero-valent iron (ZVI), ferrous iron, or sulfide. The most common bulk reductant in PRB is ZVI which has previously been proposed for the reductive precipitation of Tc [5]. In addition, Tc may be reduced by adsorbed or precipitated Fe(II) [6], or Fe(II)-bearing minerals [7]. Biotic reductive immobilization is stimulated by the addition of organic electron donor into the subsurface to enhance the growth of metal-reducing bacteria that catalyze Tc reduction *in situ* [8-12].

Despite the effectiveness of both biotic and abiotic reductive immobilization of Tc, the immobilized forms of Tc still reside in the subsurface where they may be re-oxidized and re-mobilized by common groundwater constituents and environmental processes. For example, bioreduced Tc(IV) oxide, $TcO_2 \bullet nH_2O$, was found to be released back to the aqueous phase as reducing conditions dissipated [2] and was re-oxidized upon exposure to air/oxygen [13, 14]. The potential for *in situ* remobilization of Tc following reduction in reactive barriers raises concerns about long-term stabilization and risk abatement of these conventional approaches. Indeed, the risk associated with Tc contamination remains as long as the radionuclide persists in the subsurface. An ideal approach for remediation of radionuclide contamination would enable the extraction of the metal from the subsurface for permanent risk abatement.

Recently, an electrode-based approach for removal of radionuclides from groundwater was demonstrated to enable recovery of the metal from the subsurface. A graphite electrode carrying a potentiostat-poised cathodic potential, rapidly removed U(VI) from contaminated groundwater under circumneutral pH. The uranium was readily recovered in solution once potential was removed from the electrode [15]. Similarly, findings presented in **Chapter 3** show that U may also be removed and recovered from acidic groundwater. These findings demonstrate that an electrode-based remedial approach may be an ideal option for abatement of subsurface uranium contamination and imply that a similar approach may also be suitable for technetium.

Previous studies have examined the reaction of Tc on electrodes. Farrell and coworkers reported that anodically polarized magnetite could electrosorb Tc(VII) reduce it to Tc(IV), possibly by donating electrons to Tc(VII) and being reduced to maghemite [16]. Although effective for

immobilization of Tc, magnetite is not an ideal electrode material. It may undergo spontaneous reordering to maghemite or biological dissolution. Graphite is more stable under environmental conditions and less costly than magnetite.

The objectives of this research are to: a) demonstrate pertechnetate removal and recovery using graphite electrodes, and b) determine the impact of environmental conditions on removal rates and extents. Experiments were designed to evaluate the feasibility of Tc remediation of Tc from Area 3 groundwater at Oak Ridge National Laboratory. The groundwater has characteristically high concentrations of radionuclide contaminants in a heterogeneous system that is buffered at a low pH (pH < 4) [17]. Stimulated *in situ* bioremediation and ZVI-based permeable reactive barriers have both proven to be challenging in the acidic groundwater in Area 3. The electrode-based remedial approach may be an effective alternative under these challenging conditions.

Although *in situ* electrode-based remediation offers significant advantages over conventional remediation, it is relatively nascent technology and many questions remain about its applicability and effectiveness under complex chemical and geochemical conditions experienced in the environment. For example, similar to U(VI) removal, applied potential may also influence the rate of Tc(VII) removal rate. Additionally, high ionic strength affects conductance of groundwater and potential on electrodes, and it may also cause change in Tc(VII) removal rate. And major dissolved organic constituents may interact with electrodes and interfere Tc(VII) removal [18]. While U(VI) can readily be recovered from electrodes across a broad range of pH [19], by removing the electrostatic force, it remains to be seen whether Tc(VII) can be as easily recovered. Removing the external potential provides a means by which the electrode may be

regenerated and Tc recovered from the subsurface, thereby offering a unique opportunity to permanently restore Tc contaminated groundwater. Herein, we describe experiments that investigate whether Tc(VII) can be effectively removed and recovered from groundwater using polarized graphite electrode, and how common aqueous geochemical factors and operational conditions may impact the remedial design.

4.3 MATERIALS AND METHODS

Batch, 2-electrode experiments were performed in covered, 250 mL beakers containing 150mL of synthetic contaminated solution. Electrodes were cylindrical graphite rods (Graphite Engineering & Sales, Co., Greenville, MI) with a diameter of 2.54 cm and length of 7.62 cm. The electrodes were connected to each lead via neoprene-coated cables (Teledyne Impulse, San Diego, CA). The electrodes were connected to the power supply by neoprene-coated cables and connectors (Teledyne Impulse, San Diego, CA) affixed with silver epoxy (Epoxy Technology, Billerica, MA). 40 nCi/L (23.8 nmol/L) ammonium pertechnetate (NH_4TcO_4) solution was prepared by adding 0.6 mL 10 μCi/L (6 μmol/L) NH_4TcO_4 stock to 150 mL solution at pHs pre-adjusted using HNO_3 or NaOH solution. Buffered solutions were prepared from four buffer agent: sodium phosphate monobasic (pK_a=2.15), sodium bicarbonate (pK_a=6.35), sodium phosphate (pK_a=10.3), and sodium carbonate (pK_a=12.3). Each solution contained 50 mM of buffer ions, and was amended with $NaNO_3$ as needed to ensure an ionic strength of 0.3 M. pH of buffered solutions was adjusted with their corresponding acid solutions. Ionic strength of solutions was adjusted with $NaNO_3$ as needed. Different concentrations of humic acid (Acros Organics, Morris Plains, NJ) were added as desired. All experiments were conducted at aerobic condition. Duplicate reactors were stirred at 300 rpm on a multi-position stir plate (Variomag

Poly 15, Thermo Scientific). External potential between the electrodes was established using an Agilent E3620A power supplies (Englewood, CO). Currents were measured via a multi-channel multimeter. Liquid samples were taken at intervals to monitor pH and ^{99}Tc concentration. Tc on electrode was dissolved with 50 mM Na_2CO_3 solution and collected for quantification. ^{99}Tc concentration was measured with Liquid Scintillation Counter (LSC) (LS6500 Multi-Purpose Scintillation Counter, Beckman Coulter).

4.4 Results and Discussion

4.4.1 Influence of Applied Potential on Tc Removal

Removal of pertechnetate from solution containing 40 nCi/L NH_4TcO_4 at pH 3, a concentration level commonly observed at Area 3, was first studied at different applied external potential. Removal of ^{99}Tc was strongly influenced by external potential. **Figure 4.1** illustrates a predictable trend that as potential increased, removal of pertechnetate became faster. Little removal was observed at 0-1.0 V. As potential increased to 1.5 V, about 50% of ^{99}Tc was removed after 24 hours. A further potential increase to 2.0 V resulted in 79.8% removal within 8 hours, and 88.6% removal was achieved within 8 hours at 2.5 V. Similar trend has been observed in electrode-based U(VI) removal in **Chapter 3**. Possible reason for this trend is that increasing the applied potential will also change the potential distribution in the EDL by enhancing cathodic potential [20]. As potential gradient between cathode and bulk solution increases, ions are expected to migrate faster towards the electrodes according to Eq. 3.2. Therefore a faster reaction on the electrode is also expected. The impact of potential is similar to what has been reported for pertechnetate removal with anodically polarized magnetite [16]. However, beyond 2.5 V, the benefit of additional potential diminished and no significant

difference in removal rate or extent was observed for pertechnetate removal at 2.5-5.0 V.

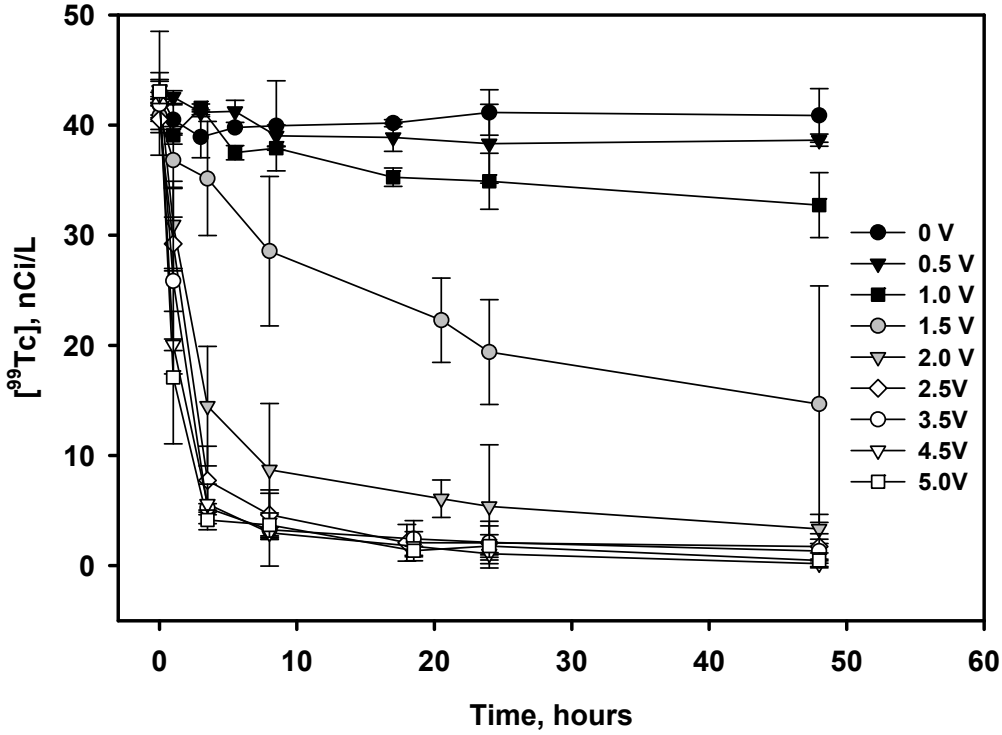

Figure 4.1 Removal of Tc(VII) from pH 3, 40 nCi/L Tc(VII) solution at different external potentials. The data markers represent the average and range of duplicate experiments.

Observed pertechnetate removal rates were calculated by fitting concentration versus time into first-order kinetic equation. **Figure 4.2** shows that removal rate reached a plateau at 2.5-5.0 V. The highest k_{obs} was around 0.3 hr^{-1}, which is three orders of magnitude higher than what has been reported for pertechnetate removal with adsorbed Fe(II) at similar concentration [6]. The removal may be limited by electron-transfer on electrode surface to reduce Tc(VII), or affected by hydrogen evolution on cathode at higher potentials. Based on this result, 2.5 V were selected as applied potential for future Tc removal studies.

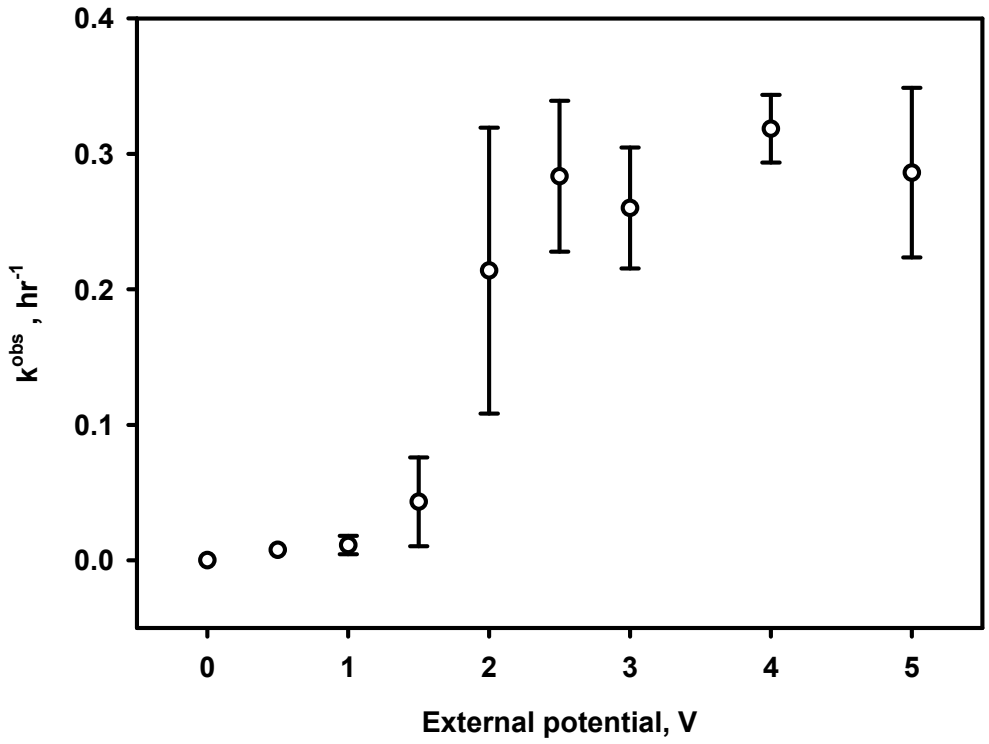

Figure 4.2 Change of first-order rate constant with external potentials from pH 3, 40 nCi/L Tc(VII) solution.

Since diminishing return on external potential above 2.5V was observed for Tc removal, another experiment was performed to measure potential of anode and cathode versus Ag/AgCl electrode (0.20 V versus standard hydrogen electrode) by stepwisely increasing externally applied potential from 0 V to 5.0 V, same as what has been previously describe in **Figure 3.6**. It was found that at 1.5 V, potential of cathode stabilized at around -0.078 V versus Ag/AgCl, or 0.122 V versus SHE, while overall potential between the electrode did not exceed 1.0 V, which is not sufficient for water electrolysis. The reduction potential of Tc(VII) to Tc(IV) is 0.343 V versus standard hydrogen electrode (SHE) at pH 3 (**Figure 2.4**). Therefore, Tc reduction is feasible with an external potential at 1.5 V and it is possible that electroreduction of Tc was the principle mechanism of removal. As externally applied potential continued to increase from 2.5 V to 5.0 V, same as what has been shown in **Figure 3.6**, cathode potential did not increase dramatically.

However, real potential between anode and cathode exceeded 1.23 V, the threshold potential for water hydrolysis [21].

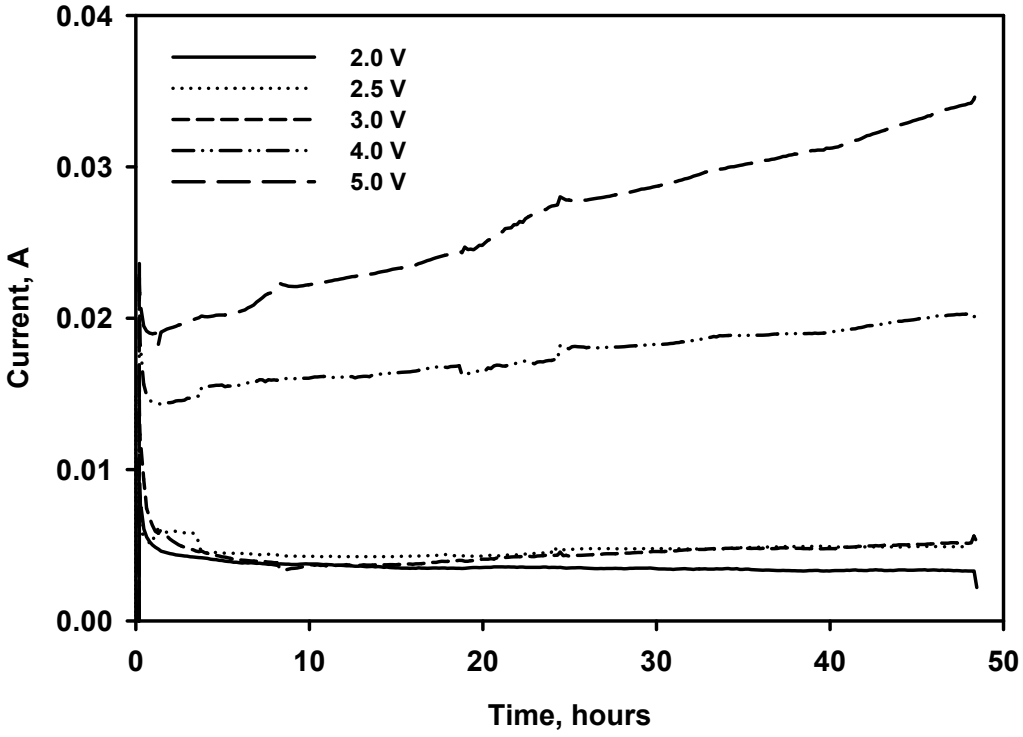

Figure 4.3 Change of current versus time during the removal of Tc(VII) at varied external potentials from pH 3, 40 nCi/L Tc(VII) solution.

Figure 4.3 shows that currents began to increase at potential beyond 2.0 V, which further suggests that side reactions, likely water hydrolysis occurred. As applied potential was partial used in side reactions, less electrons were available for Tc reduction. Moreover, pertechnetate may be prevented from approaching electrode surfaces by gas formation at the electrode surface and getting reduced [19]. Therefore, it is not surprising that pertechnetate removal did not become faster as potential exceed 2.5 V.

4.4.2 Tc Recovery after Removal at Different Potentials

The ability to recover Tc from the electrodes following removal is a chief advantage of the electrode based approach. Recovery of Tc from the electrodes was examined after 48 hours of pertechnetate removal shown in **Figure 4.1**, anode and cathode were taken out from the reactors and directly put into separate containers with polarity removed. They were rinsed with buffer reagents for Tc recovery. However, whether Tc was electrosorbed or electro-reduced affects the easiness of Tc recovery. Recovery method, especially electrode rinsing reagents should be selected to meet the most difficult Tc recovery scenario. Here is how electrode regeneration method was determined.

Pertechnetate exist as $Tc(VII)O_4^-$ even under acidic conditions (**Figure 2.4**), which favors anodic migration. Tc(VII) is the most oxidized form of Tc and anode is an oxidizing electrode. No interactions other than electrosorption could be expected between Tc(VII) and anode. If $Tc(VII)O_4^-$ is electrosorbed by anode, as suggested by recovery of electrosorbed $U(VI)O_2^{2+}$ from cathode [19], removing poise from the electrodes will cause the recovery of Tc(VII) from electrode since the anode losses electrostatic force to attract and trap Tc(VII) in the double layer.

If Tc was recovered from cathode, it should be reduced because as an anion, the only possible reason for cathodic Tc recovery is the reduction of Tc(VII) on cathode. If all Tc(VII) ($10^{-7.4}$ M) was reduced to Tc(IV) oxides and adsorbed on the electrode surface as postulated by other researchers [22], it may be recovered via re-solubilization of Tc(IV) or re-oxidation to Tc(VII). Re-solubilized Tc(IV) should be no higher than $10^{-8.4}$ M according to its solubility[1]:

$$TcO_2 \cdot 1.6H_2O_{(s)} \rightleftarrows 0.6H_2O_{(l)} + TcO(OH)_{2(aq)}, \text{ pK=-8.4} \qquad \text{Eq. 4.1}$$

Solubilization of Tc(IV) with water is considered to be slow at anaerobic condition [2]. However,

according to a recent study, in carbonate media, Tc(IV) exists as an electrically neutral aqueous species, $TcCO_3(OH)_2$, at pH 3 and E_H between +0.2 V and –0.4 V [23]. The same Tc species at pH 3 was reported by another group of researchers, but between E_H value of +0.4V and -0.17V [24]. Therefore, rinsing the electrodes with carbonate media is probably an effective way of solubilizing Tc. Tc may also return to the solution via re-oxidation. Previous studies have already shown that re-oxidization of Tc(IV) by air is a major contribution to Tc re-immbolization [13, 14]. In order to determine which electrode played a major role in Tc removal, a 50 mM Na_2CO_3 solution was used to clean the electrodes along with ultrasonic cleansing. Since the experiments were run at open-to-atmosphere condition, it is expected that most reduced Tc(IV) can be re-oxidized and/or re-mobilized during this cleansing process.

After the electrodes were cleaned 20 minutes ultrasonically and repeated 5 times, washing solutions were collected and measured to calculate the mass balance of Tc. As shown in **Table 4.1**, no obvious trend was observed in terms of the amount of Tc recovered from anode and cathode at different potentials. Although total recovered Tc is far less than the amount initially introduced, most recovered Tc was from cathode. Tc recovered from anode is almost negligible.

If Tc(VII) is electrosorbed onto anode, the recovery is expected to be fast, as observed in U recovery [19]. Therefore, the results suggest that anode had little interaction with Tc during the removal; otherwise, Tc should recover immediately from the anode to the solution if it were removed via electrosorption.

Therefore, Tc(VII) should be reduced on the cathode during the removal. The reason why

Tc(VII), an anion, was reduced on cathode may be explained as follows. On the cathode side, although electromigration favors the collection of cations near the cathode, the cathodic electric double layer dominated by cations also contain small amount of counterions ($Tc(VII)O_4^-$, OH^- in this case). When cathode potential favors Tc(VII) reduction, Tc(VII) can accept electrons and be removed from the cathode. As Tc(VII) continues to be removed, electric charge in the electric double layer became unbalanced, so does Tc(VII) concentration gradient. Therefore, more Tc(VII) enters the cathodic electric double layer to the re-balance the equilibrium, and gets further reduced by the cathode.

Since remaining Tc concentration in bulk solution was low and no precipitate was observed, it is hypothesized that un-recovered Tc residual remained on cathode. 33.5%-56.5% recovery of total Tc demonstrates that some reduced Tc was not easily re-mobilized by these recovery methods.

Table 4.1 Mass balance (%) on recovery of ^{99}Tc from solutions after 48 hours of removal. Total amount of ^{99}Tc introduced was 6 nCi (defined as 100%). Electrodes were ultrasonically cleaned in 50mM Na_2CO_3 solution for 5 times, with 20 minutes each. Data are average of duplicate samples.

Potential /V	Anode	Cathode	Total on electrodes	Total in solution	Sum
2.0	0.68	47.83	48.50	8.00	56.50
3.0	5.33	25.17	30.33	3.17	33.50
4.0	0.30	39.00	39.33	0.43	39.83
5.0	0.57	38.50	39.17	1.13	40.17

4.4.3 Influence of Unbuffered pH on Tc Removal and Recovery

Reduction of Tc(VII) to insoluble Tc(IV) involves both electrons and protons [1], as shown below:

$$TcO_4^- + 4H^+ + 3e \rightleftarrows 0.4H_2O_{(l)} + TcO_2 \cdot 1.6H_2O_{(s)} \qquad \text{Eq. 4.2}$$

Therefore, pH is also expected to influence Tc removal with poised electrodes, and a group of experiments were conducted to investigate the impact from pH. To ensure the conductivity of

solution at neutral pH, 0.1 M $NaNO_3$ was added to all studied pH conditions as supporting electrolyte. No buffer reagent was amended. As shown in **Figure 4.4(a)**, unbuffered pH had no significant impact on pertechnetate removal at 2.5 V. 38.6%-68.6% of total Tc was removed within the first 1 hour of reaction. Majority of the removal was completed within the first 5 hours. During the removal process, pH of the solutions all shifted towards neutral (**Figure 4.4(b)**), especially for alkaline solutions, which indicates that water hydrolysis or some other side reactions probably occurred under these conditions. Since Tc was poorly recovered by simple extraction from electrodes, recovery process of this experiment was initiated by reversing the polarity of the electrodes, so that reduced Tc may be re-oxidized on the former cathode. After 24 hours of removal, polarity of anode and cathode was immediately reversed and maintained for 1 hour for solutions with pH 2-9. Percentage of recovered Tc within 1 hour ranged between 52.4% and 85.9%, but had little correlation with pH. Comparing Tc recovery with Tc removal within the first 1 hour of reaction, it was found that recovery process was slightly faster than removal within studied pH range.

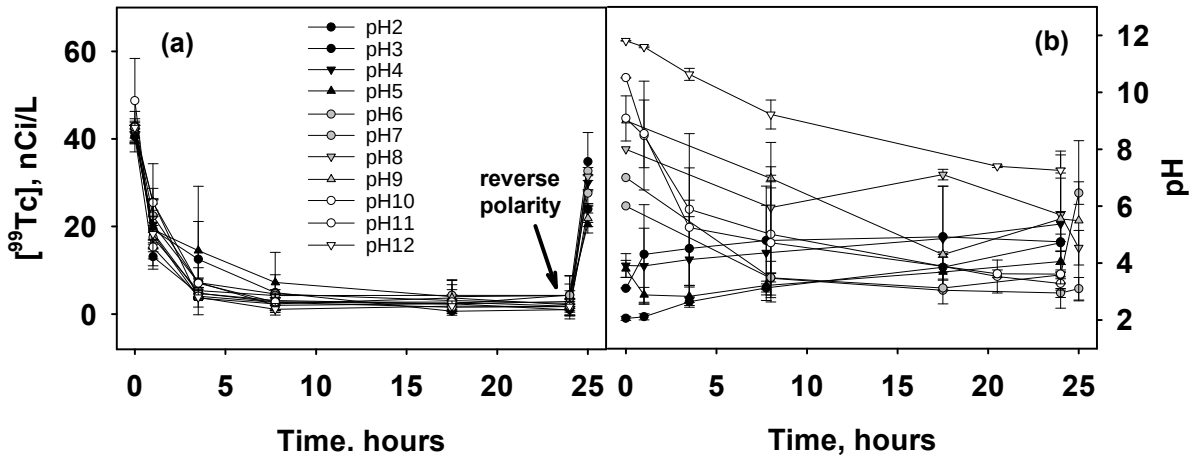

Figure 4.4 (a) Removal of Tc(VII) from unbuffered 40 nCi/L Tc(VII) solution at 2.5 V at different pHs. 0.1 M $NaNO_3$ was added to the solutions as supporting electrolyte. Polarity of electrodes was reversed at hour 24 and remained for 1 hour. (b) pH change in unbuffered solutions during Tc(VII)

removal.

Table 4.2 Mass balance (%) on recovery of ^{99}Tc from solutions after 24 hours of reaction and 1 hour of polarity reverse (pH 6-9). Total amount of ^{99}Tc introduced was 6 nCi. Electrodes were ultrasonically cleaned in 50mM Na_2CO_3 solution for 5 times, with 20 minutes each. Data are average of duplicate samples.

pH	Anode	Cathode	Total on electrodes	Total in solution	Sum	Note
6	23.67	7.00	30.67	77.83	108.50	With 1 hr polarity reverse
7	21.50	6.67	28.33	65.83	94.00	
8	32.50	8.33	41.33	74.83	115.67	
9	41.17	9.17	50.50	52.17	102.50	
10	4.17	86.67	90.83	4.00	94.83	Without polarity reverse
11	2.33	76.83	79.17	4.33	83.50	
12	1.60	76.17	77.83	4.00	81.83	

After the polarity was reversed for 1 hour, electrodes were cleaned with 50 mM Na_2CO_3 solution. Mass balance of Tc recovery for pH 6-9 solutions was listed in **Table 4.2**. Reversing the polarity changes the anode potential to a cathodic potential. Therefore it is not surprising that most of the recovered Tc came from the former anode. About 94% to 116% of Tc was recovered, which is significantly higher than the recovery observed when only poise removal and no reverse polarity was used for Tc recovery (shown in **Table 4.1**). Therefore, reverse polarity for a short period of time may be a useful pretreatment step for regenerating the electrodes and recovering Tc from the groundwater. Electrodes from pH 10-12 solutions were directly rinsed with 50 mM Na_2CO_3 solution after 24 hours of reaction. **Table 4.2** shows that recovery of Tc from these electrodes pH 10-12 was not as high as process with polarity reversed. However, 81.8%-94.8% recovery at 2.5 V and pH 10-12 was still much higher than the recovery at pH 3 and 2.5 V. pH may to be an important factor during the recovery. Since the system was not buffered, the influence of pH may be interfered by side reactions. Therefore, another group of tests were conducted to examine the influence of pH in buffered systems.

4.4.4 Influence of Buffered pH on Tc Removal and Recovery

Pertechnetate was removed faster under buffered basic conditions (**Figure 4.5**), demonstrating that, as with U(VI) [19], pertechnetate removal rate is also influenced by pH. Possible reason for the discrepancy between **Figure 4.4(a) and 4.5** is that, in an unbuffered system, pH in close proximity of electrode may be different from in bulk solution due to the occurrence of side reactions such as hydrogen evolution. Comparing pH 2-12 solutions at a specific time during the removal, the difference in their pHs near the electrodes may be not as significant as that in the bulk solutions. From this perspective, the removal of pertechnetate proceeded at similar rate in the unbuffered systems. However, in buffered systems change of pH was controlled in a narrow range. Therefore, dissociation of buffer reagent can maintain a high proton concentration at acidic condition, and provide strong competition with pertechnetate for reactive sites on the electrode and electrons when at a sufficient potential for electrolysis. Under basic conditions, consumption of H^+ was controlled by the buffer reagent. Hydrogen production was expected to slow down and electrode surface should be more accessible to pertechnetate, resulting in relative faster removal at higher pH.

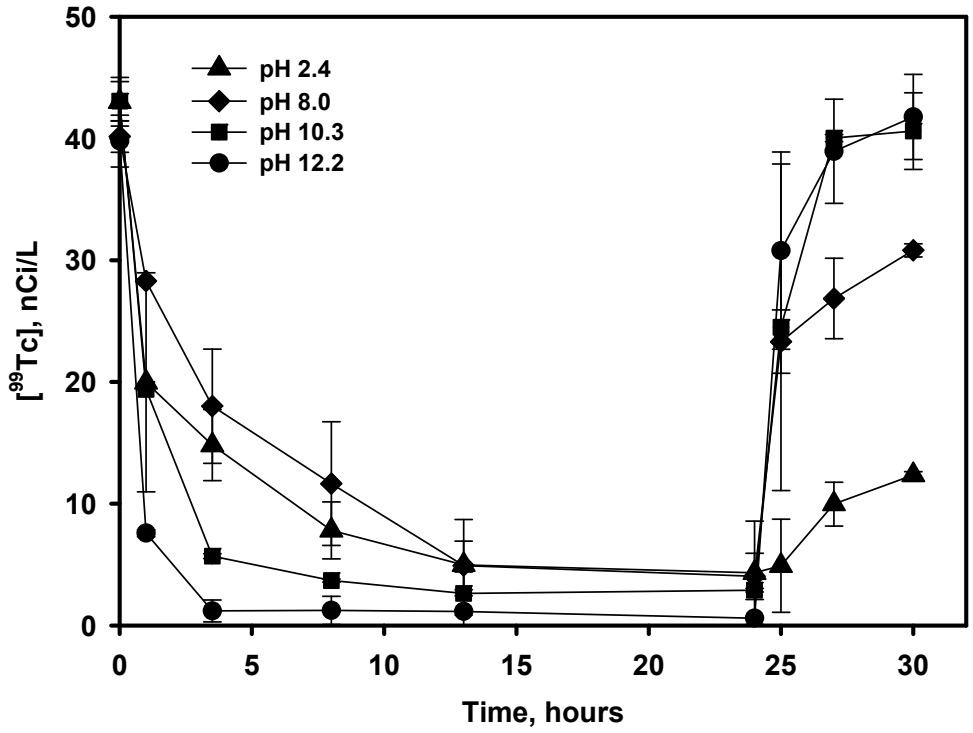

Figure 4.5 Removal of Tc(VII) from buffered 40 nCi/L Tc(VII) solution at 2.5 V at selected pHs. Power was removed after 24 hours.

The recovery of Tc from buffered systems began directly following removal of the external potential. Tc concentration in the bulk solutions was monitored for 5 additional hours. It was found that almost all Tc was recovered at pH 10.3 and 12.2 after 5 hours, whereas only 79.5% and 30.2% was achieved at pH 8.0 and 2.4, respectively. This may be related to complexation of reduced Tc with buffer ligands (carbonate or phosphate) at higher pH [1, 23].

4.4.5 Tc Removal with Repeated Addition

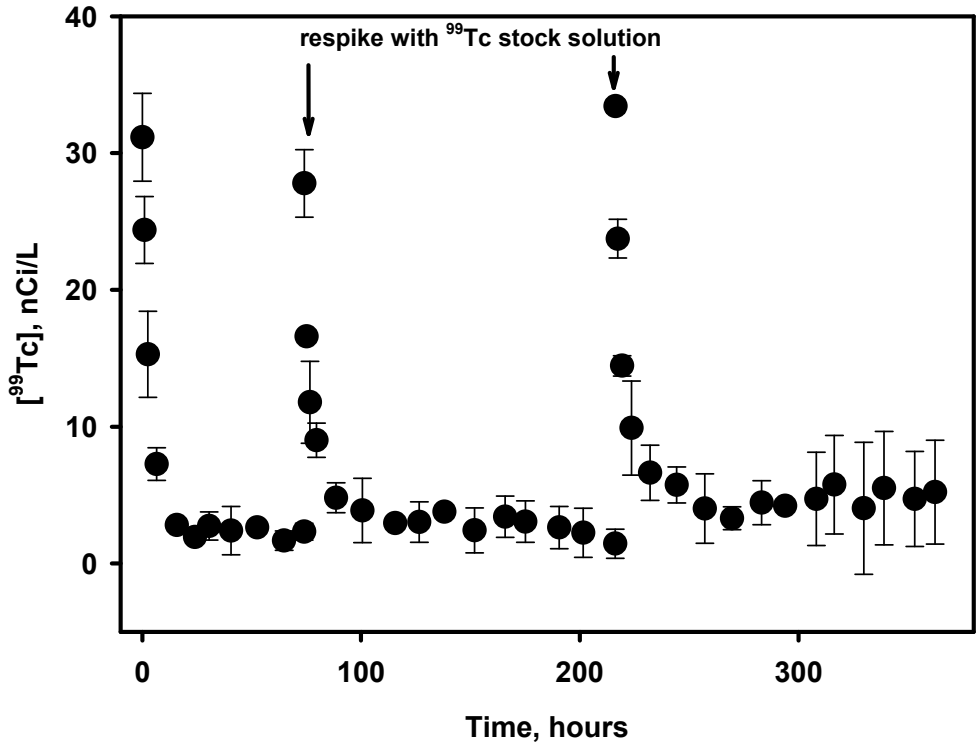

Figure 4.6 Semi-continuous removal of Tc(VII) at pH 3 and 2.5 V. The data markers represent the average and range of duplicate experiments.

A semi-continuous removal of pertechnetate was conducted at pH 3 and 2.5 V. The result was plotted in **Figure 4.6**. Two additional pertechnetate spikes were added from stock solution to the reactor after technetium concentration in bulk solution stabilized at a low concentration. Technetium was quickly removed from the solution at all three spikes. No significant decrease in either removal rate or extent was observed. This finding further supports the conclusion that Tc was reduced rather than merely electrosorbed. In an electro-reduction process, ideally the electrode is expected to have infinite capacity, as long as sufficient potential is provided, conductivity of the electrode does not decrease, and electrode is not covered by non-conductive precipitates. In an electrosorption process, the electrode has a limited capacity; as more ions are sorbed, the electrode could accommodate less ions, resulting in declining removal rate and extent

after each additional spike. This hypothesis for electrosorption has been verified in **Chapter 6**. Unlike similar removal extent with each subsequent spike in Tc electroreduction (**Figure 4.6**), U(VI) removal extent by electrosorption decreased with each subsequent spike (**Figure 6.3**)

4.4.6 INFLUENCE OF IONIC STRENGTH ON TC REMOVAL

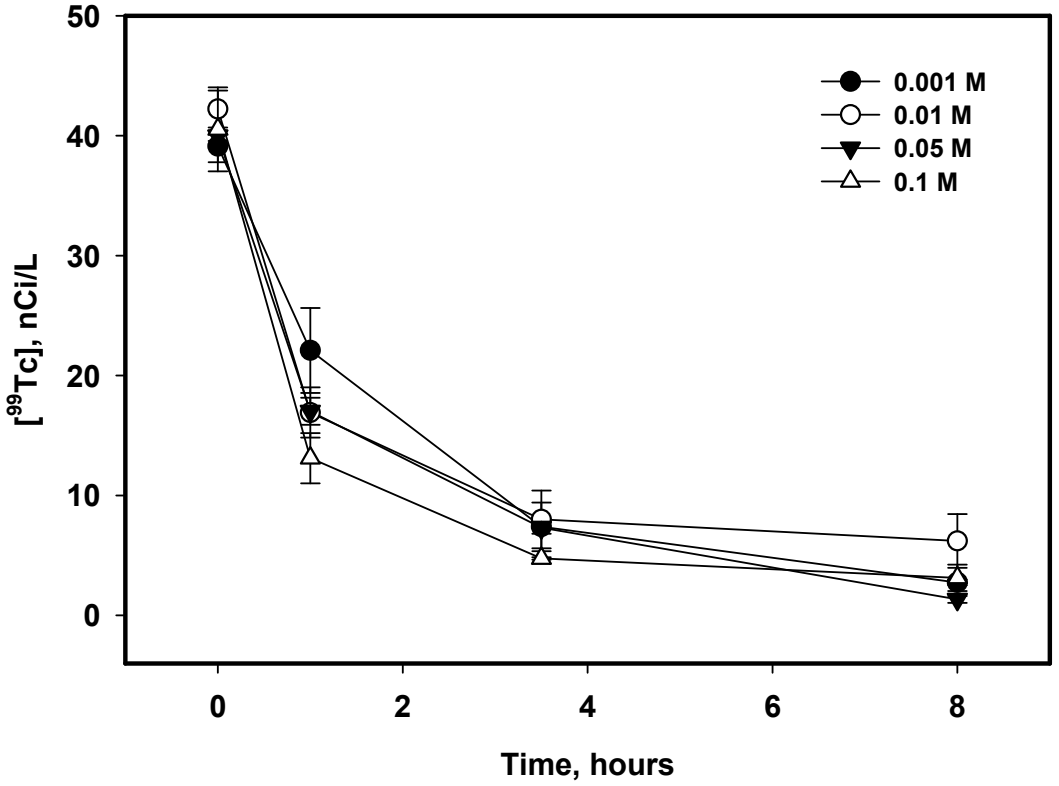

Figure 4.7 Removal of Tc with different ionic strength at pH 3 with 150 μM U(VI) solution. Ionic strength of the solutions was adjusted by adding desired concentration of $NaNO_3$; external potential applied was 2.5 V. Error bar represents standard deviation from duplicate experiments.

As discussed in **Chapter 3**, ionic strength is an important term determining ionic activity, solution conductance, and electrode capacity. However, ionic strength is found to have little impact on U(VI) removal rate. Tc removal in solutions with different ionic strength was also studied. It was found that same as U(VI) removal, Tc removal rate is not influenced by a change

in electrode capacity, or, not affected by ionic strength within 10^{-3} to 10^{-1} M range (**Figure 4.7**). Since Tc removal in this study is considered an electroreduction process, which has little relationship with electrode capacity, this result indicates that Tc removal is more vulnerable to influential factors that directly interact with electrode or affect electron transfer or distribution. Ionic strength, in this case, is not a factor of concern.

4.4.6 Influence of Humic Acid on Tc Removal

Another factor that may influence pertechnetate removal is the presence of humic acid. Previous studies on interaction between technetium and humic substances mostly support for a limited binding for both Tc(VII) and Tc(IV) [25]. Even with soil containing organic matter as high as 12%, obvious change in solubility of Tc(IV) was not observed [26]. However, a recent study revealed that humic substances could increase mobility of Tc(IV) in groundwater by forming strong complex at acidic pH [27]. Humic acid was added in concentrations between 5 and 25 mg/L, which are considered environmentally relevant concentrations, to study whether humic acid can affect pertechnetate removal with electrode-based method. Humic acid had no impact on Tc removal at pH 3 and 0.1 M ionic strength (**Figure 4.8**). Similar to the influence of humic acid on U removal (**Figure 3.11**), this result also indicates that humic acid is probably not a factor of concern for pertechnetate removal with electrodes within out studied concentration.

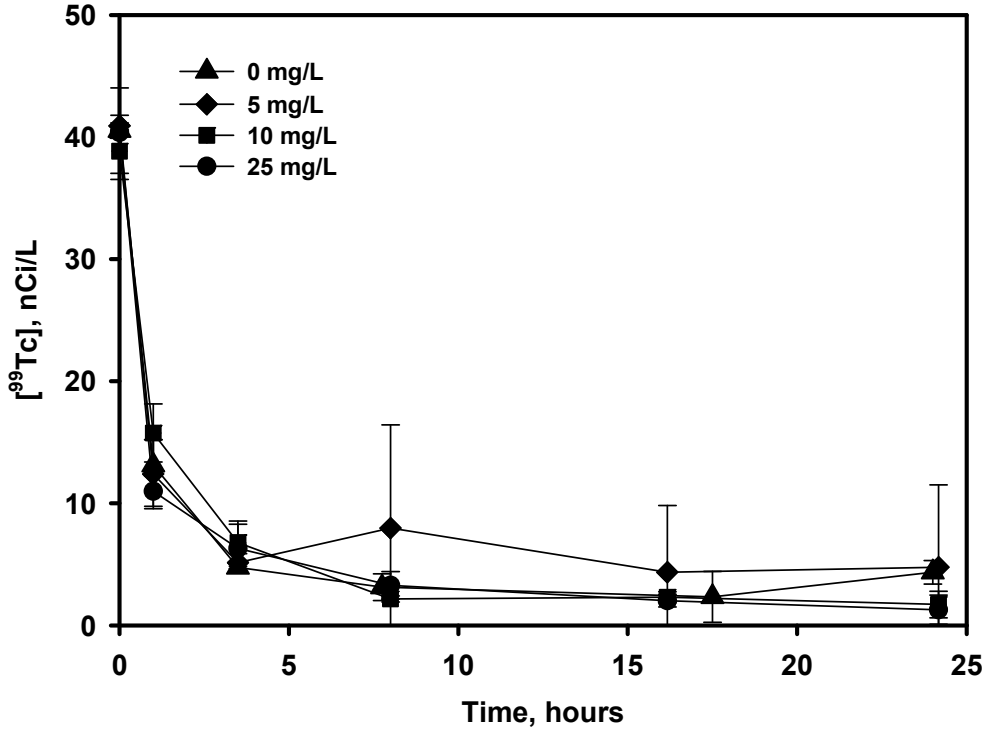

Figure 4.8 Removal of Tc(VII) from 40 nCi/L Tc(VII) solution at 2.5 V and pH 3 with different concentration of humic acid. 0.1 M $NaNO_3$ was added as supporting electrolyte. Power was removed after 24 hours. The data markers represent the average and range of duplicate experiments.

4.5 SUMMARY

Technetium was effectively removed from buffer solutions using poised graphite electrodes. Removal of pertechnetate could occur at potential as low as 1.5 V. Observed removal rate increased with higher externally applied potential. The highest k_{obs} was around 0.3 hr^{-1}, but this rate is about two times lower than removal from anodically polarized magnetite [16]. Farrell and coworkers postulated that Tc was removed by anodic sorption and reduction on magnetite anodes [16]. However, since they also used carbon as a cathode and applied similar potentials across their electrode system, we think it may also be possible that Tc in their system was reduced on the cathode. No improvement in observed removal rate constant was observed as potential

continued to increase beyond 2.5 V, probably due to the occurrence of side reactions. Removal of technetium was greatly affected by pH in a buffered system. Basic condition seemed to be more favorable for both technetium removal and recovery. Humic acid is considered to be a factor that may re-mobilize technetium in subsurface; however, it did not have evident impact on technetium removal within our studied range. Recovery of removed technetium can be achieved simply by removing the poise on electrodes. But technetium was found to return to bulk solution faster at more alkaline pH. Reversing polarity of electrodes followed by carbonate rinsing was an effective and efficient way to remove any technetium attached to the electrode surface and regenerate the electrodes.

Although Tc(IV) is the most important technetium species at reducing condition, this study does not exclude the possibility of pertechnetate reduction to more reduced form, such as Tc(III). It does not affect the key findings of this study that technetium removal and recovery could be quickly achieved using graphite electrodes, and that electrodes could be easily regenerated and reused. Electro-based removal and recovery of technetium with cost-effective graphite electrodes can be possibly applied to contamination situations requiring quick response and permanent elimination.

4.6 REFERENCES

(1) Rard, J. A.; Rand, M. H.; Anderegg, G.; Wanner, H. *Chemical thermodynamics of technetium*; Elsevier Science: Amsterdam, The Netherlands, 1999.

(2) Fredrickson, J. K.; Zachara, J. M.; Kennedy, D. W.; Kukkadapu, R. K.; McKinley, J. P.; Heald, S. M.; Liu, C. X.; Plymale, A. E. In *Reduction of TcO_4^- by sediment-associated biogenic Fe(II)*, 2004; Pergamon-Elsevier Science Ltd: 2004; pp 3171-3187.

(3) Abdelouas, A.; Grambow, B.; Fattahi, M.; Andres, Y.; Leclerc-Cessac, E. Microbial reduction of Tc-99 in organic matter-rich soils. *Sci. Total Environ.* 2005, *336* (1-3), 255-268.

(4) Lieser, K. H.; Bauscher, C.; Nakashima, T. Dissolution of TcO_2 in aqueous-solutions under various conditions. *Radiochim. Acta* 1987, *42* (4), 191-200.
(5) Darab, J. G.; Amonette, A. B.; Burke, D. S. D.; Orr, R. D.; Ponder, S. M.; Schrick, B.; Mallouk, T. E.; Lukens, W. W.; Caulder, D. L.; Shuh, D. K. Removal of pertechnetate from simulated nuclear waste streams using supported zerovalent iron. *Chem. Mater.* 2007, *19* (23), 5703-5713.
(6) Cui, D. Q.; Eriksen, T. E. Reduction of pertechnetate by ferrous iron in solution: Influence of sorbed and precipitated Fe(II). *Environ. Sci. Technol.* 1996, *30* (7), 2259-2262.
(7) Cui, D. Q.; Eriksen, T. E. Reduction of pertechnetate in solution by heterogeneous electron transfer from Fe(II)-containing geological material. *Environ. Sci. Technol.* 1996, *30* (7), 2263-2269.
(8) Lloyd, J. R.; Macaskie, L. E. A novel PhosphorImager-based technique for monitoring the microbial reduction of technetium. *Appl. Environ. Microbiol.* 1996, *62* (2), 578-582.
(9) Lloyd, J. R.; Cole, J. A.; Macaskie, L. E. Reduction and removal of heptavalent technetium from solution by *Escherichia coli*. *J. Bacteriol.* 1997, *179* (6), 2014-2021.
(10) Lloyd, J. R.; Ridley, J.; Khizniak, T.; Lyalikova, N. N.; Macaskie, L. E. Reduction of technetium by *Desulfovibrio desulfuricans*: Biocatalyst characterization and use in a flowthrough bioreactor. *Appl. Environ. Microbiol.* 1999, *65* (6), 2691-2696.
(11) Wildung, R. E.; Gorby, Y. A.; Krupka, K. M.; Hess, N. J.; Li, S. W.; Plymale, A. E.; McKinley, J. P.; Fredrickson, J. K. Effect of electron donor and solution chemistry on products of dissimilatory reduction of technetium by *Shewanella putrefaciens*. *Appl. Environ. Microbiol.* 2000, *66* (6), 2451-2460.
(12) Marshall, M. J.; Plymale, A. E.; Kennedy, D. W.; Shi, L.; Wang, Z. M.; Reed, S. B.; Dohnalkova, A. C.; Simonson, C. J.; Liu, C. X.; Saffarini, D. A.; Romine, M. F.; Zachara, J. M.; Beliaev, A. S.; Fredrickson, J. K. Hydrogenase- and outer membrane c-type cytochrome-facilitated reduction of technetium(VII) by *Shewanella oneidensis* MR-1. *Environ. Microbiol.* 2008, *10* (1), 125-136.
(13) Burke, I. T.; Boothman, C.; Lloyd, J. R.; Livens, F. R.; Charnock, J. M.; McBeth, J. M.; Mortimer, R. J. G.; Morris, K. Reoxidation behavior of technetium, iron, and sulfur in estuarine sediments. *Environ. Sci. Technol.* 2006, *40* (11), 3529-3535.
(14) McBeth, J. M.; Lear, G.; Lloyd, J. R.; Livens, F. R.; Morris, K.; Burke, I. T. Technetium reduction and reoxidation in aquifer sediments. *Geomicrobiol. J.* 2007, *24* (3-4), 189-197.
(15) Gregory, K. B.; Lovley, D. R. Remediation and recovery of uranium from contaminated subsurface environments with electrodes. *Environ. Sci. Technol.* 2005, *39* (22), 8943-8947.
(16) Farrell, J.; Bostick, W. D.; Jarabek, R. J.; Fiedor, J. N. Electrosorption and reduction of pertechnetate by anodically polarized magnetite. *Environ. Sci. Technol.* 1999, *33* (8), 1244-1249.
(17) Gu, B. H.; Brooks, S. C.; Roh, Y.; Jardine, P. M. Geochemical reactions and dynamics during titration of a contaminated groundwater with high uranium, aluminum, and calcium. *Geochim. Cosmochim. Acta* 2003, *67* (15), 2749-2761.
(18) Sun, M.; Yan, F.; Zhang, R. L.; Reible, D. D.; Lowry, G. V.; Gregory, K. B. Redox control and hydrogen production in sediment caps using carbon cloth electrodes. *Environ. Sci. Technol.* 2010, *44* (21), 8209-8215.
(19) Peng, J.; Gregory, K. B. Geochemical conditions affecting the removal and recovery of uranium from acidic solutions using electrodes. *Under review*.
(20) Bard, A. J.; Faulkner, L. R. *Electrochemical methods: fundamentals and applications*; John

Wiley & Sons, Inc.: New York, 2001.
(21) Benjamin, M. M. *Water chemistry*; McGraw Hill: New York, 2002.
(22) Lawson, B. L.; Scheifers, S. M.; Pinkerton, T. C. The Electrochemical reduction of pertechnetate at carbon electrodes in aqueous non-complexing acid-media. *J. Electroanal. Chem.* 1984, *177* (1-2), 167-181.
(23) Alliot, I.; Alliot, C.; Vitorge, P.; Fattahi, M. Speciation of technetium(IV) in bicarbonate media. *Environ. Sci. Technol.* 2009, *43* (24), 9174-9182.
(24) Wildung, R. E.; Li, S. W.; Murray, C. J.; Krupka, K. M.; Xie, Y.; Hess, N. J.; Roden, E. E. In *Technetium reduction in sediments of a shallow aquifer exhibiting dissimilatory iron reduction potential*, 2004; Elsevier Science Bv: 2004; pp 151-162.
(25) Icenhower, J. P.; Martin, W. J.; Qafoku, N. P.; Zachara, J. M. *The geochemistry of technetium: A summary of the behavior of an artificial element in the natural environment*; U.S. Department of Energy: Richland, WA, December 2008.
(26) Maset, E. R.; Sidhu, S. H.; Fisher, A.; Heydon, A.; Worsfold, P. J.; Cartwright, A. J.; Keith-Roach, M. J. Effect of organic co-contaminants on technetium and rhenium speciation and solubility under reducing conditions. *Environ. Sci. Technol.* 2006, *40* (17), 5472-5477.
(27) Boggs, M. A.; Minton, T.; Dong, W. M.; Lomasney, S.; Islam, M. R.; Gu, B. H.; Wall, N. A. Interactions of Tc(IV) with humic substances. *Environ. Sci. Technol.* 2011, *45* (7), 2718-2724.

Equilibrium Isotherm and Kinetic Model for U(VI) Electrosorption by Graphite Electrodes

6.1 ABSTRACT

The selection, design and operation of an electrode-based remediation approach for metals-contaminated groundwater will be greatly facilitated by the ability to model removal extents and removal rates under variable environmental conditions. In this study we demonstrate that the graphite electrodes have a finite capacity for uranium electrosorption and model the sorption using a Langmuir isotherm. In addition, we simulate the kinetics of of U(VI) removal via electrosorption. A semi-continuous study showed that 150 μM of U(VI) was removed on electrode surfaces following nine repeated spikes of U(VI) at the same concentration level. However, while the initial rates of removal remained constant, the percent removed decreased with each subsequent spike, demonstrating a finite capacity of polarized graphite for electrosorption of U. A mathematic model was developed based on empirical first-order kinetics, to predict k_{obs} for U(VI) removal under the influence of major environmental and operational effectors. Previous kinetic models utilize an S/V ratio to address the influence of electrode surface area (S) and volume of aqueous solution (V) on k_{obs}. However, the S/V ratio cannot reflect the expected changes in k_{obs} caused by concentration changes of contaminant. Therefore, we introduce a novel term created to stress the combined effect of electrode surface area (S), solution volume, and adsorbate concentration. The S/m ratio, or surface area to molar mass of adsorbate (m) ratio enables modeling of removal rates k_{obs} during contaminant mass loss in solution. Double layer capacity, C_d was selected as a term to define the influence of applied potential. Ionic strength considerations were based on Gouy-Chapman-Stern (GCS) theory. The

output model equation is $k_{obs} = 0.022(pH - 1.6)\ln(0.85C_d \frac{S}{m})$. Verification of the model suggests that it is applicable to predict k_{obs} in our studied ionic strength range (10^{-3} – 0.24 M). C_d remained 2.8-11.1 μF/cm^2 within this ionic strength range at 2.0 V and 2.5 V. The model was not suitable to predict k_{obs} when reactions other than contaminant removal are occurring; for example when hydrolysis is a significant side reaction.

6.2 INTRODUCTION

Dissolved radionuclides such as uranium are common groundwater contaminants at several U.S. Department of Energy sites. Uranium is highly soluble in an oxidized state and moves with the groundwater. *In situ* bioremediation has been demonstrated to be an effective remedial strategy for reductive precipitation of U(VI) from groundwater. However, groundwater at Area 3 in Oak Ridge National Laboratory exhibits characteristically high U(VI) (~210 μM), ^{99}Tc (~4000 pCi/L), and other metal concentrations. Moreover, up to 160 mM nitrate concentrations are reported along with and low pH (<4) [1, 2]. These unique geochemical conditions render bioremediation approaches prohibitively challenging [3, 4]. A more promising approach for remediation of U(VI) under low pH conditions may be the use of polarized electrodes to adsorb ions from the groundwater to prevent further migration [5, 6].

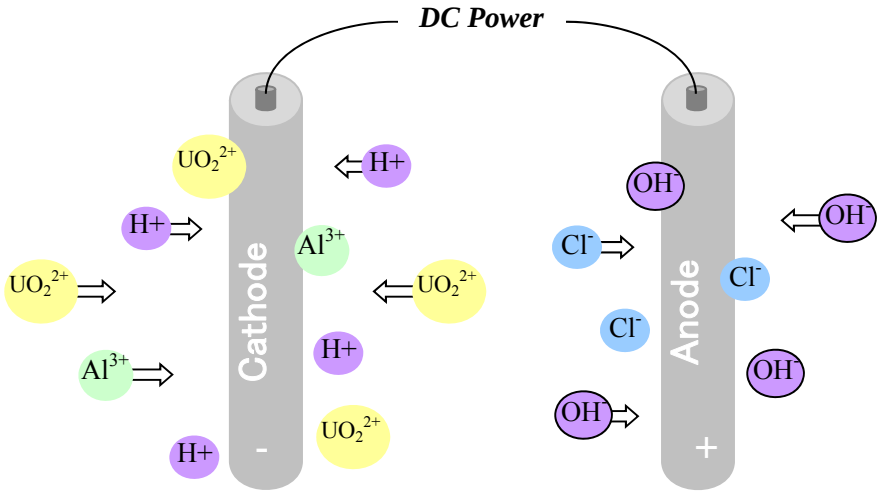

Figure 6.1 Conceptual model for electrostatic attraction process.

Electrosorption of metal cations from groundwater on polarized electrodes may be an effective and less costly approach for environmental restoration of contaminated water [7-9]. In brief, polarized electrodes are introduced to bulk solution. Cations, such as uranyl ions and protons, move towards negatively charged cathode, and anions, such as chloride and hydroxide ions, move towards positively charged anode, as illustrated in **Figure 6.1**. The ions then interact with electrode and other ions nearby, and are eventually trapped in the electric double layer via electrostatic force. This process is call electrosorption, or Capacitive Deionization (CDI). Electrostatic attraction is the driving force of electrosorption. In this approach, materials with high specific surface area and electrical conductivity such as carbon aerogel (400-1100 m^2/g), carbon fiber (>400 m^2/g) are utilized for electrode materials. Research shows that sorption and desorption of inorganic cations could be achieved by these carbonaceous materials with high surface area and polarizability, and low electrical resistance [10, 11]. Although there have been some studies on kinetics and modeling of CDI process with porous carbonaceous electrodes, study on electrosorption by graphite electrodes is limited. To date, no study on electrosorption

isotherms and kinetics has been reported on U(VI) removal at acidic condition, which is essential to system selection, design, and operation of an electrode-based remedial strategy.

Electrodes have a limited capacity in the electric double layer to accommodate ions sorbed during electrosorption. This generates two major concerns for U(VI) removal. One is the competition from other cations for spaces, which has been studied and discussed in detail in **Chapter 3**. The other is the operation lifetime of electrodes, or how much U(VI) may be removed before the EDL is at capacity and the electrodes require replacement or regeneration. This necessitates two investigations for the benefit of electrode-based remediation system design, one is to determine the maximum capacity of electrode, the other is to model the kinetics of U(VI) removal.

6.2.1 ELECTROSORPTION EQUILIBRIUM ISOTHERMS

Maximum capacity is usually obtained by developing an equilibrium isotherm of adsorption process. The most popularly used adsorption isotherms includes Langmuir isotherm, Freundlich isotherm, and BET isotherm. When sorbent surface is homogeneous, Langmuir isotherm is often used as an approximation [12]. Langmuir isotherm assumes single layer adsorption, the reaction between the ligand (L) and adsorbent (X) is defined as:

$$L + X = LX \qquad \text{Eq. 6.1}$$

The reaction rate constant equation is then:

$$k[L][X] = [LX] \qquad \text{Eq. 6.2}$$

where k is the reaction rate constant. Langmuir isotherm also assumes fixed number of adsorption sites, and total electrode adsorption capacity X_T is calculated as:

$$X_T = [X] + [LX] \qquad \text{Eq. 6.3}$$

Therefore, the Langmuir isotherm equation can be described as:

$$[LX] = X_T \frac{k[L]}{1 + k[L]}, \text{ or } \frac{[L]}{[LX]} = \frac{1}{k} \cdot \frac{1}{X_T} + \frac{[L]}{X_T} \qquad \text{Eq. 6.4}$$

Electrosorption of NaCl with carbon aerogel electrodes was found to fit well with the Langmuir isotherm [9]. Because U(VI) is not expected to be reduced by the electrode [5, 13], it is likely that the Langmuir isotherm will also accurately predict removal of U onto graphite.

6.2.2 Electrosorption Kinetics and Gouy-Chapman-Stern (GCS) Electric Double Layer Theory

Kinetic studies help develop understand influential factors during the process and predict rates of removal, and provides valuable guidance for practical engineered operation. Electrosorption of metal ions are often explained with empirical reaction order kinetic models while a recent body of work examined CDI adsorption/desorption with an electric double layer model [14]. The difference between the two approaches is that traditional reaction order models explain electrosorption results with empirical first- and second- order kinetic equations, or possibly a combination of both (Langmuir Kinetics) without theoretical support. Double layer models consider the electrode as a capacitor, and examines electrode based adsorption to ion charging in local electric field using ideal double layer theories (**Figure 6.2**).

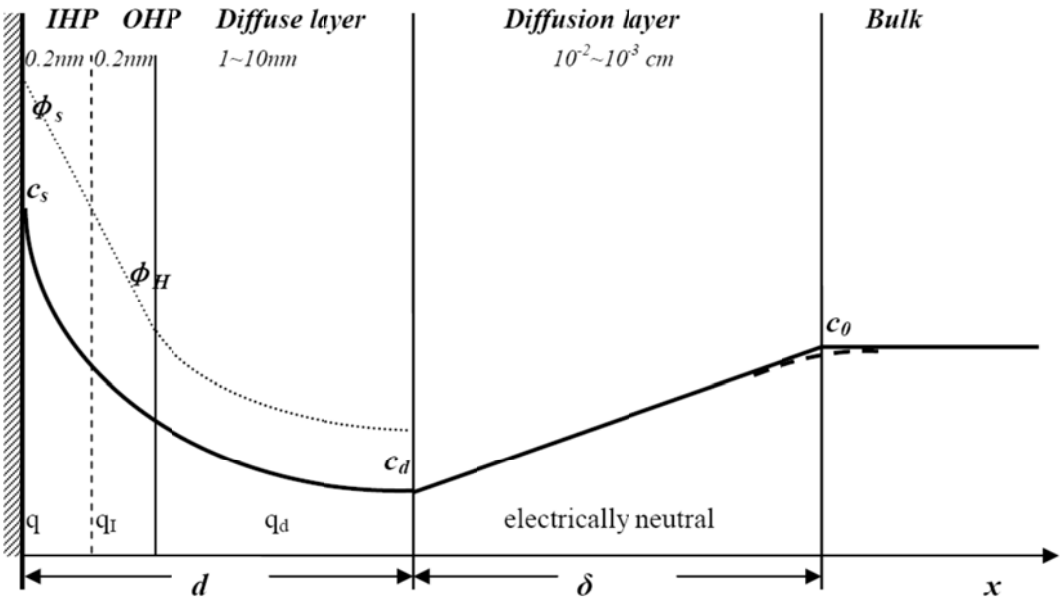

Figure 6.2 Conceptual model of the electric double layer around the electrode. IHP: Inner Helmholtz Plane, OHP: Outer Helmholtz Plane, Φ_s: potential difference in the EDL, Φ_H: potential at OHP and diffuse layer interface, c_s: concentration at electrode surface, c_d: concentration at diffuse layer, c_o: concentration at bulk solution, q: surface charge on electrode, q_I: charge in the IHP, q_d: net charge in diffuse layer, d: thickness of electric double layer (EDL), δ: thickness of diffusion layer, x: distance from electrode surface. Assume no convection in diffusion layer [15]. Assume the electrode to be planar electrode since the thickness of EDL is much smaller than the radius of curvature of the electrode.

The GCS model is often utilized to analyze this process. According to Gouy and Chapman's theory, particles are loosely distributed in solution under electric field (diffuse layer in **Figure 6.2**), and distribution follows Boltzmann distribution. Stern added a compact layer, or Helmholtz layer on electrode surface, and treated electrodes as parallel capacitor where ions are tightly compacted close to electrode surface. Gouy-Champman-Stern model is based on a combination of both theories.

According to **Figure 6.2**, average U(VI) concentration in the diffusion layer is expected to be constantly lower than that in the bulk solution, therefore in an electrosorption process, the amount of U(VI) inside the diffusion layer is not considered significant comparing with that

trapped inside the electric double layer during the removal process. In other words, U(VI) electrosorption is primarily attributed to double layer adsorption. As for the mass transfer in the diffusion layer, it only takes 24 seconds for UO_2^{2+} to move across a diffusion layer as thick as 10^{-2} cm according to the following equation [16]:

$$t_d = \frac{L^2}{D} \qquad \text{Eq. 6.5}$$

where t_d is the diffusion time, L is the diffusion distance and D is diffusion coefficient of a certain ion. The diffusion coefficient of UO_2^{2+} (dominant U(VI) species at pH 3) is 0.426×10^{-5} cm^2/s (**Table 3.1**). Comparing with the length for U(VI) removal (hours), mass transfer of U(VI) in diffusion layer is not considered a rate limiting step for U(VI) electrosorption, instead, electric double layer process may play a more vital role.

If capacitance of the Helmholtz planes is assumed to be independent of potential, for a z:z electrolyte, capacitance of electric double layer could be stated as [17]:

$$\frac{1}{C_d} = \frac{x_H}{\varepsilon\varepsilon_0} + \frac{1}{\frac{\varepsilon\varepsilon_0}{\lambda}\cosh(\frac{zF\phi_H}{2RT})} \qquad \text{Eq. 6.6}$$

where C_d is the differential capacitance of double layer, the first term on the right is the inverse of Helmholtz planes capacitance (x_H, thickness of Helmholtz planes; ε, dielectric constant of the medium; ε_0, permittivity of free space, $\varepsilon_0 = 8.85419 \times 10^{-12}$ $C^2N^{-1}m^{-2}$), and the second term on the right is the inverse of diffuse layer capacitance (λ, Debye length; I, ionic strength of electrolyte; F, faraday's constant; φ_H, potential on outer Helmholtz plane; R, universal gas constant; T, temperature). Debye length is calculated from:

$$\lambda = \sqrt{\frac{\varepsilon\varepsilon_0 RT}{2F^2 I}} \qquad \text{Eq. 6.7}$$

However, GCS model is still based on an ideal solution and not as practically as the empirical kinetic models. The empirical reaction order kinetics, on the other hand, only applies to reactions at a given condition, and does not consider the influence of geochemical and operational factors. Therefore, we propose to incorporate the environmental factors (pH, applied potential, ionic strength, and S/m ratio) described in **Chapter 3** into the empirical kinetic model, so that U(VI) removal rate can be estimated within a wider operational range.

The objective of this study was to evaluate electrode capacity and develop a mathematical kinetic model for U(VI) removal from aqueous solution. Semi-continuous U(VI) removal in a batch system was investigated to study the capacity of graphite electrode for U(VI) removal. A mathematical model was also developed to predict first-order reaction rate constant combining major geochemical factors, operational factors and GCS theory. The capacity studies and model will aid in the selection of electrode materials and provide a more fundamental understanding of removal processes for U on electrodes. The kinetic model will provide valuable predictive ability for system design under the unique geochemical conditions observed at Area 3 of ORNL.

6.3 MATERIALS AND METHODS

6.3.1 SEMI-CONTINUOUS U(VI) REMOVAL WITH GRAPHITE ELECTRODES

Semi-continuous removal of 150 μM U(VI) was conducted in 500 mL of synthetic solution in batch reactors at 2.5 V with graphite rods as electrodes. The cylindrical graphite rods (Graphite Engineering & Sales, Co., Greenville, MI) have a diameter of 2.54 cm and length of 7.62 cm. When U(VI) removal rate became slow and equilibrium was reached, uranyl acetate (Electron Microscopy Sciences, Hatfield, PA) was respiked to 150 μM. After the solutions were re-spiked

nine times and further uranium removal ceased, external potential was increased from 2.5 V to 3.0 V and another spike was added to ensure that capacity was reached. Amount of adsorbate unadsorbed (C_w) is calculated from amount left in solution measured, amount of U(VI) adsorbed (C_s) by electrode is calculated from by substracting C_w from intial amount of U(VI) before electrosorption started (CT). Then C_w and C_s were fitted into adsorption isotherm.

6.3.2 Analytical Methods

Uranium was measured using a modified kinetic phosphorescence analysis [18] with a kinetic phosphorescence analyzer (KPA-11, Chemchek Instruments, Richland, WA). In brief, 100 µL of unfiltered sample was removed from reactors with a pipetter and diluted as necessary to meet the high-range calibration of the KPA (0-20 µM), complexed with 1.5 mL of Uraplex® (Chemchek Instruments, Richland, WA), and let stand for 5 minutes prior to analysis with KPA instrument (KPA-11, Chemchek Instruments, Richland, WA).

6.3.3 Experiments for Kinetic Model Development and Verification

Three experiments were conducted to help develop and verify developed kinetic model. Experimental set-up was the same as above. The first experiment was done in the same manner as previously described in **Figure 3.6** and **Figure 4.2**. Potential distribution as well as current and conductance of solutions at different ionic strength and external potential was calculated. These data and details may be seen in **Appendix E**. The second experiment was the removal of 10 µM U(VI) from 500 mL solutions at pH 2-6. The third experiment was the removal of 150 µM U(VI) from 100 mL solutions at pH 3; ionic strength was adjusted to 0.1 M with $NaNO_3$.

6.4 Results and Discussion

6.4.1 Electrode Capacity for U(VI) Removal at pH 3

Figure 6.3 illustrates U(VI) removal with time with several additional spikes. The solution initially contained 150 μM U(VI), which was quickly removed after the electrodes were poised at 2.5 V. When less than 5% removal could be observed over 12 hours, more U(VI) was added from a uranyl acetate stock solution to increase U(VI) concentration back to ~150 μM. The re-spike was repeated for 9 times. Not only was U(VI) removed slower each following spike, U(VI) residual concentration was also higher at the end of each following spike. Percentage of U(VI) removed further decline after 6th spike, and only ~10% U(VI) removal can be achieved thereafter. This trend indicates that individual capacity for U(VI) removal at each spike decreased after each addition, and electrode adsorption capacity does exist at a defined condition. This decreased capacity for removal was partially overcome by increasing the applied potential. At the 9th spike, when U(VI) concentration was stabilized, external potential was slightly increased by 0.5 V to 3.0 V. Continuous U(VI) removal was observed. However, no more U(VI) removal was observed at the 10th spike with external potential remained 3.0 V. It is also consistent with electric double layer theory (Eq. 6.6) that increase of electrode capacity can be achieved by increasing potential. Although charging of electric double layer is generally a fast process, previous researchers also revealed a slow-charging phenomena with graphite and other types of electrode [19], which may be related to up to hours of U(VI) removal in this study.

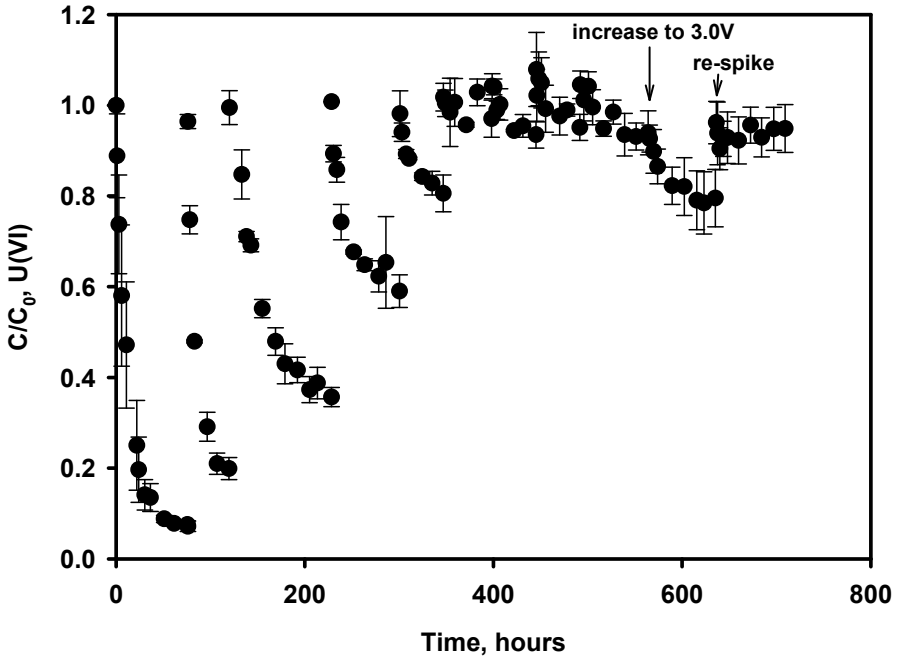

Figure 6.3 Semi-continuous removal of U(VI) with graphite electrodes at 2.5 V initially. Additional U(VI) stock solution was added to the reactor after U(VI) concentration stabilized. Each increase in normalized concentration to ~1.0 represents a spike of uranium acetate stock solution. Nine additional spikes were added before overall potential was increased to 3.0 V. Final spike was added at 3.0 V after more U(VI) was removed at higher potential. The data markers represent the average and range of triplicate experiments.

The last data point in each spike was re-calculated in order to correlate the amount of U(VI) removed (C_s) with that remained in the bulk solution (C_w). C_w is the molar mass of U(VI) in the solution and was calculated by multiplying concentration with solution volume (500 mL). C_s represents U(VI) molar mass on the electrode surface, and was calculated cumulatively by adding the mass difference between initial and final U(VI) molar mass in the solution after each spike. Here C_w = [L], Cs = [LX] in Langmuir isotherm. C_s was plotted versus C_w in **Figure 6.4**. Fitting of the all nine spikes at 2.5 V yields a Langmuir equation:

$$\frac{C_w}{C_s} = 0.063 + 0.0036C_w \qquad \text{Eq. 6.8}$$

According to the constants defined in Eq. 6.8 and Langmuir equation displayed as Eq. 6.4, $1/X_T$

equals to 0.0036, and $1/(kX_T)$ equals to 0.063. Therefore, total electrode capacity X_T = 277.78 μM, and rate constant k = 0.0572. However, some artifact may effected the final two points on the isotherm curve, as the electrosorption was approaching electrode maximal capacity; these data did not fit well into the equation. Considering only the first 7 spikes, the Langmuir equation is:

$$\frac{C_w}{C_s} = 0.0595 + 0.0038C_w \qquad \text{Eq. 6.9}$$

with X_T = 263.16 μM and k = 0.0638. Therefore, capacity of graphite electrodes for U(VI) removal at 2.5 V is 263.16 μmoles of U(VI) under our studied condition. The blue curve is the fitting to Langmuir equation. It suggests that the Langmuir isotherm model is appropriate to explain equilibrated electrosorption of U(VI).

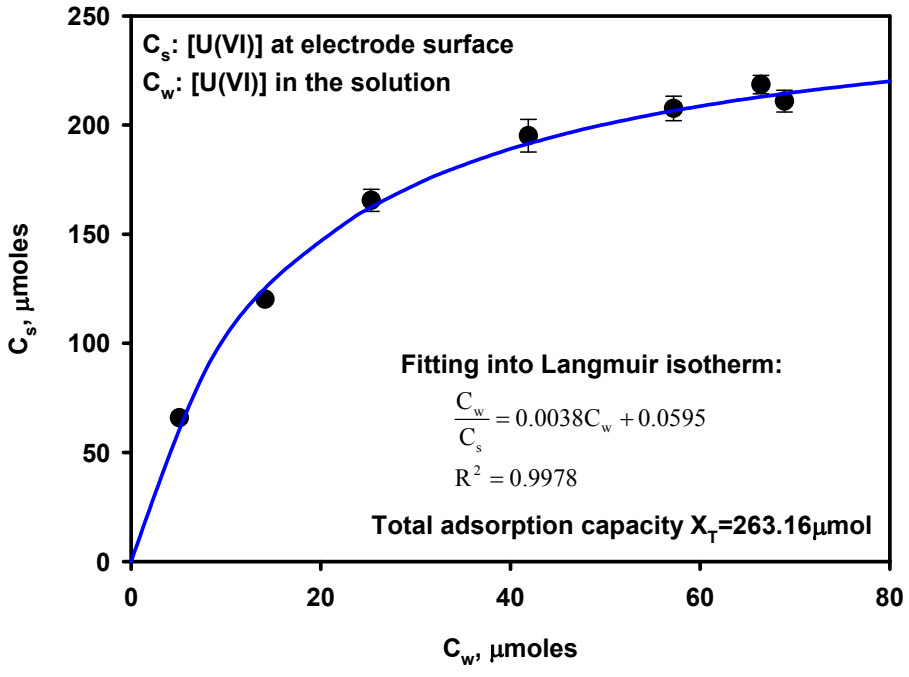

Figure 6.4 Concentration of U(VI) in the solution against that on the electrode surface. C_s is U(VI) concentration on the electrode surface, and was calculated cumulatively from the difference between initial and final concentrations during each spike. C_w is U(VI) concentration in the

solution and was directly measured. The blue curve is the fitting curve of Langmuir isotherm.

6.4.2 Surface Area of Graphite Calculated from Electrode Capacity

Maximum capacity of the electrode was estimated to be ~263 μmol according to Langmuir isotherm fitting. Using the single layer adsorption assumption of the Langmuir isotherm, electrode surface area available for 263 μmol uranyl ions can be estimated as follows. A conceptual depicture of a single UO_2^{2+} adsorbed onto negatively charged cathode is shown in **Figure 6.5**. The dimensions of the uranyl ion are indicated. Since U is the one positively atom of the charged compound, the figure illustrates the scenario in which the U atom is in direct with electrode surface and face inwards.

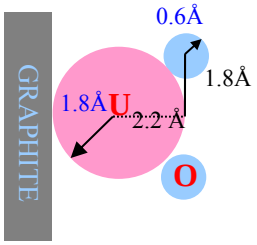

Figure 6.5 Dimensions of UO_2^{2+} ion and attachment of the ion to graphite. Data were obtained from reference [20].

Radius of oxygen ion is about 0.6 Å, radius of uranium ion is about 1.8 Å. Considering the largest projected rectangular area on electrode, one uranyl molecule can occupy $[(1.8+0.6)*2]*[1.8*2]=1.7*10^{-17}$ m^2 on electrode surface according to the dimensions indicated in **Figure 6.5**. 263 μmol of uranyl ions equals to $263*6.02*10^{23} = 1.6*10^{20}$ ions. As suggested by Langmuir isotherm, uranyl ions covered electrode via single layer adsorption. 263 μmol uranyl ions will need a surface area of $1.6*10^{20}*1.7*10^{-17}$ m^2 = 2720 m^2. Average weight of graphite

rod electrode used is 63 g. Therefore, specific surface area of the electrode, estimated from the U sorption capacity was **43.2m^2/g**. This is about an order of magnitude higher than the specific surface area of this graphite usually reported (~4 m^2/g) [21], and 3 times higher the surface area of commercial graphite powders (10 m^2/g) [21]. This result suggests that additional adsorption capacity may have been created inside the electric double layer during electrosorption, resulting in larger electrode capacity than that was defined by gas adsorption measurement.

6.4.3 MATHEMATICAL KINETIC MODEL FOR U(VI) REMOVAL

6.4.3.1 SELECTION OF FACTORS

Results presented in **Chapter 3** demonstrate that the roles of pH, external potential, and initial U(VI) concentration are important factors that determine kinetic rate of U(VI) removal. Electrode surface area is another crucial parameter for electrode-based remediation system design. Maslennikov and coworkers, used an S/V ratio to address the importance of electrode surface area; where S is reactive electrode surface area, and V is volume of aqueous solution [22, 23]. At given conditions, metal removal rate constant is considered to be proportional to S/V ratio [22]. An increase in S/V ratio caused faster Tc(VII) removal by electrodes [23]. S/V ratio is considered to be proportional to first-order Tc removal rate by electrodes [22]. However, since concentration of ions varies in different groundwater and metal ions directly interact with electrodes during electrode-based removal, the term S/V ratio could not predict a change in removal rate when initial concentration varies. For example, although U(VI) removal was found to fit first-order kinetics best under the conditions tested, it obviously also varied with initial U(VI) concentration (**Figure 3.7**), suggesting U(VI) removal reaction is not a strict first-order reaction. It should be more accurate to consider the amount or molar mass of targeted ions

instead of solution volume. Therefore we normalize the surface area to the molar mass of the contaminant to create an S/m ratio, where S is reactive electrode surface area and m is the total molar mass of studied ions at the beginning of the experiments. This will better address the importance of electrode surface area per mole of ions. If we arbitrarily define 1 S/m unit as batch reactor with one anode and one cathode and 150 μM U(VI) at 500 mL solution, **Figure 3.7** can be converted to a k_{obs}-S/m curve, as shown in **Figure 6.6**. It suggests a great impact from S/m on k_{obs}. A possible reason is that when pH remains constant, electrode surface area per U(VI) ion increases with higher S/m, offering U(VI) higher chance of be absorbed while chance of H^+ being absorbed remains the same.

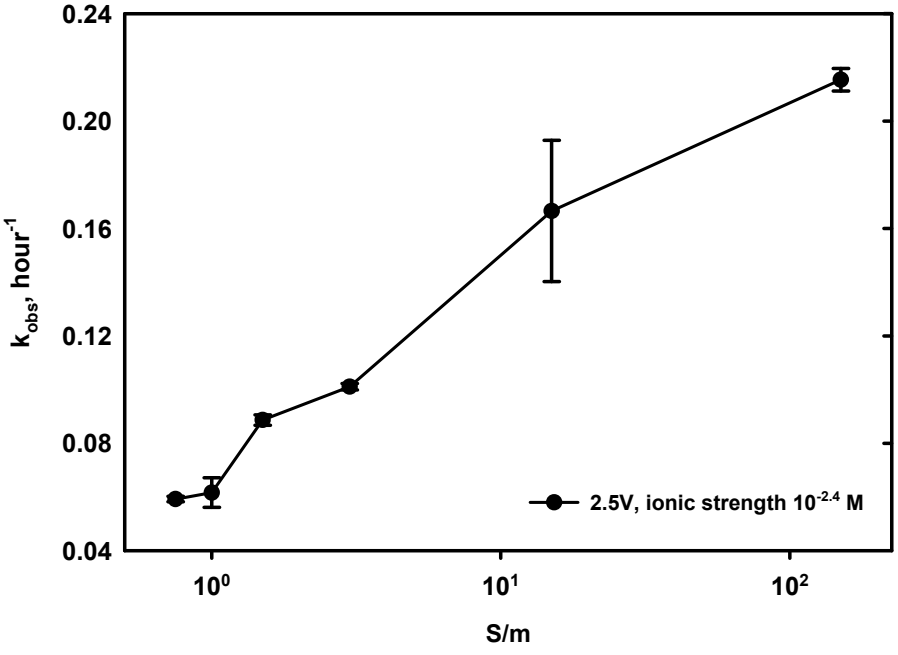

Figure 6.6 Impact of S/m ratio on initial removal rates (k_{obs}) of U(VI). S/m ratio of a system with two graphite electrodes and 500 mL 150 μM U(VI) solution is arbitrarily defined as 1 S/m. The external potential was 2.5 V and starting concentration of U(VI) was 150 μM at pH 3. The data markers represent the average and range of duplicates.

As has been suggested by **Figure 6.3**, the overall rate of U(VI) removal diminished as the system

was approaching the maximal adsorption capacity. Since both ionic strength and external potential influence electric double layer capacity (Eq. 6.6), differential capacitance of electric double layer per unit area, C_d, is another important determinant of U(VI) removal rate. When ionic strength and potential are constant, differential capacitance of the electric double layer is also constant for a defined electrolyte solution. Therefore, the factors that are considered closely related to k_{obs} are pH, double layer potential (included in C_d term), ionic strength (included in C_d), and S/m ratio. As a reminder, since U(VI) initial concentration is included in S/m term, U(VI) removal reaction is actually not a strict first-order reaction.

6.4.3.2 MODEL DEVELOPMENT

Assuming that initial U(VI) removal rate obeys first-order kinetics [13], k_{obs} could be interpreted by a combined effect of S/m, C_d, and $[H^+]$, where C_dS/m represents the theoretical vacancy per ion, $[H^+]$ represents the influence of a competing ion. k_{obs} expression is schemed as

$$k_{obs} = c_1 f(pH) g(C_d \frac{S}{m}) \qquad \text{Eq. 6.10}$$

where c_1 is an unknown constant, $f(pH)$ is the function related to pH, and $g(C_d \frac{S}{m})$ is the function for S/m and C_d. As a reminder, in this study, S/m ratio of a system with two graphite electrodes and 500 mL 150 μM U(VI) solution is arbitrarily defined as 1. Parameters for C_d calculation are listed below:

Table 6.1 Parameters used for C_d estimation with Equation 6.6 and 6.7

x_H	0.4 nm	z	2
ε_0	8.85419×10^{-12} F/m	R	8.314
ε	5 for Helmholtz layers 80 for diffuse layer	T	298 K
F	96485 C/mol	φ_H	-

The only parameter that is undetermined for C_d estimation is the potential of diffuse layer, φ_H, or the potential on the outer Helmholtz layer in relative to bulk solution. In our previous experiments, potential on electrode versus Ag/AgCl was measured at different external potentials to address the potential distribution in the solution. However, since the reference electrode can not be placed several nanometers away from the electrode surface, and overpotentials can not be accurately defined, cathode potential measured is still not as negative as the real φ_H. A group of experiments were done to measure potential distribution as well as current and conductance of solutions at different ionic strength and external potential, detailed results were put in **Appendix E**. Ohmic loss was calculated from measured current, conductance and estimated electrode distance to solution cross section area ratio (0.1 cm^{-1}) (**Table 6.2**). Assuming potential other than ohmic loss is distributed evenly between the two identical graphite electrodes; cathode potential on electrode surface (φ_s in **Figure 6.2**) can be estimated by dividing this potential value by 2. Then potential at about 0.4 nm from electrode surface can be estimated from $\varphi_H = \varphi_s e^{-x/\lambda}$, where x is the distance from electrode surface and λ is Debye length [17]. φ_H and C_d can then be estimated, and the results for two selected applied potential, 2.0 V and 2.5 V, were listed in **Table 6.2**. It shows that the Debye length is large with more diluted solution (lower ionic strength) and solution conductance increases with ionic strength. The results suggest that at ionic strength ranging from 10^{-3} M to 0.24 M, capacity of electric double layer does not change as dramatical at 2.0 V and 2.5 V; only with an increase from 2.8 to 11.1 $\mu F/cm^2$. Therefore, within our studied range, S/m is expected to be more influential on k_{obs} since C_d remained stable at a wide range of ionic strength. The next step is to develop k_{obs} equations related to pH and S/m.

Table 6.2 φ_H and C_d estimation at various ionic strength conditions with 2.0 V and 2.5 V externally

applied potential. Measured cathode potential was calculated versus SHE (Ag/AgCl is 200 mV versus SHE)

	Ionic strength	10^{-3} M	$10^{-2.5}$ M	$10^{-1.6}$ M	0.24 M
	Conductance (mS/cm)	0.47	0.6	2	12
	$x_H/\varepsilon\varepsilon_0$	9.04	9.04	9.04	9.04
	λ (nm)	9.71	5.46	1.94	0.63
2.0 V	Measured cathode potential (V)	0.08	-0.01	-0.2	-0.5
	Current (A)	0.007	0.01	0.013	0.046
	Ohmic loss (V)	1.489	1.667	0.650	0.383
	φ_s (V)	-0.255	-0.167	-0.675	-0.808
	φ_H (V)	**-0.245**	**-0.155**	**-0.549**	**-0.427**
	C_d (μF/cm^2)	**9.1**	**9.1***	**11.1**	**11.1**
2.5 V	Measured cathode potential (V)	0.07	-0.2	-0.52	-0.66
	Current (A)	0.01	0.011	0.023	0.089
	Ohmic loss (V)	2.128	1.833	1.150	0.742
	φ_s (V)	-0.186	-0.333	-0.675	-0.879
	φ_H (V)	**-0.178**	**-0.309**	**-0.549**	**-0.464**
	C_d (μF/cm^2)	**2.8**	**11**	**11.1**	**11.1**

* calculated as 2.2 μF/cm^2, which should be an error caused by experimental artifacts since theoretically C_d increases with ionic strength at given potential. Therefore 9.1 μF/cm^2 was used instead as its minimum possible value.

Removal of 10 μM U(VI) from 500 mL solution (15 S/m unit) was compared with that of 150 μM U(VI) from **Figure 3.2** (1 S/m unit) and plotted together in **Figure 6.7.** It shows that k_{obs} is higher at 15 S/m at acidic pH. Assuming C_d remains unchanged, Linear fitting of the two k_{obs} versus pH curve in **Figure 6.7** yields the relationship between k_{obs} and pH at two different S/m ratios, as listed in **Table 6.3**. Linear fitting of k_{obs}-S/m curve in **Figure 6.6** generates another equation defining k_{obs} with S/m, shown as the third equation in **Table 6.3**.

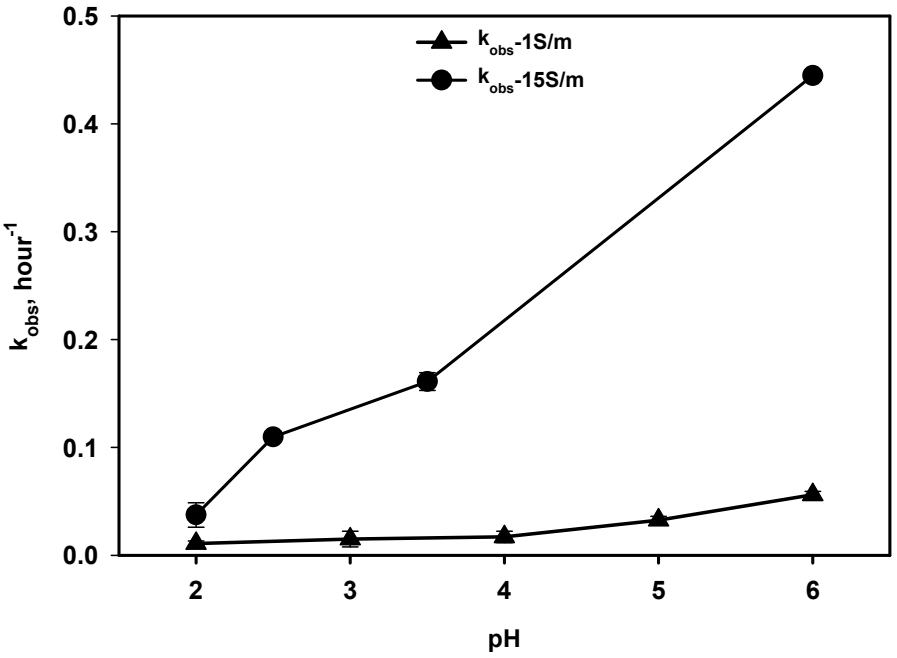

Figure 6.7 k_{obs} at different pHs with two tested S/m ratios (initial U(VI) concentration were 10 μM and 150 μM, respectively) at 2.0 V. Error bar represents standard deviation from duplicates.

Table 6.3 Fitting results of k_{obs}-pH and k_{obs}-S/m

Factor	Fitting equation	S/m	pH	Potential	Ionic strength
pH	k_{obs} = 0.0996(pH-1.61) R^2=0.9870	15	-	2.0 V	10^{-2} -10^{-5} M
pH	k_{obs} = 0.0108(pH-1.56) R^2=0.8472	1	-	2.0 V	10^{-2} -10^{-5} M
S/m	k_{obs} = 0.0306[ln(S/m) + 2.25] R^2 = 0.9812	-	3	2.5 V	$10^{-2.4}$ M

For a condition with defined potential and ionic strength, C_d is constant. Therefore C_d is included in the constant in the k_{obs}-S/m equation. According to **Table 6.2**, C_d for the k_{obs}-S/m equation is 11 μF/cm^2. Therefore, k_{obs}-S/m equation can be rewritten as k_{obs} = 0.0306 ln(0.85C_dS/m). From the hypothesized k_{obs} formula, $c_1 f(\text{pH}) = 0.0306$. Using either (pH-1.61) or (pH-1.56) as f(pH), and we could eventually get $c_1 = 0.022$. The k_{obs} equation can be put as:

$$k_{obs} = 0.022(pH - 1.6)\ln(0.85C_d \frac{S}{m}) \qquad \text{Eq. 6.11}$$

where unit of k_{obs} is hour^{-1}, unit of C_d is μF/cm^2, and unit of S/m is cm^2/mol.

6.4.3.3 MODEL VERIFICATION

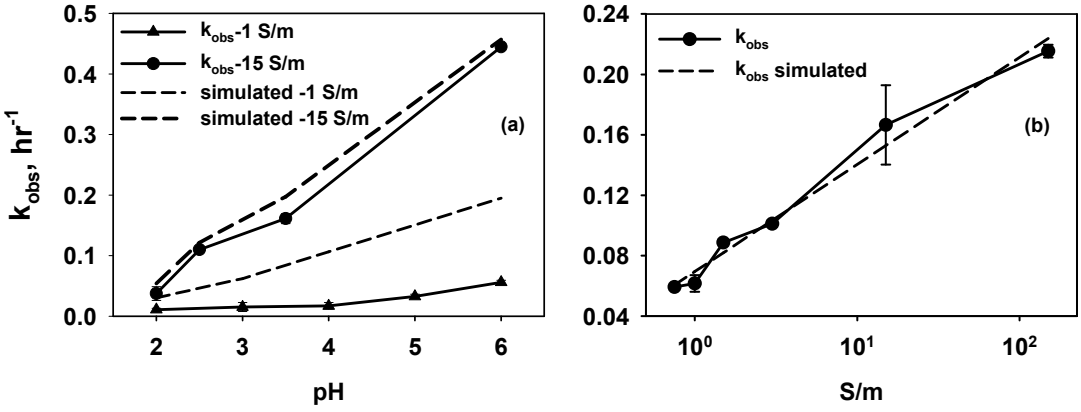

Figure 6.8 Modeling fitting of k_{obs} change with (a) pH and (b) S/m ratio. Dashed lines represents modeling results; solid symbols and lines were experimental results.

Bring the Eq. 6.11 back to conditions examined in **Figure 6.6 and Figure 6.7**, with C_d calculated as 9.1 μF/cm^2 and 11.1 μF/cm^2 respectively, comparison of experimental results and model simulation results is shown in **Figure 6.8**. The model successfully predicts k_{obs} change with pH at 15 S/m ratio, but not so well at 1 S/m. It was found that the simulated results tend to overestimate k_{obs} by 65%-253% with 1 S/m scenario at high pHs. Since ionic strength of solutions at pH 5 and 6 was actually two orders of magnitude lower than our lowest studied condition, 10^{-3} M, it is likely that the assumption of constant C_d caused the discrepancy since the actual C_d is expected to be lower at ionic strength lower than 10^{-3} M. When S/m ratio is as high as 15, the large value reduces the error introduced by the higher value of C_d. Therefore, the model equation is more effective in predicting k_{obs} in our studied ionic strength range (10^{-3} – 0.24 M) than in ionic strength below 10^{-3} M.

The model equation also explains the finding in **Chapter 3** [13] that ionic strength did not influence U(VI) removal rate at pH 3 (**Figure 3.10**), since C_d only changes in a narrow range at ionic strength between 10^{-3} M and 10^{-1} M. Another experiment was performed with changes both in S/m ratio and ionic strength. The results as well as its fitting curve are shown in **Figure 6.9(a)**. It appears that the model does not predict the change in rate constant as expected. It underestimates rate constant at low pH. However, the pH of the bulk solution was not constant throughout the adsorption reaction (**Figure 6.9(b)**). Unlike U(VI) removal from lower ionic strength and constant pH (data not shown), when ionic strength was as high as 0.1 M, the solution pH all converged on a value of 4, which suggests the occurrence of side reactions. Treatment of Area 3 groundwater with ionic strength of 0.24 M with electrodes poised at 2.5 V reported evolution of hydrogen during U removal (**Figure 5.9**). For ionic strength as high as 0.1 M, low ohmic loss probably causes a high φ_s value. The synergic effect of increased S/m and φ_s may result in more complicated situations, and lessen the impact of pH on U(VI) removal, causing significant deviation from the observed results. Another reason for model failure in predicting trend in **Figure 6.9(a)** is that the pH value incorporated in the model equation for verification was not real solution pH but rather initial pH. Therefore, the model seems to be more suitable for prediction of k_{obs} with simple electrosorption process without the occurrence of side reactions such as electrolysis.

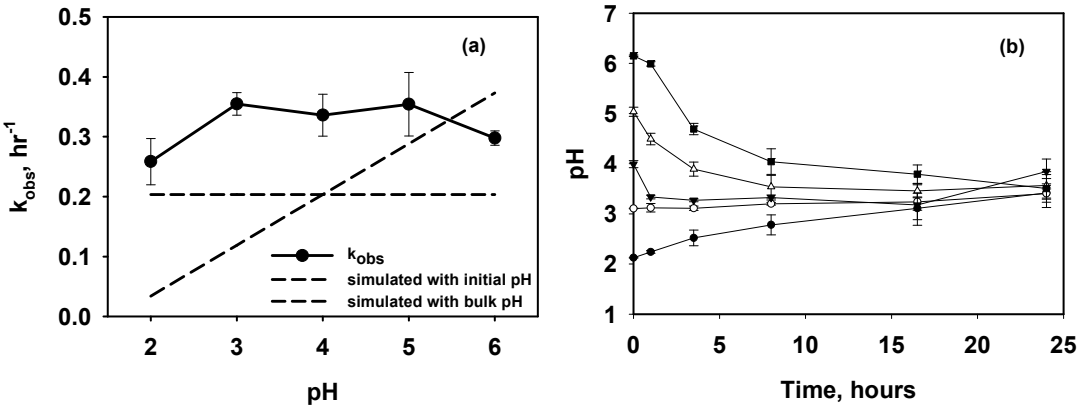

Figure 6.9 (a) k_{obs} at different pHs at ionic strength of 0.1 M. The external potential was 2.5 V, and S/m ratio was 5. Dashed lines represent modeling results; solid symbols and lines were experimental results. (b) Shift of solution pH with time during the removal. The data markers represent the average and range of duplicate experiments.

6.5 SUMMARY

The extent and kinetics of electrosorption of U(VI) on graphite electrodes has not been investigated before. Models for predicting electrosorption of metals under environmental conditions must also include terms for aqueous geochemical conditions. The model presented here includes influence of potential, ionic strength, molar mass of adsorbate, and pH that was not considered in previous kinetic reaction models.

A semi-continuous study of U removal on graphite electrodes shows that U(VI) can be removed repeatedly as solution U(VI) concentration stabilized and additional U(VI) was spiked. However, stabilized U(VI) concentration by the end of each spike gradually increased, suggesting electrosorption of U(VI) was also limited by a capacity. When little U(VI) removal was observed with the 9th spike, externally applied potential was adjusted from 2.5 V to 3.0 V. U(VI) was continued to be remove after this slight increase of potential, but stopped at the second spike. Calculating U(VI) concentration on electrode surface versus in the bulk solution

shows that the removal fits well with Langmuir isotherm. Maximum electrosorption capacity is 263.16 μmol for U(VI), which required a specific surface area of 43.2 m^2/g theoretically.

Electrode surface area to solution volume ratio is usually considered as an influential factor for removal. However, since we discovered U(VI) removal was not a strict first-order reaction and initial concentration also affected removal rate, an S/m term, or surface area to molar mass of adsorbate, was created to combine the three effects. However, although double layer capacity, C_d, changes with potential and ionic strength, no significant shift was observed according to our approximate calculation. C_d remained 2.8-11.1 $\mu F/cm^2$ within 10^{-3} M - 0.24 M ionic strength range at 2.0 V and 2.5 V. The final model equation combines the effects of pH, C_d and S/m, and is conceived as:

$$k_{obs} = 0.022(pH - 1.6)\ln(0.85C_d \frac{S}{m}) \qquad \text{Eq. 6.11}$$

The strength of this model is that it can predict change of k_{obs} when more than one condition is changed. Influence of electrode surface area (S), solution volume, and adsorbate concentration can also be reflected and quantified by the S/m term of the model. The natural logarithm of S/m is linearly correlated to k_{obs} in the model output equation, implicating that for practically remedial design, a balance between electrode surface area and reactor volume can be evaluated to optimize k_{obs}. However, it may not be applicable to solutions with ionic strength out of the range of 10^{-3} M - 0.24 M. Another weakness of this model is that it may over-emphasize the importance of pH for some conditions, such as higher ionic strength environment. It was also found that pH used for the model simulation needs to be real bulk solution pH rather than initial pH, since the change in pH may cause a great shift in the resulted k_{obs}. This study only estimated the value of C_d within 10^{-3} M - 0.24 M ionic strength range at applied potential 2.0 V and 2.5 V.

If the model is to be further improved, C_d should be more thoroughly evaluated in a broader potential range to better reflect the influence of applied potential.

6.6 REFERENCES

(1) Gu, B. H.; Brooks, S. C.; Roh, Y.; Jardine, P. M. Geochemical reactions and dynamics during titration of a contaminated groundwater with high uranium, aluminum, and calcium. *Geochim. Cosmochim. Acta* 2003, *67* (15), 2749-2761.

(2) Wu, W. M.; Carley, J.; Fienen, M.; Mehlhorn, T.; Lowe, K.; Nyman, J.; Luo, J.; Gentile, M. E.; Rajan, R.; Wagner, D.; Hickey, R. F.; Gu, B. H.; Watson, D.; Cirpka, O. A.; Kitanidis, P. K.; Jardine, P. M.; Criddle, C. S. Pilot-scale *in situ* bioremediation of uranium in a highly contaminated aquifer. 1. Conditioning of a treatment zone. *Environ. Sci. Technol.* 2006, *40* (12), 3978-3985.

(3) Moon, H. S.; Komlos, J.; Jaffe, P. R. Uranium reoxidation in previously bioreduced sediment by dissolved oxygen and nitrate. *Environ. Sci. Technol.* 2007, *41* (13), 4587-4592.

(4) Senko, J. M.; Istok, J. D.; Suflita, J. M.; Krumholz, L. R. In-situ evidence for uranium immobilization and remobilization. *Environ. Sci. Technol.* 2002, *36* (7), 1491-1496.

(5) Gregory, K. B.; Lovley, D. R. Remediation and recovery of uranium from contaminated subsurface environments with electrodes. *Environ. Sci. Technol.* 2005, *39* (22), 8943-8947.

(6) Xu, Y.; Zondlo, J. W.; Finklea, H. O.; Brennsteiner, A. Electrosorption of uranium on carbon fibers as a means of environmental remediation. *Fuel Process. Technol.* 2000, *68* (3), 189-208.

(7) Farmer, J. C.; Bahowick, S. M.; Harrar, J. E.; Fix, D. V.; Martinelli, R. E.; Vu, A. K.; Carroll, K. L. Electrosorption of chromium ions on carbon aerogel electrodes as a means of remediating ground water. *Energ. Fuel* 1997, *11* (2), 337-347.

(8) Alfarra, A.; Frackowiak, E.; Beguin, F. Mechanism of lithium electrosorption by activated carbons. *Electrochim. Acta* 2002, *47* (10), 1545-1553.

(9) Gabelich, C. J.; Tran, T. D.; Suffet, I. H. Electrosorption of inorganic salts from aqueous solution using carbon aerogels. *Environ. Sci. Technol.* 2002, *36* (13), 3010-3019.

(10) Seron, A.; Benaddi, H.; Beguin, F.; Frackowiak, E.; Bretelle, J. L.; Thiry, M. C.; Bandosz, T. J.; Jagiello, J.; Schwarz, J. A. Sorption and desorption of lithium ions from activated carbons. *Carbon* 1996, *34* (4), 481-487.

(11) Ying, T. Y.; Yang, K. L.; Yiacoumi, S.; Tsouris, C. Electrosorption of ions from aqueous solutions by nanostructured carbon aerogel. *J. Colloid Interface Sci.* 2002, *250* (1), 18-27.

(12) LaGrega, M. D.; Buckinghan, P. L.; Evans, J. C.; Management, E. R. *Hazardous waste management*; McGraw-Hill: New York, NY, 2001.

(13) Peng, J.; Gregory, K. B. Geochemical conditions affecting the removal and recovery of uranium from acidic solutions using electrodes. *Under review*.

(14) Biesheuvel, P. M.; van Limpt, B.; van der Wal, A. Dynamic adsorption/desorption process model for capacitive deionization. *J. Phys. Chem. C* 2009, *113* (14), 5636-5640.

(15) Brett, C. M. A.; Brett, A. M. O. *Electrochemistry: principles, methods, and applications*; Oxford University Press: New York, 1994.

(16) Socolofsky, S. A.; Jirka, G. H. Advective diffusion equation. In *Special topics in mixing and transport processes in the environment*; Eds.; College Station, TX, 2005.
(17) Bard, A. J.; Faulkner, L. R. *Electrochemical methods: fundamentals and applications*; John Wiley & Sons, Inc.: New York, 2001.
(18) Brina, R.; Miller, A. G. Direct detection of trace levels of uranium by laser-induced kinetic phosphorimetry. *Anal. Chem.* 1992, *64* (13), 1413-1418.
(19) Oren, Y.; Soffer, A. The electrical double layer of carbon and graphite electrodes : Part II. Fast and slow charging processes. *J. Electroanal. Chem.* 1985, *186* (1-2), 63-77.
(20) Burns, P. C.; Finch, R. *Uranium: Mineralogy, Geochemistry and the Environment*; Mineralogical Society of America: Washington, DC, 1999.
(21) Kinoshita, K. *Carbon: electrochemical and physicochemical properties*; Wiley-Interscience: 1988.
(22) Farrell, J.; Bostick, W. D.; Jarabek, R. J.; Fiedor, J. N. Electrosorption and reduction of pertechnetate by anodically polarized magnetite. *Environ. Sci. Technol.* 1999, *33* (8), 1244-1249.
(23) Maslennikov, A.; Masson, M.; Peretroukhine, V.; Lecomte, M. Technetium electrodeposition from aqueous formate solutions: Electrolysis kinetics and material balance study. *Radiochim. Acta* 1998, *83* (1), 31-37.